BIODIESEL PRODUCTION FROM PALM FATTY ACID DISTILLATE (PFAD) CATALYZED BY ACID CATALYSTS AND BIODIESEL PURIFICATION VIA POLYMERIC MEMBRANES

By

FONG YONG SHENG

A dissertation submitted to Lee Kong Chian Faculty of Engineering and Science,

Unviersiti Tunku Abdul Rahman,

in partial fulfilment of the requirements for degree of Master of Engineering Science

July 2016

ABSTRACT

BIODIESEL PRODUCTION FROM PALM FATTY ACID DISTILLATE (PFAD) CATALYZED BY ACID CATALYSTS AND BIODIESEL PURIFICATION VIA POLYMERIC MEMBRANES

Fong Yong Sheng

In the study, biodiesel has been successfully produced from a low cost feedstock of palm fatty acid distillate (PFAD) using acid catalysts. The most promising catalyst for the biodiesel production was screened among the three types of catalysts (Al_2O_3-SO_3H, SiO_2-SO_3H and TiO_2-SO_3H). During the catalyst development stage, the optimum immersion time and acid concentration for good catalyst were defined. Characterizations of these catalysts were investigated by using Scanning Electron Microscope (SEM) with X-ray energy dispersive spectra (EDX), X-ray Diffractometer (XRD), Fourier Transform Infra Red (FTIR), Inductively Coupled Plasma-optical Emission spectrometer (ICP-OES) and Brunauer-Emmett-Teller (BET) surface area measurement. For biodiesel purification process, types of membranes (PES and PVDF), effect of molecular cut-off and transmembrane pressure were studied. Among the developed catalysts, sulfonated aluminium oxide (Al_2O_3-SO_3H) exhibited the most desired characteristic with high sulphur content of 3.71 wt %. The specific surface area and pore specific volume of Al_2O_3-SO_3H were 7.64 m^2/g and 0.0987 cm^3/g respectively. FTIR spectrum of Al_2O_3-SO_3H was detected at band 1077 cm^{-1} which indicated the presence of SO_3 species.

The maximum biodiesel yield of 57.49 % was achieved in 6 hours for esterification reaction catalyzed by sulfonated aluminium oxide. During catalyst development, aluminium oxide immersed in 5 M acid concentration with 18 hours duration appeared as the good catalyst for esterification reaction. For the downstream process, biodiesel mixture were purified using two types of polymeric membranes (PES and PVDF) at different molecular weight (5 kD, 20 kD, 30 kD and 100 kD) under different transmembrane pressure. 5 kD of PES with transmembrane pressure of 5 bar exhibited the stable permeate flux with the highest percentage reduction in palmitic acid (78.76 %) and oleic acid (93.73 %) during membrane purification process.

ACKNOWLEDGEMENTS

I would like to thank everyone who had contributed to the successful completion of this project. I would like to express my gratitude to my research supervisor, Asst. Prof. Dr. Sim Jia Huey for her invaluable advice, guidance and her enormous patience throughout the development of the research. Thank you for believing in me and constantly encouraging me to do my best. I am grateful to her for advising me to be humble and hardworking in life.

I would also like to express my gratitude to my loving parent who had given me encouragement and for guiding me through my ups and downs. Special thanks to my beloved mother for being emotionally strong for me and family. Thank you for teaching me: to face the problems, to solve them, and to let it go.

Lastly, I am grateful to UTAR for giving me this opportunity to carry out my research and providing me with the facilities.

APPROVAL SHEET

I certify that this project report entitled **"BIODIESEL PRODUCTION FROM PALM FATTY ACID DISTILLATE (PFAD) CATALYZED BY ACID CATALYSTS AND BIODIESEL PURIFICATION VIA POLYMERIC MEMBRANES"** was prepared by **FONG YONG SHENG** and submitted as partial fulfilment of the degree of Master of Engineering Science at Universiti Tunku Abdul Rahman.

Approved by,

_____ Date: _____

(Asst. Prof. Dr. Sim Jia Huey)

Supervisor

Department of Chemical Engineering

Lee Kong Chian Faculty of Engineering and Science

Universiti Tunku Abdul Rahman

_____ Date: _____

(Asst. Prof. Dr. Lee Poh Foong)

Co-Supervisor

Department of Biomedical and Mechatronic Engineering

Lee Kong Chian Faculty of Engineering and Science

Universiti Tunku Abdul Rahman

LEE KONG CHIAN FACULTY OF ENGINEERING AND SCIENCE

UNIVERSITI TUNKU ABDUL RAHMAN

Date: 15 JULY 2016

SUBMISSION OF THESIS

It is hereby certified that **FONG YONG SHENG** (ID No: **12UEM07837**) has completed this thesis entitled "**BIODIESEL PRODUCTION FROM PALM FATTY ACID DISTILLATE (PFAD) CATALYZED BY ACID CATALYSTS AND BIODIESEL PURIFICATION VIA POLYMERIC MEMBRANES**" under the supervision of **ASST. PROF. DR. SIM JIA HUEY** (Supervisor) from the Department of Chemical Engineering, Lee Kong Chian Faculty of Engineering and Science, Universiti Tunku Abdul Rahman.

I understand that university will upload the softcopy of my thesis in pdf format into UTAR institutional Repository, which may be made accessible to UTAR community and public.

Yours truly,

_____

(FONG YONG SHENG)

DECLARATION

I **FONG YONG SHENG** hereby declare that the thesis/dissertation is based on my original work except for quotations and citations which have been duly acknowledged. I also declare that it has not been previously or concurrently submitted for any other degree at UTAR or other institutions.

_____

(FONG YONG SHENG)

Date _____

TABLE OF CONTENTS

LIST OF TABLES

LIST OF FIGURES

LIST OF APPENDIXES

LIST OF SYMBOLS/ ABBREVIATIONS

n_{FAME}	Total mole of biodiesel in sample, mol
R_a	Ratio between the areas under curve of methyl esters to the area under curve of methyl heptadecanoate obtained from sample
R_s	Ratio between the areas under curve of methyl esters to the area under curve of methyl heptadecanoate obtained from standard
c_E	Biodiesel concentration in internal standard
DF	Dilution factor
$(V)_{PFAD}$	Total volume of PFAD used, L.
Al_2O_3-SO_3H	Sulfonated aluminium oxide
SiO_2-SO_3H	Sulfonated silicon dioxide
TiO_2-SO_3H	Sulfonated titanium (IV) oxide
GHG	Green house gases
ASTM	American society for testing and materials
FAME	Fatty acid methyl ester
B20	Blends of 20 % biodiesel and 80 % petrodiesel
B100	100 % biodiesel
FFA	Free fatty acid
MT	Metric tons
PFAD	Palm fatty acid distillate
RSM	Response surface methodology
SEM	Scanning electron microscopy
EDX	Energy dispersive x-ray spectroscopy

BET	Brunaur-Emmett-Teller
FTIR	Fourier Transform Infa-Red
XRD	X-ray Diffaction
ICP-OES	Inductively coupled plasma-optical emission spectrometer
ANOVA	Analysis of variance
MWCO	Molecular cut-off

CHAPTER 1

INTRODUCTION

1.1 Background

Rapid growth of human population and industrialization has accelerated the diminishing of energy resources. The International Energy Outlook 2013 subjects that the total world energy consumption will grow by 54 % between 2010 and 2040. In Figure 1.1, it can be seen that especially in the second half of 20th century, the global production of energy source was growing rapidly. As the fossil fuels (coal, oil and natural gas) take millions of years to form naturally, the rate of replenishment could not catch up with the current consumption rate of the energy. Therefore, fossil fuels are categorized as non-renewable resources (Nyambuu and Semmler, 2014). Besides, the experts have predicted that the fossil fuels will be depleted in next 10 decade if no new oil wells are found (Lam et al., 2010). In view of the increasing global energy demands and the exhaustion of fossil fuels, the era of the renewable energy like biofuels are important to ensure the sustainability of energy resource (Balat and Balat 2009).

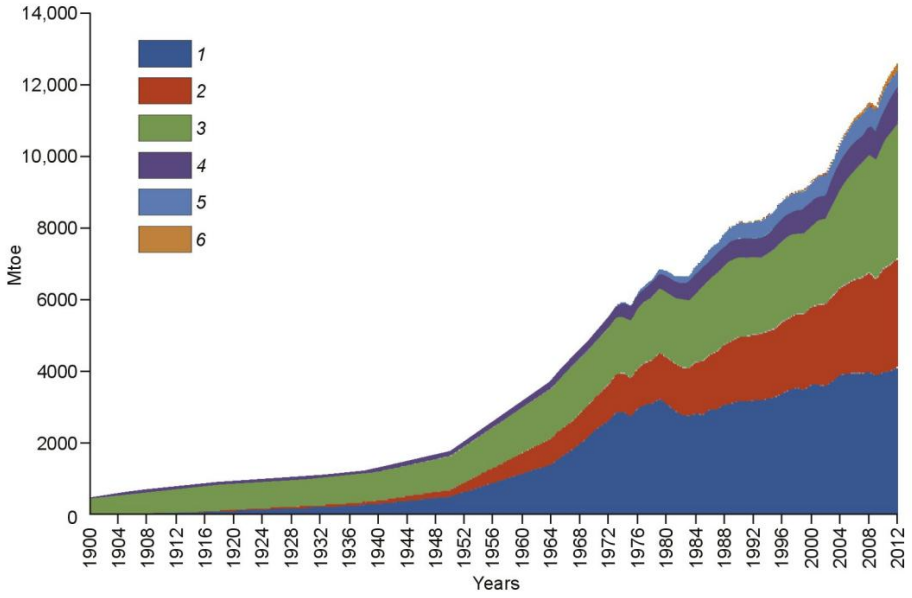

Figure 1.1: Global production of energy source in 1990-2012. 1. Oil; 2. Natural gas; 3. Coal; 4. Hydro; 5. Nuclear; 6. Other (Kontorovich et al., 2014)

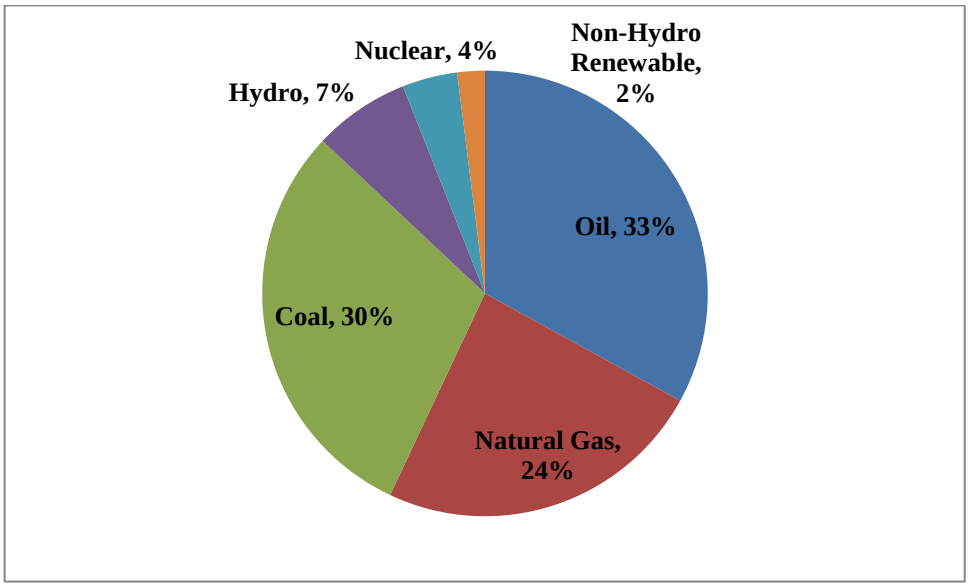

Figure 1.2: World Energy Consumption Year 2012 (BP, 2013).

Biofuels such as bioethanol and biodiesel derived from renewable resources could replace non-renewable resources such as crude oil. Biodiesel is a sustainable fuel because it is non-toxic, renewable, biodegradable and environmental friendly. The physical properties of biodiesel are similar to the diesel fuel. Thus, biodiesel shows a great potential to be used as a substitute fuel for diesel engines as it is derived from renewable sources and it allows the substitution of fossil diesel oil without engine modification (Berrios and Skelton, 2008; Jaichandar and Annamalai, 2011).

In this study, palm fatty acid distillate (PFAD) as side products from palm oil refining process was used as feedstock for biodiesel production. Heterogeneous acid catalysts like sulfonated aluminium oxide (Al_2O_3-SO_3H), sulfonated silicon dioxide (SiO_2-SO_3H) and sulfonated titanium (IV) oxide (TiO_2-SO_3H) were screened for the suitability to catalyze esterification reaction. The selected catalyst was further optimized to improve its performance with the aid of statistical approach. In the study, two types of polymeric membranes (PES and PVDF) were used to purify produced biodiesel. The effects of transmembrane pressure and pore sizes of polymeric membranes on the separation performances were also studied.

1.2 Problem Statement

The current production cost of biodiesel is 1.5 – 3 times higher than petroleum based diesel (Domingues et al., 2012). The cost is not competitive enough compared to diesel fuels due to expensive cost of feedstocks such as vegetable oil and heterogeneous catalyst. In order to lower the production cost of biodiesel, relatively cheap feedstocks such as the waste cooking oil or palm fatty acid distillate (PFAD) side products from palm oil refining process were proposed to be used. In this study, PFAD with the high free fatty acid (FFA) content of 72.7 % - 92.6 % was used in biodiesel production.

To accelerate the rate of reaction, catalyst plays an important role in the esterification reaction for biodiesel production. Liquid acid catalysts were employed for the commercial production of biodiesel. However, homogeneous catalysts would cause equipment corrosion and difficulty in catalyst recovery from reaction mixture. Although heterogeneous solid base catalyst has high catalytic performance on the high quality vegetable oils, it will result in soap formation with waste oils due to the FFA content. Solid acid catalyst is more suitable to process the low grade oils because the solid acid catalysts are insensitive to FFA and water content in the oil (Lam et al., 2010). In this study, the use of heterogeneous acid catalyst was for esterification of PFAD was proposed and studied.

The composition of biodiesel must comply with the ASTM D6751 and EN 14214 standards in order to enhance the biodiesel performance in diesel engine (Atadashi et al., 2011). Several researchers have studied the conventional technologies used for biodiesel separation such as gravitational settling, decantation, filtration and biodiesel purification such as water washing, acid washing and washing with ether and absorbents (Atadashi et al., 2011). The disadvantages of conventional technologies are high amount of water usage, high energy and time consumption, lower cost effectiveness (Atadashi et al., 2010). In comparison, membrane technology can be operated at moderate operating conditions with low energy consumption and low investment cost (Atadashi et al., 2011; Shuit et al., 2012). Membrane technology for biodiesel separation is still at the infant stage. Research on finding the suitable membrane for biodiesel separation is still in progress. The further study on membrane separation technology needs to be carried out. In the study, two types of polymeric membranes which include PES and PVDF were tested on their efficiency in biodiesel separation process.

1.3 Aim and Objectives

The research project aims to achieve the following objectives:

1. To screen for the most suitable catalyst support for esterification of PFAD. The types of catalyst supports were Al_2O_3, SiO_2 and TiO_2.
2. To study the effects of immersion time and acid concentration on the catalyst performance in catalyzing the esterification of palm fatty acid distillate (PFAD) reaction.
3. To optimize the catalyst performance in catalyzing esterification reaction for high biodiesel yield achieved in the shortest reaction time.
4. To study the effects of transmembrane pressure and molecular cut-off of polymeric membranes used for the biodiesel purification. Types of polymeric membranes used for the study include 5 kD and 20 kD polyethersulfone (PES), and 30 kD and 100 kD polyvinylidene fluoride (PVDF).

1.4 Scope of the Study

The different heterogeneous acid catalysts (sulfonated Al_2O_3, sulfonated SiO_2 and sulfonated TiO_2) were developed through sulfonation process. The performances of the developed acid catalysts were tested on the esterification reaction of PFAD to biodiesel. The developed heterogeneous acid catalysts were characterized to obtain catalysts' physical and chemical properties. The most suitable acid catalyst for esterification reaction was selected based on the highest biodiesel yield achieved in the shortest time.

The most efficient catalyst determined in the screening process was used in the subsequent studies. The effect of immersion time (6h, 12h and 18h) and the acid concentration (2M, 3M, 4M and 5M) on the catalyst performance was studied. Besides, the catalyst was further developed for optimum catalyst performance with the aid of statistical tool.

5 kD and 20 kD of PES and 30 kD and 100 kD of PVDF were selected to purify the biodiesel from reaction mixture after the esterification reaction. The effects of different transmembrane pressures (5 bar, 3 bar, 2 bar and 1 bar) on biodiesel membrane performance were studied. The membranes performances were examined based on the membrane flux and the percentage rejection of palmitic acid and oleic acid.

CHAPTER 2

LITERATURE REVIEW

2.1 Biodiesel as fuel

Compared to diesel fuel, biodiesel produces no sulphur, no net carbon dioxide, less carbon monoxide, particulate matters, smoke and hydrocarbons emission. Generally, biodiesel contains about 10 wt % of oxygen. Higher oxygen content favours biodiesel as a fuel because of better combustion characteristics (Atabani et al., 2012). Moreover, biodiesel production requires no drilling and refining like petroleum diesel (Atabani et al., 2012).

Biodiesel can be used in diesel engine in any proportion blended with conventional diesel fuel without any modification at all or minor modification (Mo et al., 2013). Several studies have been investigated to assess the engine performance with different biodiesel blends (Mohan et al., 1991; Agarwal, 2007; Gopal et al., 2014). For example, B20 (20 vol % biodiesel and 80 vol % petroleum diesel) is often used in diesel engine and heating systems, rather than as B100 (Joshi and Pegg et al., 2007). The relevant combustion parameters (ignition delay, peak pressure and rate of pressure rise) of biodiesel are found to be similar to the characteristic of petroleum diesel combustion at the same engine load, speed, timing and nozzle diameter.

Biodiesel has been applied in many countries such as United States of America, Malaysia, Indonesia, Brazil, Germany, France, Italy and other European

countries. The current mandate and planned targets for biodiesel are summarized in Table 2.1. For example, Canada started to use 2 % biodiesel in diesel fuel in 2012 and the blend will be increased to 5 % in 2015 (Hossein et al., 2014).

Table 2.1: Summary of worldwide biofuel current mandate and planned targets (Hossein et al., 2014).

Country	Official biofuel targets
Brazil	40% rise in ethanol production, 2005–2010; mandatory blend of 20–25% anhydrous ethanol (E 20–25) with petrol; minimum blending of 5% (B5) biodiesel to diesel by January 2013 20% biodiesel (B20) in fossil fuel by 2015
Canada	5% renewable fuel standard in all Canadian fuel and 2% biodiesel content in diesel fuel by 2012
European Union	10% in 2020 (biofuels); target set by European Commission in January, 2008
UK	5% by 2020 (biofuels, by energy content)
Indonesia	20% biodiesel and 15% ethanol blend in fossil fuel by 2025
India	20% Biodiesel content in diesel fuel by 2012
Malaysia	EnvoDiesel (B5) in all fuel stations and industrial sectors from 2008
Thailand	10% replacement of diesel in 2012

2.2 Biodiesel production

In general, different approaches have been introduced for the production of biodiesel. Biodiesel or fatty acid methyl ester (FAME) produced can be produced from the transesterification of triglycerides (TG) or esterification of free fatty acids (FFAs).

2.2.1 Transesterification reaction

Biodiesel produced from the transesterification of triglycerides (vegetable oils or animal fats) with short chain alcohols (mainly ethanol and methanol) have been studied by researchers. The transesterification reaction had been widely used in industry to convert renewable resources into biodiesel (Juan et al., 2011). In transesterification reaction, the triglycerides will be converted to one mole of glycerol and three moles of fatty acid methyl ester of biodiesel (Vyas et al., 2010). The transesterification process is shown in Figure 2.1.

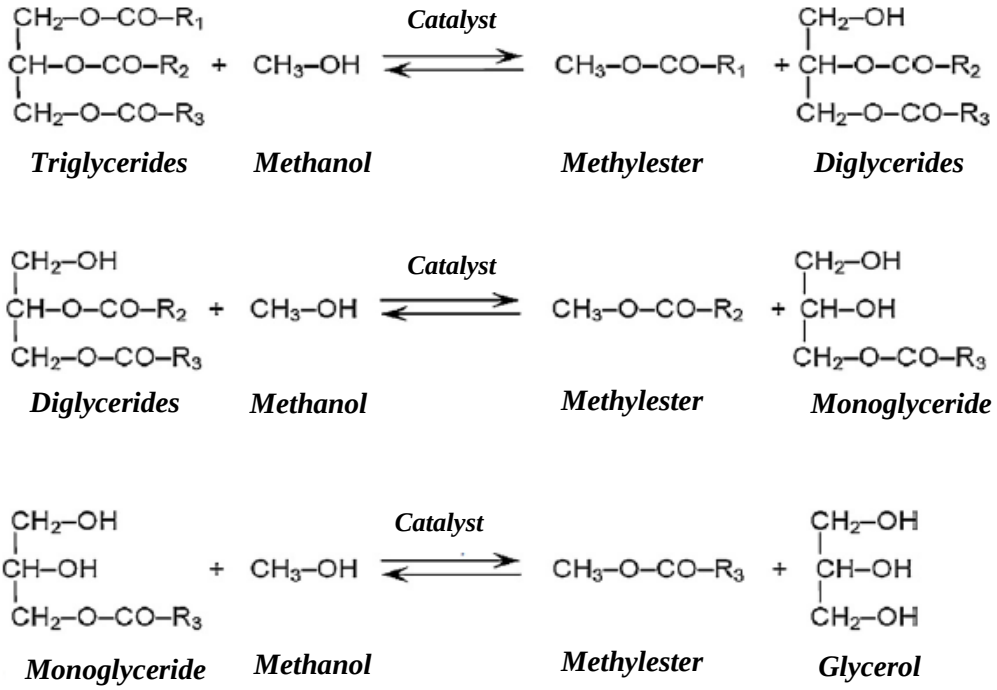

Figure 2.1: Transesterification Reaction Steps (Borges and Díaz, 2012).

2.2.2 Esterification reaction

Transesterification of low quality oils or fats which are high in FFA content will produce soap and thus reduce the ester yields (Borges and Díaz 2012). Hence, esterification reaction offers a better solution as only biodiesel an water are produced. Secondly, it can reduce the cost of production with the use of cheap raw feedstocks with high FFA contents. And the use of a heterogenous acid catalyst could simplify the steps of biodiesel purification and minimize the corrosion problem (Lam et al., 2010).

The biodiesel can be synthesized through the esterification of low quality of oils that contains high FFA (> 90%) waste cooking oils or palm fatty acid with alcohols as shown in Figure 2.2.

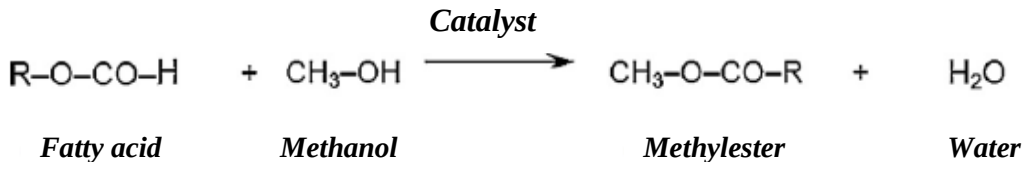

Figure 2.2: Esterification Reaction (Borges and Díaz, 2012).

2.3 Feedstocks for biodiesel production

The raw material cost is the primary obstacle to commercialize biodiesel compare to petroleum-based diesel (Domingues et al., 2012). The main biodiesel feedstocks were tabulated in Table 2.2. The cost of manufacturing accounts for 60% to 75% of the total production cost of biodiesel (Huang et al., 2010). Cheap feedstocks such as waste cooking oils, grease and PFAD have great potential to substitute the expensive vegetable oils as feedstock for biodiesel production (Cho et al., 2012).

Non-edible oils and animal fats are considered as second generation feedstocks. More recently, microalgae have become the third generation of biodiesel feedstock. They eliminate food competition and they are very economical compared to the edible oils. Moreover, the use of those feedstocks in biodiesel production will help to lower the production cost besides the issues of competition between food and biodiesel feedstocks will not exist (Atabani et al., 2012).

In the previous study, brown grease was used as feedstocks for biodiesel production catalyzed by zircronia supported metal oxide catalyst (Kim et al,. 2012). Besides Canakci (2007) and Wen et al. (2010) had studied on the esterification of waste cooking oil for biodiesel production. Recently, microalgae which contains high lipid content was also found to be a potential feedstock for biodiesel production (Huang et al., 2010). As mentioned, biodiesel feedstock accounts for about 70% of the production cost (Huang et al., 2010). In the study, a less expensive feedstock with high FFA of PFAD was used in the biodiesel production to reduce the production cost.

Table 2.2: Main feedstocks of biodiesel production (Atabani et al.,2012)

Edible oils	Non-edible oils	Animal fats	Other sources Bacteria
Soybeans	Jatropha curcas	Pork lard	Bacteria
Rapeseed	Mahua	Beef tallow	Algae
Safflower	Pongamia	Poultry fat	Microalgae
Rice bran oil	Camelina	Fish oil	Tarpenes
Barley	Cotton seed	Chicken fat	Poplar
Sesame	Karanja or honge		Switchgrass
Groundnut	Cumaru		Miscanthus
Sorghum	Cynara cardunculus		Latexes
Wheat	Abutilon muticum		Fungi
Corn	Neem		
Coconut	Jojoba		
Canola	Passion seed		
Peanut	Moringa		
Palm and palm kernel	Tobacco seed		
Sunflower	Rubber seed tree		
	Salmon oil		
	Carnegiea gigantean		
	Coffee ground		
	Nagchampa		
	Croton megalocarpus		
	Pachira glabra		
	Aleurites moluccana		
	Terminalia belerica		

2.3.1 Palm Fatty Acid Distillate (PFAD)

Malaysia is one of the most productive palm oil producers in the world. In year 2014, 25.07 million tonnes of palm oil products from Malaysia were exported (Awalludin et al., 2015). It is reported that about 700,000 MT of PFAD were produced in Malaysia during the palm oil refining process. PFAD is the by-product of palm oil being naturally obtained in the palm oil refining process (Cheah et al., 2008). Based on previous researches, biodiesel can be produced from the esterification of PFAD with alcohols. Therefore, Malaysia has a great advantage to develop the biodiesel production industry since PFAD can be used as feedstocks for biodiesel production.

PFAD can be considered as low-cost but valuable feedstock for the production of biodiesel due to the high FAME yield (93.7 %) being achieved previously (Mongkolbovornkij et al., 2010). Initially, PFAD is generally used in non-food applications such as soap making and also used as a power source in power plants and industrial boilers (Cheah et al., 2008).

From Table 2.3, PFAD contains 72.7 to 92.6% of FFA, with a small amount of unsaponifiable components (1 to 2.5%) and the remainder neutral oil (Tay et al., 2009). The general characteristics of PFAD produced in Malaysia are shown in Table 2.3. Unsaponifiable components include higher aliphatic alcohols, sterols, squalene, pigments and hydrocarbon. Saponification value is the measure of the free and esterified acids present. The saponification value ranged from 200.3 - 215.4 mg KOH/g. Iodine value is used to define the total unsaturation in PFAD. The iodine

value ranged from 46.3 - 57.6 g/100g. Titer is the measure of temperature of solidification of the material. The range of the titer falls between 46.0 - 48.3 °C.

Table 2.3: General Characteristic of PFAD Produced in Malaysia (Tay et al., 2009)

Catalyst	Mean	Range
FFA - palmitic (%)	86.4	72.7 - 92.6
Unsaponifiable matter (%)	1.61	1.0 - 2.5
Saponification value (mg KOH/g)	209.5	200.3 - 215.4
Titer (°C)	46.7	46.0 - 48.3
Specific gravity at 50°C (g/cc)	0.8725	0.8640 - 0.8880
Water content (%)	0.104	0.03 - 0.24
Iodine value, W_{ijs} (g/100g)	54.8	46.3 - 57.6

2.4 Heterogeneous catalysts

Heterogeneous catalyst is suitable to produce biodiesel because of the ease of catalyst separation from biodiesel mixture. Besides that, the equipment corrosion problem can be avoided. In comparison, homogeneous catalyst has the ability to catalyze the reaction at low temperature and pressure with high biodiesel yield in short time (Lotero et al., 2005). But the catalysts would cause equipment corrosion problem and the difficulty in catalyst separation from reaction mixture. The biodiesel produced by using homogeneous catalyst need to be neutralized by undergoing extra washing step and purification step in order to meet the biodiesel standard. Eventually, it leads to higher cost of biodiesel production because of the large amount of water usage in the washing process and the additional expenses for the waste water treatment (Sharma et al., 2011).

2.4.1 Heterogeneous acid catalysts

Heterogeneous acid catalyst is insensitive to water and free fatty acids. Unlike the heterogeneous base catalyst, it is sensitive to water and free fatty acid. The heterogeneous base catalyst has high catalytic performance on the high quality vegetable oils but it will result in soap formation with low quality of oils. The undesirable soap formation will eventually reduce the yield of biodiesel (Lam et al., 2010). To overcome this problem, many researchers have done the study on the esterification of FFA by using heterogeneous acid catalysts. The heterogeneous acid catalysts which had been tested are sulphated zirconium oxide, sulphated titanium oxide, sulphated tin oxide, sulfonic ion-exchange resin, sulfonic modified mesostructure silica, sulfonated carbon-based catalyst, heteropolyacids (HPAs) (Lam et al., 2010). Table 2.4 summarizes the heterogeneous catalysts used in biodiesel production.

Table 2.4: Summary of heterogeneous catalysts used for biodiesel production.

Catalyst	Feedstock	Reaction time (h)	Reaction temp. ^{o}C	Catalyst conc. (wt %)	Oil to methanol ratio	FAME yield (%)	Reference
Al_2O_3	Soybean oil	3	160	1	1:0.4	89	Mello et al., 2010
SnO	Soybean oil	3	160	1	1:0.4	87	
Carbon-based solid acid	Cottonseed oil	4.5	220	0.2	1:16.8	94.8	Shu et al., 2010
SO_4^{2-}/ZrO_2	Purified palm oil	0.17	250	0.5	1:6	90	Petchmala et al., 2010
	PFAD	0.017	250	0.5	1:6	75	
SO_4^{2-}/SnO_2	Waste cooking oil	3	150	6	1:30	91.5	Lam et al., 2010
SO_4^{2-}/SnO_2- SiO_2	Waste cooking oil	3	150	3	1:15	92.3	
SO_4^{2-}/SnO_2-Al_2O_3	Waste cooking oil	3	150	3	1:10	82.3	
SO_4^{2-}/TiO_2	Soybean oil	1	120	1	1:20	40	Almeida et al., 2008
	Castor oil	1	120	1	1:20	25	
SO_4^{2-}/TiO_2-SiO_2	Waste vegetable oil	6	200	3	1:9	92	Peng et al.,2008

Zirconium oxides are the heterogeneous acid catalyst which had gained much attention from researchers for esterification reaction. Zirconium oxides contain large number of Brönsted acid sites which is an important factor to be an efficient support (Lee and Saka 2010). Strong solid acid catalysts, such as SO_4^{2-}/ZrO_2, SO_4^{2-}/Al_2O_3, SO_4^{2-}/SiO_2, WO_3/ZrO_2 (powder type) have been tested in the esterification of waste cooking oils. SO_4^{2-}/ZrO_2 and WO_3/ZrO_2 catalysts were found to be effective in catalyzing the conversion of FFA to biodiesel (Park et al., 2008). Even though zirconium oxides showed a promising performance in the esterification of FFAs, it has not been widely used in the industry process because it is non-cost effective as zirconium is rare and costly metal (Lee and Saka 2010). Therefore, it is necessary to find a cheap and readily available support.

Besides zirconium oxide, alumina (Al_2O_3) as metal oxide of heterogeneous catalysts also presented promising results in the esterification of soybean oil with the reaction yields as high as 89 % after 3 hours (Mello et al., 2010). Tin oxide (SnO) catalyst has been found to be reusable up to ten times in the esterification reaction without significant losses in its catalytic activity. In other words, the possibility of recycling tin oxide will then reduce the cost of production. The surface areas of Al_2O_3, SnO, $(Al_2O_3)_8(SnO)_2$ and $(Al_2O_3)_8(ZnO)_2$ were 119 m^2/g, 15 m^2/g 22 m^2/g and 33 m^2/g. The decreasing order for catalyst activities was: Al_2O_3> SnO > $(Al_2O_3)_8(SnO)_2$ >$(Al_2O_3)_8(ZnO)_2$. This can be explained by the surface areas of the catalysts. The authors have concluded that solid metal oxides as heterogeneous catalysts especially alumina and tin oxide results in the high biodiesel yields, ease the

catalyst separation from products and provide good results on catalyst recycling (Mello et al., 2010).

Catalyst SiO_2 is another promising heterogeneous catalyst for biodiesel production. It was found that SiO_2 has a strong generation of acid surface sites after the pretreatment with either H_2SO_4, HCl, HNO_3, or HF. SiO_2 after treated with HF showed the highest number of acid surface sites. SiO_2 (HF) as heterogeneous catalyst achieved 86% of FFA conversion. The catalytic activity of SiO_2 (HF) remained unchanged even after ten runs of esterification reaction (Corro et al., 2010). The recycling of catalyst for many times can reduce the cost of biodiesel production.

TiO_2 after modified with sulphate was found to be an active catalyst for the transesterification of cottonseed oil with methanol (He et al., 2007). This might be due to its creation of new Bronsted acid sites. It was reported that higher sulphur content represents higher acidity of the catalyst and thus higher catalytic activity (Islam et al., 2013). The catalytic activities of TiO_2/SO_4 with different ratios used in transesterification of soybean oil have been studied. The order of catalytic activities was: TiO_2/SO_4 (5:1) > TiO_2/SO_4 (10:1) > TiO_2/SO_4 (20:1). TiO_2/SO_4 with the ratio of 20:1 for the transesterification reaction obtained the lowest reactivity which was probably due to inadequate amount of sulphuric acid used in during catalyst preparation (Almeida et al., 2008).

2.5 Catalyst characterization

In general, the physical and chemical properties of catalyst can be characterized by using Scanning Electron Microscopy (SEM), Energy Dispersive X-ray Spectroscopy (EDX), Brunauer-Emmett-Teller (BET), Inductively Coupled Plasma-Optical Emission Spectrometer (ICP-OES), Fourier Transform Infra-Red (FTIR) and X-Ray Diffraction (XRD) analyses.

2.5.1 Catalyst structure

Scanning electron microscope (SEM) is an electron microscope that produces images of a sample by scanning the sample with a focused beam of electron. The signals produced contain information about the sample's surface topography and composition (Nixon, 1971).

The SEM micrographs of SiO_2 and SiO_2HF were shown in Figure 2.3. The SiO_2HF catalyst was used to catalyze the esterification of waste frying oil (Corro et al., 2011). The morphological structure of sulfonated starch solid acid catalyst was visualized by SEM as shown in Figure 2.4. The catalyst performance was determined by the esterification of palm fatty acid distillate with the aid of sulfonated starch solid acid catalyst. (Lokman et al., 2015)

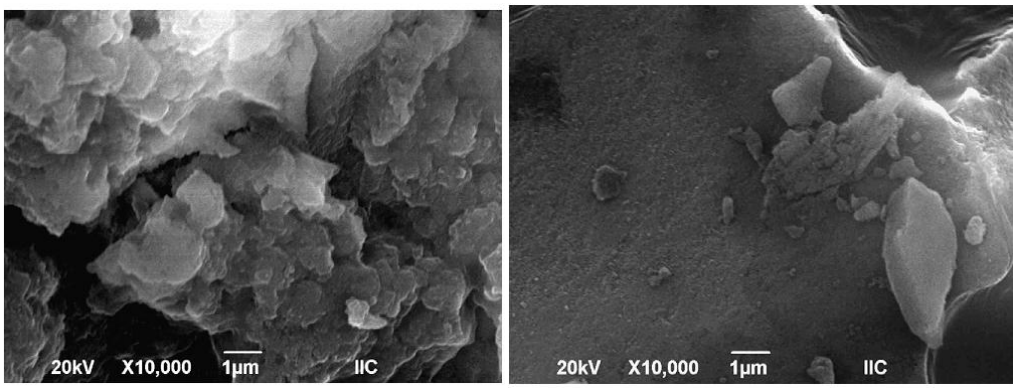

Figure 2.3: SEM micrographs of SiO_2 and SiO_2HF.

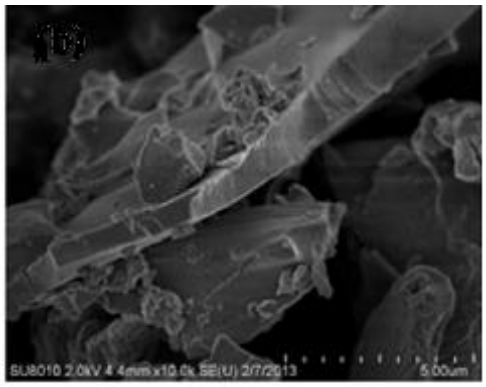

Figure 2.4: SEM micrographs of SiO_2 and SiO_2HF.

2.5.2 Sulfur concentration

EDX analysis is a technique using the emission of X-ray spectrum from the bombard of a solid sample with a focus beam of electron to acquire a confined chemical analysis. All elements from atomic number 4 (Be) to 92 (U) can be detected by EDX analysis. The determination of concentration of the elements is based on the line intensities for each element in the sample and for the same elements in calibration Standards of known composition (Goldstein et al., 2003).

Figure 2.5 indicates the EDX diagram of sulfonated carbon catalyst. The result shows the contents of C, O and S. The sulfur content of sulfonated carbon catalyst was found to be 9.12 wt% (Tao et al., 2015). Moreover, the sulfur content of sulfonated solid acid catalyst (4.89 wt%) were measured by the EDX which had been used in the esterification of palm fatty acid distillate (PFAD) (Lokman et al., 2015).

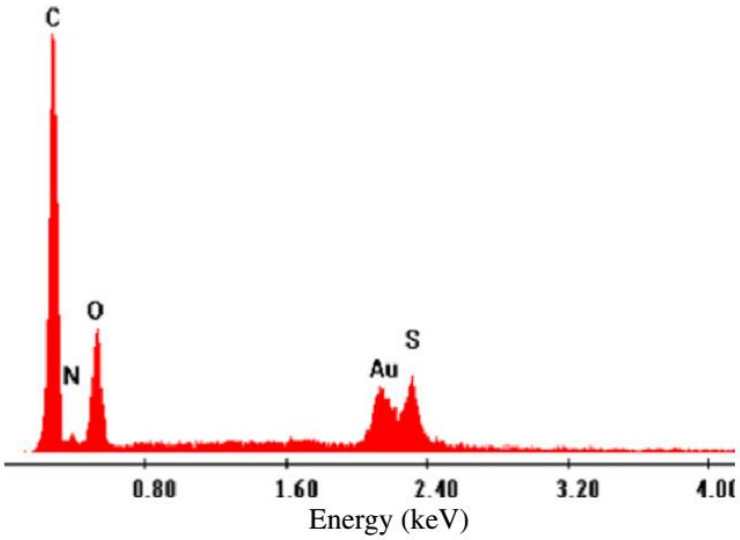

Figure 2.5: EDX diagram of sulfonated carbon catalyst (Tao et al., 2015).

2.5.3 Surface Area Measurement

The specific surface area of a powder is measured by the Brunauer-Emmett-Teller (BET). The surface area analysis involves the nitrogen adsorption-desorption at low temperature (77k), and has been used for the determination of the total specific surface area of porous catalysts.

The specific surface area of the catalyst is determined by calculating the amount of adsorbed gas corresponding to monomolecular layer on surface area using the BET equation (Brunauer et al., 1938).

$$\frac{p}{V(p_o - p)} = \frac{1}{V_m C} + \frac{(C-1)p}{CV_m p_o} \quad (2.1)$$

where V is the volume, reduced to standard conditions, i.e. the standard temperature and pressure (STP) of gas adsorbed per unit mass of adsorbent at a given pressure, p and constant temperature; p_0 is the saturation pressure at the measurement temperature; V_m is the volume of gas required to form a complete monolayer adsorbed layer at STP per unit mass of adsorbent, when the surface is covered by a monolayer of adsorbate; and C is a constant related to free energy of adsorption which is represented by the equation below:

$$C = A_{r\,exp}\left(\frac{(\Delta H_1 - \Delta H_2)}{RT}\right) \quad (2.2)$$

where A_r is the pre-exponential factor; ΔH_1 is the heat of adsorption of the first layer; ΔH_2 is the heat of liquefaction; R is the gas constant; and T is the absolute temperature in Kelvins (Ladavos et al., 2012).

BET technique has been used in the study of the directly synthesized sulphated zirconia catalyst. The surface area of directly synthesized sulphated zirconia was 169 m^2/g and the conventionally synthesized sulphated zirconia was 65 m^2/g. The directly synthesized sulphated zirconia produced 43 % of biodiesel yield,

whereas the conventionally synthesized sulphated zirconia produced 15 % of biodiesel yield (Eterigho et al., 2011).

2.5.4 Inductively Coupled Plasma-Optical Emission Spectrometer (ICP-OES)

The inductively coupled plasma is a type of emission spectroscopy which generate excited atoms and ions that emit electromagnetic radiation at wavelengths characteristic of a particular element (Hou and Jones, 2000).

The sulfur content of sulphated zirconia catalysts were determined by the ICP method. The sulfur content of sulphated zirconia was 1.73 wt%(Suwannakarn, 2008).. The result of ICP method was consistent with the sulfur content obtained by the thermogravimetric analysis (TGA) method (Suwannakarn, 2008).

2.5.5 Fourier Transform Infra-Red (FTIR)

FTIR is a method of infrared spectroscopy. In infrared spectroscopy, when IR radiation is passed through a sample, some of the infrared radiation is absorbed by the sample while some of it is passed through (transmitted). The resulting spectrum represents the molecular absorption and transmission, creating a molecular fingerprint of the sample (Wellner, 2013).

Figure 2.6 displays the FTIR spectrums of a pure methanol and crude biodiesel. The presence of biodiesel occurred between 1830-1800 cm^{-1} and 1780-1640 cm^{-1}. In Figure 2.7, FTIR spectrum of PFAD has similar pattern to the FTIR spectrum of oleic acid. The stretching of carbonyl group of carboxylic acid contributes near 1704 cm^{-1}. It was reported that PFAD is a mixture containing free fatty acids, squalene, vitamin E, sterols, glycerides and other unknown compound. The peaks at 2360 and 2340 cm^{-1} indicate those minor compounds present in PFAD (Kaijun, 2013).

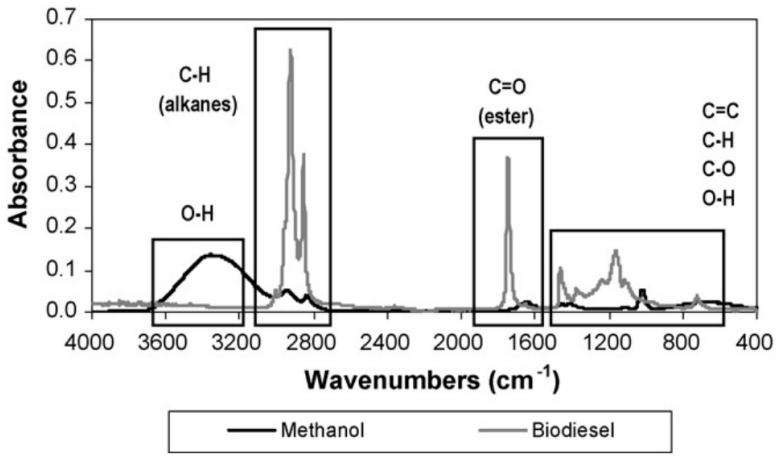

Figure 2.6: FTIR spectrums of a pure methanol and crude biodiesel (Othman et al., 2010).

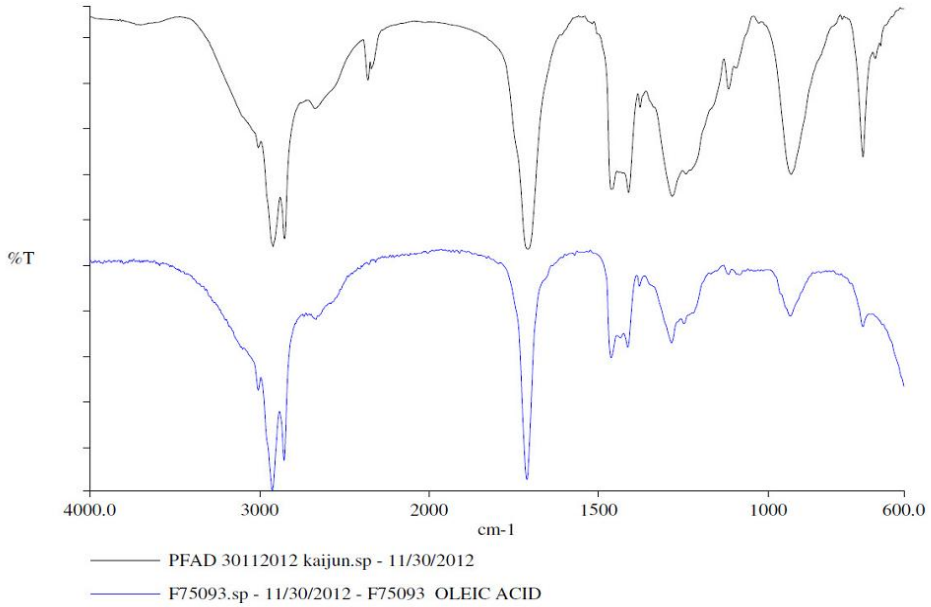

Figure 2.7: FTIR spectrums of PFAD and oleic acid (Kaijun, 2013).

2.5.6 X- ray Diffraction (XRD) analysis

XRD analysis is a technique for qualitative and quantitative analysis of crystalline compounds. The phenomenon of diffraction occurs when the penetrating radiation, X-rays enters a crystalline substance and is scattered. The scattered X-rays will undergo constructive and destructive interference in a process termed as diffraction. Resulting diffractogram will confirm the identity of a solid material. The diffraction of X-Rays by crystals is described by Bragg's Law.

X-ray diffraction has been in use in two main areas: the fingerprint characterization of crystalline materials and the determination of their structure. In catalysis, X-ray diffraction analysis is carried out to determine the phase

compositions of catalysts at ambient temperature and under normal atmospheric conditions (Klug and Alexander, 1974).

For example, Figure 2.8 shows the typical diffraction peaks (111), (311), (400) and (440) of γ-Al_2O_3 with a cubic structure (Jian-hong et al., 2009). In Figure 2.9, the distinguished diffraction peaks of all catalysts were found at 2θ = 26.5, 33.9, 37.95 and 51.8^o which indicated the presence of SnO_2 (Lam et al., 2009).

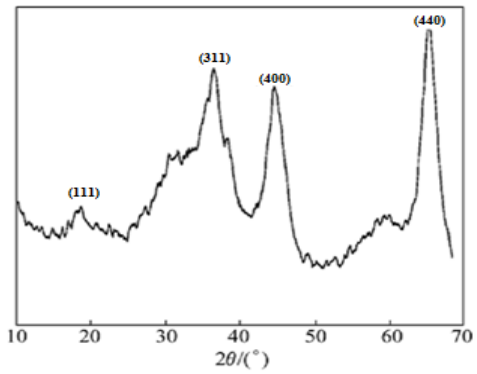

Figure 2.8: XRD pattern of γ-Al_2O_3 powder (Jian-hong et al., 2009).

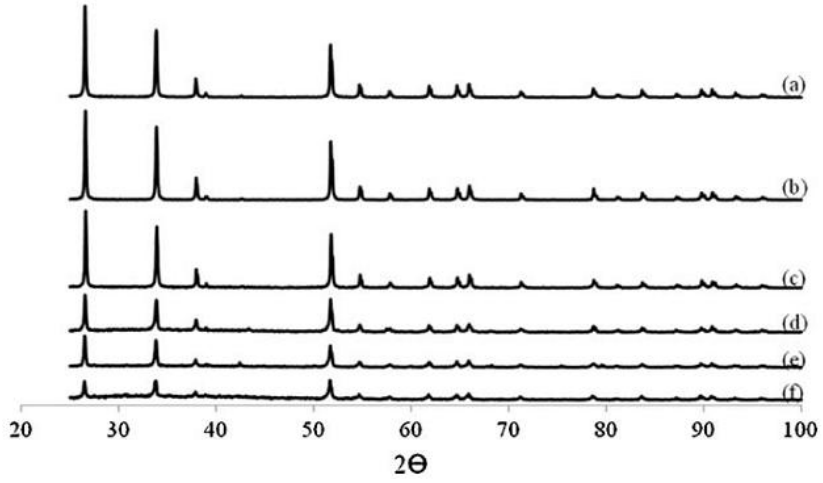

Figure 2.9: XRD patterns of catalysts calcined at different temperatures for 2 h; (a) unsulfated SnO_2, (b) 500 ^{o}C for SO_4^{2-}/SnO_2, (c) 400 ^{o}C for SO_4^{2-}/SnO_2, (d) 300 ^{o}C for SO_4^{2-}/SnO_2-Al_2O_3 (3), (e) 300 ^{o}C for SO_4^{2-}/SnO_2-SiO_2 (3) and (f) 300 ^{o}C for SO_4^{2-}/SnO_2 (Lam et al., 2009).

2.6 Catalyst performance in esterification reaction

The effects of important parameters that directly affect the performance of acid catalyst in catalyzing the esterification reaction have been studied by many researchers. These studies include the effects of calcination temperature, immersion time, and acidity of catalyst on catalyst performance in biodiesel production.

2.6.1 Effect of calcination temperature on catalyst activity

Calcination treatment has been found to improve the catalysts ($NaNO_3/Al_2O_3$ and KNO_3/Al_2O_3) performance and help to restore the catalytic activity. High calcination temperature of more than 550 ^oC decreased the catalytic activity of the catalyst (Benjapornkulaphong et al., 2009). A similar investigation has been done and the authors suggested that the decrease in catalytic activity might be due to the adsorption of organic materials, which led to the carbonization on the catalyst surface at high temperature (Wan et al., 2009). In addition, the contamination of catalyst with H_2O, O_2, CO_2 and other gases contained in air during storage, eventually reduced the catalytic activity in the reaction (Yan et al., 2008).

According to Abdoulmoumine (2010), the acid catalysts of SO_4^{2-}/ZrO_2 were calcined at 550 ^oC and 650 ^oC. The sulphur contents of these calcined SO_4^{2-}/ZrO_2 at 550 ^oC and calcined SO_4^{2-}/ZrO_2 at 650 ^oC were 1.04 wt % and 1.01 wt % respectively, whereas the sulphur content of uncalcined SO_4^{2-}/ZrO_2 was 1.22 wt%. Apparently, the catalyst underwent the calcinations pretreatment tend to have

decreased the amount of sulphur content. Consequently, the uncalcined SO_4^{2-}/ZrO_2 obtained the highest biodiesel yield (31.39 %) in comparison with calcined SO_4^{2-}/ZrO_2 at 550 ^oC (25.82 %) and SO_4^{2-}/ZrO_2 at 650 ^oC (25.04 %).

2.6.2 Surface area

The surface area was found to be influenced by calcinations temperature (Lopez et al., 2007). For example, the tungstated zirconia with 325 m^2/g surface area was prepared by dehydrating a tungstated zirconia precursor at 120 ^oC and then calcined for 3 h under air at 800 ^oC. The surface area of tungstated zirconia was reduced to 20 % (58 m^2/g) after the calcination at 800 ^oC. It is probably due to the loss of the tetragonal phase for ZrO_2 structure at 800 ^oC (Lopez et al., 2007).

The effect of surface area for TiO_2, ZrO_2, TiO_2-SO_4, ZrO_2-SO_4 were investigated in the transesterification of cottonseed oil with methanol at 230 ^oC. The study showed that the specific surface area of TiO_2 and ZrO_2 were increased by merging of sulphate to both TiO_2 and ZrO_2 structure. Subsequently, the large accessibility of the catalyst enhanced the FAME yield of transesterification (He et al., 2007).

The different ratios of superacid sulphated TiO_2/SO_4 catalysts were studied in the transesterification of soybean with methanol at 120 ^oC. The specific surface area of TiO_2/SO_4 (5:1), TiO_2/SO_4 (10:1) and TiO_2/SO_4 (20:1) were 266, 235, 193 m^2/g respectively. From the study, the catalyst TiO_2/SO_4 (5:1) exhibited the highest specific surface, average pores diameter and pore volume. It also produced the

highest FAME yield of 40 % compared TiO_2/SO_4 (10:1) and TiO_2/SO_4 (20:1) (Almeida et al., 2008).

2.6.3 Effect of immersion time

Researchers have highlighted the application of solid acids catalyst in the biodiesel field. The solid catalysts have to be immersed into a liquid acid periodically in order to produce a solid acid catalyst. For instance, SO_4^{2-}/ZrO_2, SO_4^{2-}/Al_2O_3, SO_4^{2-}/SnO_2 have been used in catalyzing the transesterification of vegetable oils (Park et al., 2008). In an example, an inexpensive and environmental friendly SO_4^{2-}/TiO_2-SiO_2 solid acid catalyst has been immersed in 0.5 M H_2SO_4 for one day. The prepared catalyst showed good catalytic activity and ease of separation characteristic. Besides, the catalyst was able to catalyze either esterification reaction or transesterification reaction for biodiesel production (Peng et al., 2008).

SO_4^{2-}/SnO_2–SiO_2 catalyst was prepared by immersing in 2 M H_2SO_4 for 6 hours (Lam et al., 2009). Transesterification of waste cooking oil in the presence of SO_4^{2-}/SnO_2 –SiO_2 have resulted in 92.3 % high biodiesel yield. On the other hand, the zirconia powder was immersed in 0.5 M H_2SO_4 for only 30 minutes. With 1 wt % of the SO_4^{2-}/ZrO_2, the biodiesel yield was obtained higher than 90 % (Jiputti et al., 2005).

2.6.4 Effect of acidity of catalyst

The researchers have reported that higher sulphur content corresponded to higher catalyst acidity and thus higher catalytic activity in biodiesel production (Kiss et al., 2006). Several acid catalysts at different TiO_2/SO_4 molar ratios were used to catalyze transesterification of soybean oil with methanol at 120 ^oC. The increasing order of reactivity was TiO_2/SO_4 (5:1) > TiO_2/SO_4 (10:1) > TiO_2/SO_4 (20:1). The TiO_2/SO_4 with ratio 20:1 has the lowest catalytic which is probably due to inadequate amount of sulphuric acid used during catalyst preparation. In contrast, the catalyst which is immersed in high concentration of sulphuric acid resulted in the highest specific area, high average pore diameter and pore volume, and the catalyst contained the highest concentration of sulphate groups. In the transesterification of soybean oil, the catalysts TiO_2/SO_4 (5:1) and TiO_2/SO_4 (10:1) achieved 30 % and 40 % biodiesel yield, respectively. Thus, the acidity of catalyst affected the catalyst performance in biodiesel production (Almeida et al., 2008).

The catalysts ZrO_2 and SO_4^{2-}/ZrO_2 were investigated in transesterification of crude palm kernel oil. The SO_4^{2-}/ZrO_2 with sulphate groups contained high acid strength whereas the ZrO_2 without sulphate group has low acid strength. Transesterification reaction catalyzed with the ZrO_2 resulted in lower biodiesel yield compared to the SO_4^{2-}/ZrO_2 catalyst (Garcia et al., 2008). The SO_4^{2-}/TiO_2-SiO_2 solid acid catalyst with 2.2 wt % of sulphur content showed good stability in the reaction. It can be recycled and the catalyst can simultaneously catalyze both the transesterification and esterification reactions (Peng et al., 2008).

The alumina sulfonated with 0.8 M sulphuric acid has larger surface area and average pore size compared to alumina immersed in 3.6 M sulphuric acid. The 43.4 % biodiesel yield was achieved with sulphated alumina in 0.8 M sulphuric acid whereas the reaction catalyzed by sulphated alumina in 3.6 M sulphuric acid had resulted in lower biodiesel yield of 33.4 % (Kim et al., 2004).

2.7 Operating parameters for esterification reaction

The operating parameters that affect the biodiesel yield during esterification reaction include reaction temperature, alcohol to oil molar ratio, mixing intensity, reaction time and catalyst loading. The effects of those factors on biodiesel yield are discussed in the following section.

2.7.1 Reaction temperature

The temperature is directly proportional to the production rate of biodiesel. The increase in temperature will accelerate the reaction to complete in shorter time (Othman et al., 2010). The effects of operating temperature ranging from 30 to 55 ^{o}C had been studied on the biodiesel yield. The results showed that the increased of temperature led to a rise in the biodiesel conversion (Marchetti et al., 2007). The optimum operating temperature was found to be near the boiling point of methanol which was 65 ^{o}C. Above 65 ^{o}C, the methanol started to vaporize and resulted in the formation of bubbles and the three phases (solid catalyst – oil – alcohol) formation, inevitably decreased the rate of reaction (Liu et al., 2008).

The optimum temperature also depends on the types of oil used for transesterification reaction or esterification reaction. Generally, the higher the operating temperature, the higher the reaction rate for biodiesel production was obtained. Transesterification of palm oil achieved 90 % FAME yield at 250 ^{o}C operating temperature in 10 minutes reaction time (Petchmala et al., 2010). Esterification of used vegetable oils at temperature of 75 ^{o}C achieved 85 % FFA conversion after 20 hours (Park et al., 2008).

2.7.2 Molar ratio of alcohol to oil

Triglyceride or free fatty acid reacts with alcohol will produce fatty acid methyl ester (FAME), also known as biodiesel. Alcohol acts as a very important reactant in the transesterification reaction or esterification reaction. Alcohol to oil ratio is one of the key parameters that affects the biodiesel production. From the stoichiometric reaction of transesterification (Figure 2.1), it is shown that at least three moles of alcohol must react with one mole of triglyceride to produce three moles of fatty acid methyl ester and one mole of glycerol. On the other hand, for esterification reaction, (Figure 2.2) at least one mole of alcohol must react with one mole of free fatty acid to yield one mole of fatty acid methyl ester and one mole of water (Mat et al., 2012).

Both transesterification and esterification processes are reversible reactions (Hassan et al., 2013). Thus, transesterification reaction requires a high concentration of alcohol to force the reaction shift to the forward direction. However, large excess alcohol caused the increase in solubility of glycerol in methyl ester layer which

eventually created the difficulty in separation process. If the reaction mixture largely contained the glycerol, this would drive the reaction equilibrium backward and reduced the biodiesel yield (Fillières et al., 1995).

2.7.3 Mixing intensity

Mixing intensity is very important in transesterification and esterification reactions. At the start of the reaction, the reaction mixtures (solid acid catalyst, oil and alcohol) formed three-phase system. Thus, the reaction rate was slow in the three phases since the reaction is diffusion controlled. The mixing effect was studied and the increased in mixing intensity have improved the mass transfer on the surface of solid catalyst. When the single phase was established, the mixing effect becomes negligible (Encinar et al., 2010). This was because methyl ester played the role of a mutual solvent for the reactants (Srivastava and Prasad, 2000).

In the study, the effects of stirring speed were investigated in the range of 300-800 rpm. The stirring speed did not have significant effect in the transesterification of corn oil (Rasimoglu et al., 2014). In another study, sterculia foetida oil was used as the non-edible feedstock for biodiesel production. The optimum biodiesel yield was obtained at the stirring speed of 1200 rpm (Silitonga et al., 2013). In another study by Kartika et al. (2013), the influence of stirring speed (700-900 rpm) was examined for the optimum biodiesel yield. The stirring speed at 700 rpm was found to be the optimum value for transesterification process.

2.7.4 Reaction time

In general, the conversion of biodiesel increased with the reaction time (Mat et al., 2012). The effect of reaction time with the range 1 to 10 hours was studied on the biodiesel production in the presence of KI/Al_2O_3. The biodiesel yield increased from 4 hours reaction time to 8 hours reaction time and reached the saturation thereafter. The maximum conversion of soybean oil was 90 % after 8 hours (Xie and Li, 2006).

Kim et al. (2004) reported that the biodiesel conversion achieved by using homogeneous catalyst and heterogeneous catalyst had been investigated. Both homogeneous and heterogeneous catalyst reached the maximum biodiesel yield within 1 hour of reaction time. However, the biodiesel yield achieved with homogeneous catalyst was 20 % higher than the biodiesel yield achieved with heterogeneous catalyst.

In a study by Macario et al. (2010), transesterification of vegetable oil catalyzed by heterogeneous base catalyst was compared to the conventional homogeneous catalyst (NaOH). The biodiesel yield increased steadily at the reaction time from 1 to 3 h. After 3 hours, the saturation point of biodiesel yield was achieved. Esterification of palm fatty acid distillate achieved 75 % of biodiesel conversion in 1 minute. And the 90 % of biodiesel conversion was obtained in transesterification of purified palm oil after 10 minutes reaction time (Petchmala et al., 2010). On the other hand, the esterification of waste fruit oilseeds required 48 hours to reach 87 % of biodiesel yield.

2.7.5 Catalyst loading

The amount of catalyst used for biodiesel production depends on the types of solid catalyst (Mat et al., 2012). The amount of catalyst used in the reaction can affect the amount of biodiesel being produced. In the study conducted by Mat et al. (2012), nearly 1 wt% of solid metal oxides was able to catalyze the esterification reaction between FFA and alcohol. 95 % of biodiesel yield was achieved after 3 hours when the reaction was catalyzed with 8 wt % of catalyst (Liu et al., 2008).

The authors have studied the effect of catalyst amount (2 to 7 wt%) on biodiesel yield. The results showed that the reaction rate increased with increased amount of catalyst used. 2 to 5 wt % of catalyst resulted in less significant improvement of the reaction rate. Even for a higher amount of catalyst (7 wt%), the results showed that all biodiesel conversion reached the same saturation point as expected (Marchetti et al., 2007). The effects of different amounts of catalyst loading were shown in Figure 2.10.

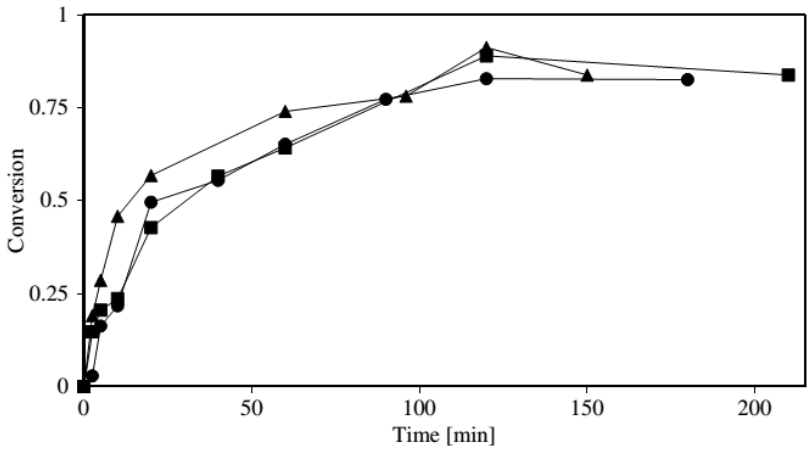

Figure 2.10: Effect of different amounts of catalyst. Catalyst = basic resin ● = 2.267 wt%, ■ = 5.099 wt%, ▲= 7.053 wt% (Marchetti et al., 2007).

2.8 Biodiesel purification via membrane separation process

Generally, the interest of biodiesel usage is still low due to its high investment cost and the historical availability of crude oil. As compared, production cost of biodiesel is 1.5 – 3 times higher than petroleum diesel (Domingues et al., 2012). Targeting to resolve the high production cost of biodiesel, the development of membrane separation technology for biodiesel separation is in favor recently due to its low capital cost, environmental friendly process and resulted in high purity of biodiesel after the separation (Atadashi et al., 2011; Shuit et al., 2012).

Besides that, membrane separation technology can be operated at moderate operating conditions with low energy consumption and resulted in high purity of biodiesel. The conventional biodiesel separation and purification technologies like (gravitational settling, decantation, filtration, water washing, acid washing and washing with ether and absorbents) have few disadvantages such as high operating cost, high energy consumption and huge amount of water usage (Atadashi et al., 2011; Shuit et al., 2012). Biodiesel separation through membrane separation is able to overcome the problem faced due to the conventional biodiesel separation and purification technologies. In this type of system, the membrane acts as a selective barrier to separate the impurities from biodiesel reaction mixtures under mild condition.

The membrane separation technology is essential as there are plenty of impurities in biodiesel. The types of impurity of biodiesel include unconverted fat

and soap, excess amount of alcohol, residual catalysts, free glycerin and water (Banga and Varshney, 2010). The impurities of biodiesel will cause instability of biodiesel on diesel engine performance. For instance, methanol gives rise to metal corrosion, especially aluminium and it also decreases the flash point, cetane number and lubricity of biodiesel. Low level of contamination of biodiesel definitely gives a better engine performance (Araujo et al., 2008; Berrios and Skelton, 2008). Table 2.5 shows the negative effect of impurities on biodiesel and engines.

Table 2.5: Negative effects of impurities on biodiesel and engines (Atadashi et al., 2011).

Contaminants	Negative effect
Methanol	Deterioration of natural rubber seals and gaskets, lower flash points (problems in storage, transport, and utilization, etc.), lower viscosity and density values, corrosion of pieces of Aluminum (Al) and Zinc (Zn)
Water	Reduces heat of combustion, corrosion of system components (such as fuel tubes and injector pumps) failure of fuel pump, hydrolysis (FFAs formation), formation of ice crystals resulting in gelling of residual fuel, Bacteriological growth causing blockage of filters, and Pitting in the pistons
Catalyst/soap	Damage injectors, pose corrosion problems in engines, plugging of filters and weakening of engines less oxidation stability, corrosion of vital engine components
Free fatty acids (FFAs)	Crystallization, turbidity, higher viscosities, and deposits formation at pistons, valves and injection nozzles
Glycerol	Decantation, storage problem, fuel tank bottom deposits Injector fouling, settling problems, higher aldehydes and acrolein emissions, and severity of engine durability problems.

2.8.1 Polymeric membranes

For biodiesel separation processes, membrane separation technology offered promising results in the biodiesel purity as high as 90 % or above (Cao et al., 2008; He et al., 2006). Lately, polymeric and ceramic membranes are commonly used in membrane separation technology. Ceramic membrane gave the promising result in glycerol and oil rejection (Cao et al., 2008; Gomes et al., 2010; Low and Cheong, 2009). Unfortunately, ceramic membrane is not economically feasible because the cost of the membrane is more expensive than polymeric membrane (Van Hoof et al., 2006). Presently, the use of polymeric membrane is common in biodiesel purification as polymeric membrane contains good mechanical and thermal stability, good chemical resistance to aliphatic hydrocarbons, alcohols and acids (Zhang et al., 2012). Many researchers highlighted the benefits of polymeric membranes for biodiesel separation from different types of oil feedstocks (He et al., 2006; Saleh et al., 2010; Low et al., 2011; Rios et al., 2011).

The types of polymeric membrane used in biodiesel production include polyacrylonitrile (PAN), polyethersulfone (PES), polyvinylidene fluoride (PVDF), polytetrafluoroethylene (PTFE), polypropylene, polysulfone (PSU) and cellulose acetate (Saleh et al., 2010; Mah et al., 2012; He et al., 2006; Low and Cheong, 2009). The polymeric membranes can be categorized into microfiltration, ultrafiltration and nanofiltration polymeric membranes (Low et al., 2009; Othman et al., 2010; Low et al., 2011). Hydrophilic 0.05 µm PAN membrane, hydrophobic 0.2 µm polypropylene and 0.2 µm PVDF, 0.45 µm polysulfone and 0.2 µm polyethersulfone were used for the biodiesel purification. The hydrophilic PAN ultrafiltration membrane was good

to retain biodiesel, but the membranes performance degraded due to fouling. The soap deposited on membrane caused the fouling effect on the membrane. Milky soap emulsions with thin layer of oil were found at the hydrophobic polypropylene and PVDF microfiltration membranes. The microfiltration PSU with large pore size, 0.45 µm produced a significant layer of oil with a thick milky soap emulsion. The PSU and mixed cellulose acetate showed good soap rejection and allowed the water and biodiesel passed through the membranes. Pre-filtration step prior to biodiesel purification process could prevent the clogging of the polymeric membrane from the biodiesel impurities (Low et al., 2009).

In a study by Low et al. (2011), a flat ultrafiltration PTFE membrane of 0.05 µm and a flat microfiltration mixed cellulose acetate (MCA) membrane of 0.45 µm were utilized to improve biodiesel purity and water consumption. PTFE membrane had better water rejection than MCA membrane due to its hydrophobicity nature of the membrane. However, both PTFE and MCA membranes presented good permeation for biodiesel. PTFE and MCA membranes are hydrophilic and hence biodiesel as permeate can pass through both membranes rapidly. The increased transmembrane pressure (TMP) is able to decrease the moisture content in biodiesel when using PTFE membrane and MCA membrane as separators. Compared to MCA membrane, PTFE membrane could provide better permeate flux and surfactant (biodiesel and catalyst) rejection due to its natural properties of the membrane.

In a study by He et al. (2006), the performance of a novel membrane extraction was compared with three traditional extraction methods of distilled water washing, acid washing, and solvent extracting. Two types of polymeric hollow fiber membranes polysulfone (PSU) and polyacrylonitrile (PAN) were used in the study. PSU hollow fiber was not suitable for biodiesel separation because the water content in biodiesel of 0.107 wt % was higher than the ASTM and EN standards (0.05 wt %) for biodiesel content. On the other hand, PAN hollow fiber membrane exhibited the promising results with the highest biodiesel yield of 99 %. In addition to this, the density, viscosity, water content and acid value of biodiesel purified using PAN hollow fiber membrane accorded with the standards.

In a study by Othman et al. (2010), eight types of commercial polymeric solvent resistant nanofiltration (SRNF) membranes were selected and sifted for the separation of methyl ester-rich effluent (biodiesel) from the mixture of the homogeneous catalyst, free glycerin and excess methanol. Biodiesel was obtained from the transesterification of refined, bleached and deodorized (RBD) palm olein and anhydrous methanol by the aid of strong base catalyst, sodium hydroxide. The effect of applied pressure from 600 to 3000 kPa and the effect of temperature from 28 to 60 ^{o}C were tested on eight types of SRNF membranes. Pure water and methanol permeation flux were examined and the results showed that no water and methanol were obtained due to the hydrophobicity nature of the membranes. The breakage of membranes and the increased in permeation flux were observed at the end of separation process. One of the membranes revealed the highest rejection to triglycerides (TG) (99.80 %), diglycerides (DG) (97.16 %), monoglycerides (MG)

(40.65 %), free glycerin (75.24 %), ester (25.37 %) and methanol (74.98 %). The transesterification products with the pH of 8.68 enhanced the membrane performance and had much less effects on the morphological structure of the membranes.

2.8.2 Effect of parameters on membrane performance

The membrane performance for biodiesel separation process can be measured by the volume flux of permeate which is defined as the permeate flow rate per unit area of membrane. The magnitude of membrane permeability is generally affected by membrane composition, temperature, pressure, velocity of flow and interaction between components of the feedstocks with membrane surface (Atadashi et al., 2011).

In addition, the effects of methanol to oil ratio, catalyst concentration, pH value, membrane pore size and thickness are the other parameters that would affect the performance of the membrane (Shuit et al., 2012). Polymeric membranes used in biodiesel purification was characterized from the membrane thermal stability, mechanical properties, fouling effect, surface and cross-sectional morphologies, membrane functional groups, contact angle measurement and surface charge (Amin et al., 2010; Sarkar et al., 2010).

The control of pressure is a key factor for the good performance of membrane during separation. Low pressure will prevent the organic solvent (methanol) intruding into the pores of hydrophilic polymeric membrane. Higher pressure creates greater forces that allow more organic solvents entering the membrane pores. The

viscosity of biodiesel may cause the alternation of pressure and the flow rate of permeate is then affected during the separation process (Araujo et al., 2008).

The trans-membrane pressure (TMP) is linearly proportional to the permeation flux during the biodiesel separation. When the TMP increases, the permeation flux is increased as well (Othman et al., 2010). The pressure difference between the feed side and permeate side of the membrane, is also known as trans-membrane pressure (TMP). The contact angle of fluids on the membrane will affect the magnitude of TMP. The fluids needs greater force to enter the more hydrophobic membrane pores. The TMP creates forces which allowing the methyl ester to pass through the membrane pore. The increase of TMP also reduces the moisture content inside the biodiesel. Higher TMP causes the soap passing through the membrane and finally altered the pH (Low et al., 2011).

In this study, two types of polymeric membranes (PES and PVDF) were screened under different of transmembrane pressure (1 to 5 bar) and the membrane molecular weight cut-off (5, 20, 30 and 100 kD).

2.9 Concluding remark

Based the literature review, three types of catalyst (Al_2O_3-SO_3H, SiO_2-SO_3H, and TiO_2-SO_3H) were selected for the study to screen for the most promising catalyst support for biodiesel production. The types of catalyst supports, immersion time (6 h, 12 h and 18 h) and acid concentration (2M, 3M, 4M and 5M) were optimized by employing response surface methodology (RSM) with a full factorial experiment design. All the catalyst supports were underwent characterization of SEM, EDX, BET, FTIR, XRD and ICP-OES. For the biodiesel purification, the polymeric membranes of polyethersulfone (PES) at 5 and 20 KD and polyvinylidene fluoride (PVDF) at 30 and 100 kD were used to purify biodiesel at different transmembrane pressure (1 to 5 bar).

CHAPTER 3

METHODOLOGY

3.1 Project work flow

In the present study, biodiesel has been successfully produced from a low cost feedstock which is PFAD using three types of catalyst (Al_2O_3-SO_3H, SiO_2-SO_3H and TiO_2-SO_3H). These catalysts were prepared by sulfonating aluminium oxides, titanium (IV) oxides and silicon dioxides with sulphuric acid. All the catalysts used were characterized by analytical equipment such as SEM, EDX, BET, FTIR, XRD and ICP-OES. The corresponding catalytic activity on esterification of PFAD had been tested. The effects of types of catalyst support, immersion time of catalyst support in the sulphuric acid and acid concentration on the catalyst performance were studied. These parameters were then optimized by using response surface methodology (RSM). For the study of biodiesel purification, the effects of types of membrane (polyethersulfone (PES) and polyvinylidene fluoride (PVDF)) molecular weight cut-off (5 and 20 kD of PES, and 30 and 100 kD of PVDF) with different transmembrane pressure (1 to 5 bar) on membrane performance were investigated using the membrane stirred cell. The performance of polymeric membranes was measured based on the volume flux of permeate after the biodiesel separation process.

Stage 1: Catalyst Screening
To screen for the most promising catalyst support for biodiesel production:
Type of catalyst: Al_2O_3-SO_3H, SiO_2-SO_3H, and TiO_2-SO_3H
Weight: 10 g of catalyst powder
Temperature: 80 ^oC
Acid concentration: 5 M
Immersion time: 18 hours
Stirring speed: 800 rpm
Calcination process: with (550 ^oC and 4 hours) and without

Stage 2: Optimization study
Optimization study on the parameters related to the catalyst development stage:
Parameters studies:
- Acid concentration: 2 M, 3 M, 4 M and 5 M
- Immersion time: 6 h, 12 h and 18 h

Software used: Design Expert Version 9.0
Method: Response surface methodology (RSM) analysis
Designed experiment: Full factorial experiment

Stage 3: Catalyst Characterization
All the catalyst supports developed at Stage 1 and Stage 2 were underwent characterization:
Characterization techniques:
- SEM, EDX, BET, FTIR, XRD and ICP

Stage 4: Biodiesel Purification
To screen the polymeric membranes used for the biodiesel purification:
Types of polymeric membrane: PES and PVDF
Molecular weight cut-off (MWCO) of polymeric membranes: 5 and 20 kD of PES, and 30 and 100 kD of PVDF.
Transmembrane pressure: 1 to 5 bar

PFAD esterification:
Reaction temperature: 80 ^oC
Methanol to oil mole ratio: 20:1
Weight: 2 (wt/wt)%
Stirring speed: 800 rpm
Reaction time: 6 hours

3.2 Materials

All the chemicals and gases used in the project with the respective purity and brands are shown in Table 3.1.

Table 3.1: List of chemicals and gases.

Chemicals	**Brand**
Palm Fatty Acid Distillate	PGEO Edible Oils
Amorphous Aluminium Oxide	Merck
Amorphous Titanium (IV) Oxide	Sigma-Aldrich
Silicon Dioxide	Gene Chemistry
Sulphuric acid	Merck
Methanol	Fisher Scientific
Hexane	Merck
Nitric acid	Merck
Methyl Heptadecanoate	Sigma-Aldrich
Methyl Palmitate	Sigma-Aldrich
Methyl Oleate	Sigma-Aldrich
Methyl Linoleate	Sigma-Aldrich
Methyl Stearate	Sigma-Aldrich
Gases	
Purified Nitrogen, N_2	Linde Malaysia
Purified Helium, He	Linde Malaysia
Purified Argon, Ar	Linde Malaysia

3.3 Equipment

The main equipment used in the project for sample analysis and catalyst characterization are shown in Table 3.2.

Table 3.2: List of main equipment used.

Instrumentation	Brand	Model
Scanning electron microscope (SEM) and Energy dispersive X-ray (EDX)	Hitachi	S3400N
Brunauer-Emmett-Teller (BET)	Thermo Scientific	Finnigan Sorptomatic 1990
Inductively Coupled Plasma-Optical Emission Spectrometer (ICP-OES)	Perkin Elmer	*Optima 2000 DV*
Fourier transform infra-red (FTIR)	Thermo Scientific	Nicolet iS10
X-ray Diffractometer (XRD)	Shimadzu	XRD-6000
Gas Chromatography (GC)	Perkin Elmer	Clarus 500

3.4 Catalyst Preparation

Catalyst sulfonation process was carried out in the 500 ml three neck round-bottom flask connected with condenser and was placed onto the heating mantle as shown in Figure 3.1. A reflux condenser was employed to condense any sulphuric acid (H_2SO_4) vapour back to reaction mixture during the reaction. A heating mantle equipped with

temperature controller and stirring speed controller was used to achieve the desired reaction temperature and stirring speed during the sulfonation process.

Figure 3.1: Apparatus setup for catalyst sulfonation.

10 g of amorphous aluminium oxide was added into 5 M of H_2SO_4 and the reaction mixture was continuously stirred at 800 rpm for 18 hours at 80 ^oC. After the sulfonation process, the resulting precipitated solid was continuously washed with the water solution to reach pH 5-6. The precipitated solid was filtered using glass filtration assembly with the aid of acid resistant pump. The solid was then dried at 100 °C for 24 hours to obtain the sulfonated solid acid catalyst for biodiesel production. Figure 3.2 shows the setup of lab glass filtration assembly for the catalyst filtration purpose. For the study of the effects of different catalyst support, all the mentioned procedures were repeated with amorphous titanium (IV) oxide and amorphous silicon dioxide.

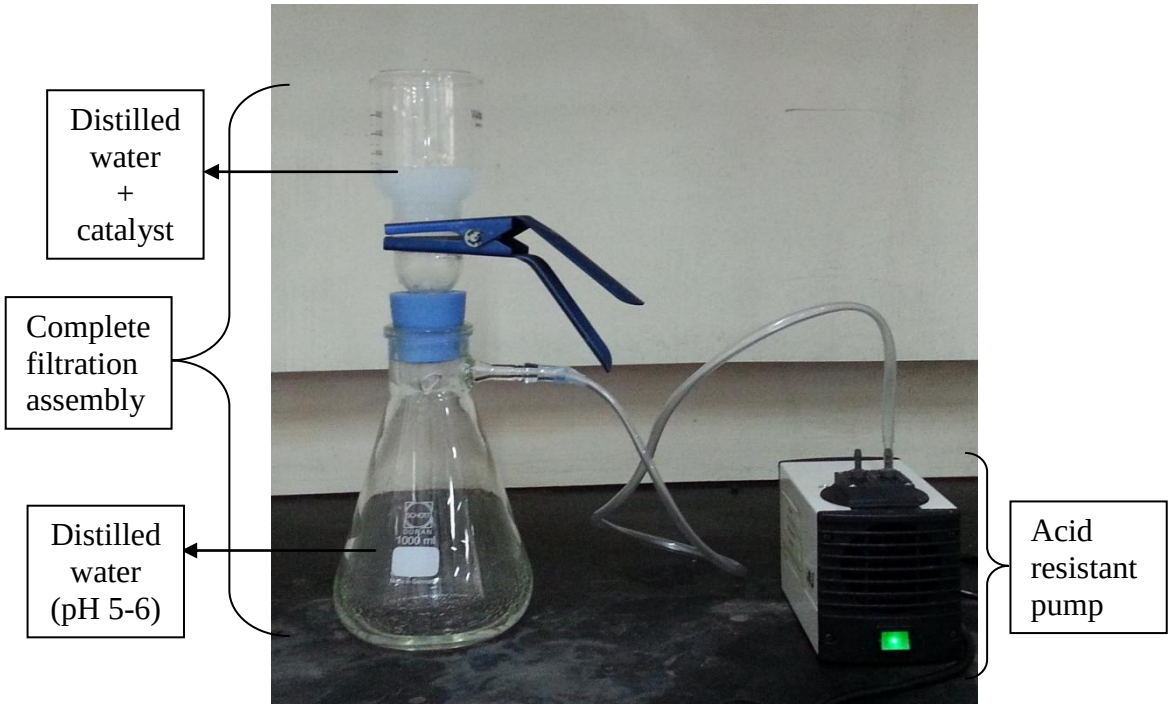

Figure 3.2: Apparatus setup for filtration process.

3.5 Catalyst Calcination

The sulfonated aluminium oxide catalyst prepared earlier in Section 3.4 was calcined in a furnace at temperature of 550 ^{o}C for duration of 4 hours. During calcination process, the catalyst was placed on combustion boat with constant flow of nitrogen gas. The same calcination procedures were applied again for the sulfonated titanium (IV) oxide and sulfonated silicon dioxide catalysts. Figure 3.3 depicts the preparation stages of calcined catalysts.

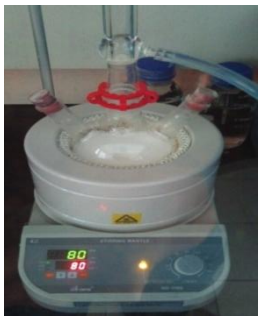

Step 1: Sulfonation process

5 M of H_2SO_4 solution mixed with 10 g of catalyst support (Al_2O_3, TiO_2, SiO_2) at temperature of 80 ^oC under agitation speed of 800 rpm.

Step 2: Filtration

Acid resistant pump was connected to complete filtration assembly for catalyst filtration.

Step 3: Drying

The catalyst was dried at temperature of 100 ^oC for 24 hours.

Step 4: Calcination

The catalyst was calcined in a furnace at temperature of 550 ^oC for duration of 4 hours.

Figure 3.3: Preparation stages of calcined catalysts.

3.6 Esterification of PFAD

The esterification of PFAD was carried out at reaction temperature of 80 ºC with 2 wt% of catalyst and methanol to PFAD molar ratio of 20:1. The reaction was operated at 800 rpm of agitation speed for 6 hours (Kartika et al., 2013; Park et al., 2008). The sample was taken for biodiesel analysis continuously for the duration of 6 hours with 1 hour interval time. The operating conditions for PFAD esterification are shown in the Table 3.3. The samples were filtered and underwent GC analysis for biodiesel yield measurements. The detail of GC analysis for biodiesel is available in Section 3.9.1.

Table 3.3: Reaction Conditions.

Parameters	Operating conditions
Methanol to PFAD Molar Ratio	20:1
Amount of Catalyst (Catalyst/PFAD), wt%	2
Reaction Temperature, T (°C)	80
Stirring Speed (rpm)	800

3.7 Catalyst Screening

Three types of catalyst supports: aluminium oxide, titanium (IV) oxide and silicon dioxide were used in the study. The catalyst with good catalyst performance was screened based on the maximum biodiesel yield obtained at the shortest reaction time.

3.7.1 Effects of different types of uncalcined catalysts

Three different types of solid acid catalysts were developed: 1) aluminium oxide, 2) silicon dioxide and 3) titanium (IV) oxide. The catalysts were used to catalyze the esterification of PFAD without calcination treatment. The good catalyst performance was based on the maximum biodiesel yield obtained at the shortest reaction time. The most efficient catalyst will be used in the subsequent study. The catalyst were prepared and calcined according to the methods described in Section 3.4 and 3.5. The esterification reaction of PFAD was carried out according to the methods described in Section 3.6.

3.7.2 Effects of different types of calcined catalysts

Three different types of solid acid catalysts were developed: 1) aluminium oxide, 2) silicon dioxide and 3) titanium (IV) oxide. The catalysts were calcined prior to be used in the esterification of PFAD. The good catalyst performance was based on the maximum biodiesel yield obtained at the shortest reaction time. The most efficient catalyst will be used in the subsequent study. The catalyst were prepared and calcined according to the methods described in Section 3.4 and 3.5. The esterification reaction of PFAD was carried out according to the methods described in Section 3.6.

3.7.3 Optimization study

In this study, the different types of catalysts were screened for the most efficient catalyst through RSM. A full factorial experiment design with two factors, types of catalyst and reaction time which were denoted as factors A and B, respectively was used in the study. Experimental design with a total of 21 experimental runs which consists of three different types of catalyst (Al_2O_3-SO_3H, SiO_2-SO_3H, and TiO_2-SO_3H), seven levels of reaction time ranging from 0 to 6 hours with intervals of 1 hour was shown in Table 3.4. In the study, biodiesel yield was the dependent response. The best performance of catalyst was optimized based on the maximum biodiesel yield achieved at minimum reaction time. Table 3.5 summarizes the independent factors with their respective high and low limits studied levels for the study.

The software Design Expert Version 9.0 (Stat Ease Inc., MN, USA) was employed for statistical analysis and regression model building.

Table 3.4: Experimental design and the respective biodiesel yield.

Run	Factor A	Factor B
	Catalyst	*Reaction Time (minutes)*
1	Al_2O_3-SO_3H	0.00
2	Al_2O_3-SO_3H	60.00
3	Al_2O_3-SO_3H	120.00
4	Al_2O_3-SO_3H	180.00
5	Al_2O_3-SO_3H	240.00
6	Al_2O_3-SO_3H	300.00
7	Al_2O_3-SO_3H	360.00
8	SiO_2-SO_3H	0.00
9	SiO_2-SO_3H	60.00
10	SiO_2-SO_3H	120.00
11	SiO_2-SO_3H	180.00
12	SiO_2-SO_3H	240.00
13	SiO_2-SO_3H	300.00
14	SiO_2-SO_3H	360.00
15	TiO_2-SO_3H	0.00
16	TiO_2-SO_3H	60.00
17	TiO_2-SO_3H	120.00
18	TiO_2-SO_3H	180.00
19	TiO_2-SO_3H	240.00
20	TiO_2-SO_3H	300.00
21	TiO_2-SO_3H	360.00

Table 3.5: Independent Factors and the Corresponding Levels for Experimental Data

Factor	Factor code	Unit	Factor type	Factor level	Study Level
Catalyst	A	-	Categorical	3	Al_2O_3-SO_3H,SiO_2-SO_3H,TiO_2-SO_3H
Reaction time	B	(hour)	Numeric	7	0,1,2,3,4,5 and 6

3.7.4 Comparison between calcined catalysts and uncalcined catalysts in producing biodiesel

Esterification of PFAD to biodiesel was catalyzed with calcined catalysts (Al_2O_3-SO_3H, SiO_2-SO_3H, and TiO_2-SO_3H) and uncalcined catalysts (Al_2O_3-SO_3H, SiO_2-SO_3H, and TiO_2-SO_3H). The efficiency of calcined catalysts were compared with uncalcined catalysts in producing biodiesel to examine the necessity of calcinations treatment. The best catalyst was selected based on the maximum biodiesel yield achieved at minimum reaction time.

3.8 Effect of preparation conditions

In the study of the effects of immersion time and acid concentration on biodiesel production, the same procedures were repeated with varied immersion time of 6 hours, 12 hours and 18 hours and with varied acid concentration of 2M, 3M, 4M and 5M.

3.8.1 Effects of preparation conditions: Acid concentration

In the study of the effects of acid concentration on biodiesel yield, the best catalyst determined in Section 'Catalyst Screening' was immersed in the 2M, 3M, 4M and 5M sulphuric acid solution for 6 hours, 12 hours and 18 hours. The catalyst was prepared according to the catalyst preparation method described in Section 3.4. The prepared catalyst was used to catalyze esterification reaction according to the method

in Section 3.6. The optimum acid concentration used in catalyst preparation was based on the catalyst that would result in maximum biodiesel yield.

3.8.2 Effects of preparation conditions: Immersion time

In the study of the effects of immersion time on biodiesel yield, the best catalyst determined in Section 'Catalyst Screening' was immersed in the 2M, 3M, 4M and 5M sulphuric acid solution for 6 hours, 12 hours and 18 hours. The catalyst was prepared according to the catalyst preparation method described in Section 3.4. The prepared catalyst was used to catalyze esterification reaction according to the method in Section 3.6. The optimum acid concentration used in catalyst preparation was based on the catalyst that would result in maximum biodiesel yield.

3.8.3 Optimization Study

In this study, the parameters related to preparation condition: immersion time and acid concentration were optimized via RSM with the aid of Design Expert Version 9.0 (Stat Ease Inc., MN, USA). A full factorial experiment design with three factors, immersion time, acid concentration and reaction time which were denoted as factors A, B and C respectively was used in the study. Experimental design with a total of 84 experimental runs consists of three levels of immersion time (6h, 12h and 18h), four levels of acid concentration (2M, 3M, 4M and 5M) and seven levels of reaction time (ranging from 0 to 6 hours). In the study, biodiesel yield was the dependent response. The optimum immersion time and acid concentration used during catalyst

preparation stage was based on the maximum biodiesel achieved at minimum reaction time. Table 3.6 summarizes the independent factors with their respective high and low levels for the study.

Table 3.6: Independent Factors and the Corresponding Levels for Experimental Data

Factor	Factor code	Unit	Factor type	Factor level	Study level
Immersion time	A	hours	Numeric	3	6, 12 and 18
Acid concentration	B	Molar	Numeric	4	2, 3, 4 and 5
Reaction time	C	hours	Numeric	7	0, 1,2,3,4,5 and 6

3.9 Catalyst Characterization

Throughout the study, a number of characterization techniques were used to examine the physical and chemical properties of the catalysts produced. The characterization techniques used includes Scanning Electron Microscope (SEM), Energy Dispersive X-ray (EDX), Brunauer-Emmett-Teller (BET), Inductively Coupled Plasma-Optical Emission Spectrometer (ICP-OES), Fourier Transform Infra-Red (FTIR) and X-ray Diffraction (XRD).

3.9.1 Scanning Electron Microscopy (SEM)

Scanning electron microscopy (SEM) analyses were done by using a Hitachi S3400N scanning electron microscope (Figure 3.4), under accelerating voltage of 15 kV. The magnification of SEM images for the catalyst supports was 10000. A small amount of fresh catalyst was placed on the surface of a carbon tape, which had been fixed on an aluminium holder (diameter 15 mm). Then the catalysts were coated with palladium and gold using Sputter Coater machine.

Figure 3.4: Hitachi S-34000N Scanning Electron Microscope coupled with Ametek EDX

3.9.2 Energy Dispersive X-ray (EDX)

Energy dispersive x-ray spectroscopy analysis was carried out using Hitachi S-3400N Scanning Electron Microscope under accelerating voltage of 15 kV. The magnification of SEM images for the catalyst supports was 500. Energy-dispersive X-ray (EDX) analyses were carried out by using EDAX software.

3.9.3 Brunaur-Emmett-Teller (BET) Surface Area Measurement

The Brunauer-Emmett-Teller (BET) surface area analysis involves the nitrogen adsorption-desorption at low temperature (77 K), has been used for the determination of the total specific surface area and porosity of catalysts. This was done by using a Thermo Finnigan Sorptomatic 1990 nitrogen adsorption-desorption analyzer (Figure 3.5).

Figure 3.5: Thermo Finnigan Sorptomatic 1990.

3.9.4 Inductively Coupled Plasma-Optical Emission Spectrometer (ICP-OES)

The bulk chemical composition was determined by using a sequential scanning inductively coupled plasma-optical emission spectrometer (ICP-OES) Perkin Elmer Optical Emission Spectrometer Optima 7000 DV (Figure 3.6). 0.025 g of sample catalyst was digested with slight heating and continuous stirring in 10 mL of 8 M nitric acid. The standard solutions of sulphur were prepared in concentrations of 0.625, 1.25, 2.5, 5 and 10 ppm, respectively. Deionised water was used as a blank control solution. All the solutions prepared were added with 10 mL of 8 M HNO_3 in order to be consistent with the sample solutions.

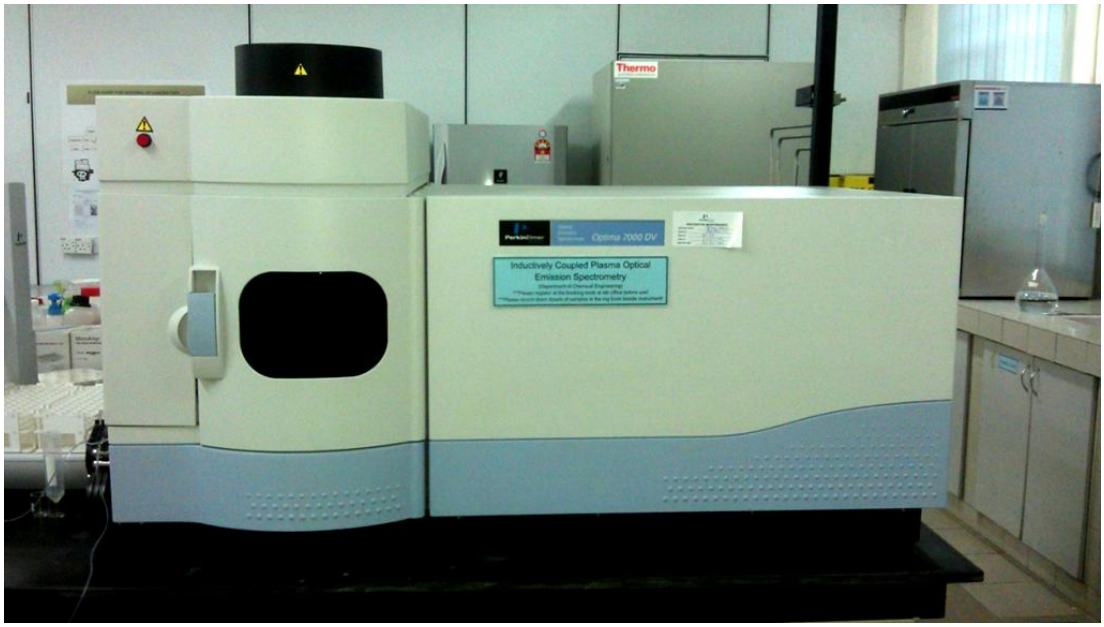

Figure 3.6: Perkin Elmer Optima 7000 DV optical emission spectrometer

3.9.5 Fourier Transform Infra-Red (FTIR)

The analyses were done by using Thermo Scientific Nicolet iS10 FTIR (Figure 3.7). As with all FTIR measurement, an infra-red background is collected from the clean diamond crystal. The FTIR spectrum is ranging from 400- 4000 wave number. The infra-red spectrum of catalyst was acquired from the computer with the OMNIC software.

Figure 3.7: Thermo Scientific Nicolet iS10 FTIR.

3.9.6 X-ray Diffraction (XRD) Analysis

X-Ray Diffraction (XRD) analysis (Figure 3.8) relies on the dual wave or particle nature of X-Rays to obtain information about the structure of crystalline materials. The sample was prepared for analysis by compressing a small amount of sample into the sample holder. The sample was scanned from 2 to 80 degree.

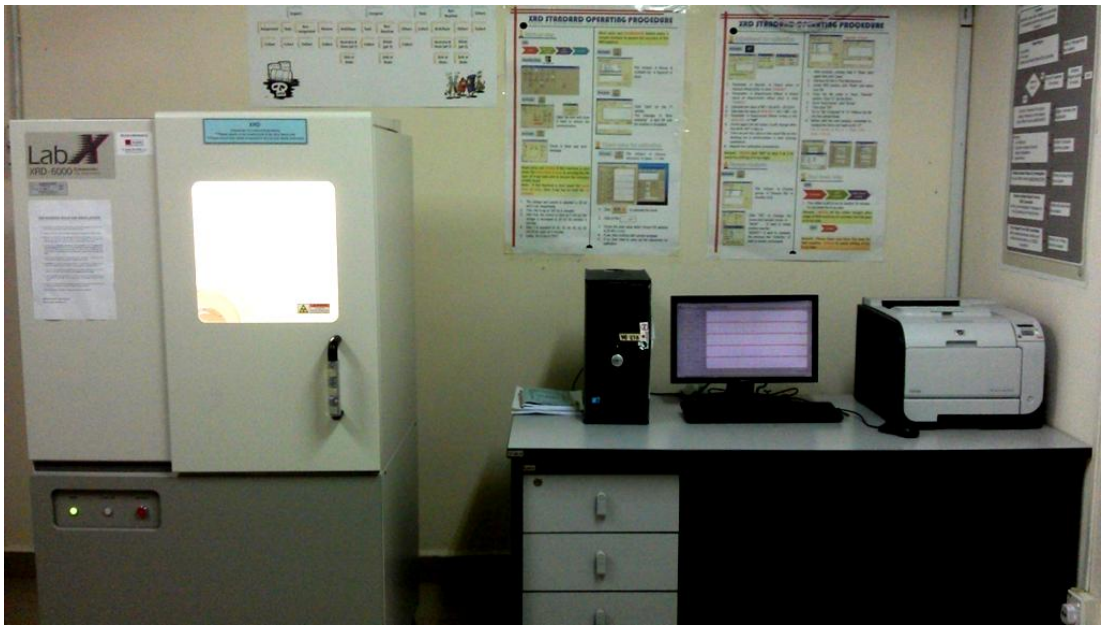

Figure 3.8: Shimadzhu diffractometer Model XRD-6000

3.9.1 Biodiesel anaylsis

The biodiesel sample collected was collected and analyzed by using Gas Chromatography (Perkin Elmer Clarus 500) (Figure 3.9). The GC is equipped with a capillary inlet (on column mode) and an Flame Ionization detector (FID). The capillary column used to detect biodiesel was Zebron^{TM} ZB-FFAP with dimensions 60 m x 0.25 mm x 0.25 μm (Phenomenex, USA). Helium was used as carrier gas with 2.00 mL/min. oven temperature was held at 110 ^{o}C for 5 minutes and then heated at a rate of 10 ^{o}C/ minute to 190 ^{o}C. Temperature of injector and detector was maintained at 250 ^{o}C. One microlitre (1 μL) of the diluted sample was injected into the GC column for analysis. The retention time for different types of biodiesel

content is determined from the GC calibration curve and tabulated into Table 3.7. The biodiesel yield was calculated based on the formula as shown below (2).

$$n_{FAME}=\sum \frac{Ra}{Rs} \text{ X } C_E \text{ x DF x } V_{PFAD} \quad (2)$$

where R_a is the ratio between the areas under curve of methyl esters to the area under curve of methyl heptadecanoate obtained from sample. R_s is the ratio between the areas under curve of methyl esters to the area under curve of methyl heptadecanoate obtained from standard. Methyl esters includes methyl palmitate, methyl oleate, methyl stearate, methyl linoleate. On the other hand, C_E represents the methyl ester concentration in internal standard, DF is the dilution factor $(V)_{sample}$ indicates the total volume. The biodiesel derived from free fatty acid: palmitic acid (44.56 %), oleic acid (34.75 %), stearic acid (3.43 %) and linoleic acid (6.62 %).

Table 3.7: Retention time for different types of biodiesel content.

Component	Molecular Weight (g/mol)	Retention Time (min)
Methyl Palmitate	270.45	13.24
Methyl Heptadecanoate (IS)	284.48	15.85
Methyl Sterate	298.50	18.99
Methyl Oleate	296.49	20.10
Methyl Linoleate	294.47	21.96

Figure 3.9: Perkin Elmer Clarus 500 Gas Chromatography.

3.10 Biodiesel Purification using Polymeric membrane

The polymeric membranes, polyethersulfone (PES) and polyvinylidene fluoride (PVDF) were used to purify the biodiesel mixture with a membrane stirred cell. Figure 3.10 illustrates the configuration of a HP4750 stirred cell system. A circular membrane disk with a diameter of 0.049 m (49 mm) was placed at the bottom of the filtration module. The membrane was installed with active top layer towards the feed solution. The membrane was sealed between a Teflon O-ring and a stainless steel porous support. In this way, the membrane surface has an active area of 0.00146 m^2 (14.6 cm^2). The Teflon coated magnetic stirrer was used to agitate the biodiesel mixtures. The maximum volume capacity of the cell is 0.3 L and the maximum operating pressure is 69 bar. The membrane stirred cell was supplied by an inert gas (N_2) for the pressure at the feed side. The operating pressure was regulated by a

nitrogen gas regulator from 1 bar to 5 bar. The analyzed pressure range were chosen based on preliminary tests in which suitable permeate fluxes were observed. The molecular weight cut-off and operating pressure are listed in Table 3.8.

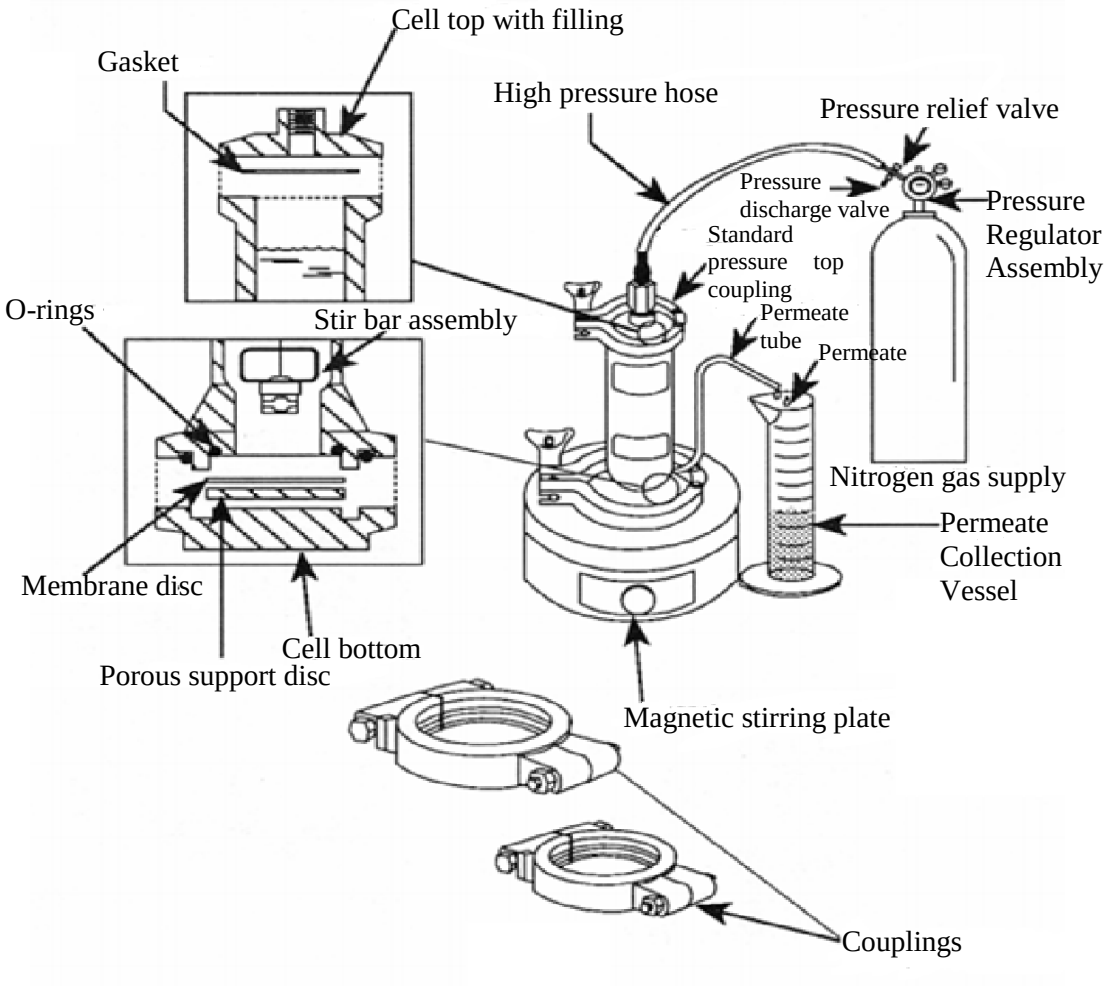

Figure 3.10: Configuration of a stirred cell system.

The study of effects of types of membrane, operating pressure and pore size were carried out using the membrane stirred cell. The performance of polymeric membranes was examined after the esterification reaction product separation prior to identifying any change on the volume flux of permeate. The volume flux of permeate is defined as ($m^3m^{-2}s^{-1}$):

$$J = \frac{\upsilon}{A\Delta t} \quad (1)$$

where J ($m^3m^{-2}s^{-1}$) is the permeate flux, υ (m^3)) is the permeate volume and t(s) is the separation time.

Table 3.8: Types of membranes used in biodiesel purification with different molecular weight and operating pressure.

Type of membrane	Molecular weight cut-off, kDa	Pressure, bar
PES	5	5
	20	3
PVDF	30	2
	100	1

The polymeric membranes were cut into circular shape with a diameter of 49 mm. After that, the polymeric membranes were soaked in deionised water for one day and then rinsed with methanol. The membrane stirred cell was filled with 100 ml of biodiesel mixture for every permeation experiment. The volume of permeate was recorded every 10 minutes for one hour. The biodiesel samples were collected every 10, 30 and 60 minutes for GC analysis. The composition of biodiesel reaction mixture before and after separation can be found in Chapter 4.

CHAPTER 4

RESULTS AND DISCUSSION

In this section, the biodiesel yield resulted from esterification of PFAD catalyzed by different types of acid catalysts (Al_2O_3-SO_3H, TiO2-SO3H, and SiO_2-SO_3H)) was discussed. The catalyst with good performance was used in subsequent study. Besides, the selected catalyst was underwent a series of characterization methods which includes SEM, BET, EDX, ICP-OES, FTIR and XRD analysis. The effects of acid concentration and effects of immersion time of catalyst in sulphuric acid on biodiesel production were studied. The catalyst preparation conditions were optimized through statistical analysis for maximum biodiesel yield at shortest reaction time. For the downstream process, biodiesel purification via membrane process was studied by using two types of polymeric membranes with different molecular weight (PES (5 kD, 20 kD) and PVDF (30 kD, 100 kD)). The effects of different transmembrane pressure on these membrane performance was carried out.

4.1 Effect of different types of uncalcined catalysts (without calcinations treatment)

The catalytic activities of different types of catalyst (Al_2O_3-SO_3H, TiO2-SO3H, and SiO_2-SO_3H) (without undergoing calcinations treatment) on biodiesel production were investigated. The esterification of PFAD were carried out at 80 ºC reaction temperature, 2 wt% catalyst to PFAD mass ratio, 20:1 methanol to PFAD molar ratio and 360 minutes reaction time. These catalysts were analyzed by SEM, EDX and FTIR to determine the physical and chemical properties that would directly and indirectly affect the catalyst activity.

4.1.1 Scanning Electron Microscopy (SEM) Analysis

SEM analysis was used to study the surface structure and morphology of the catalysts. It was reported that catalyst which consists of a large number of pores and large pore sizes would increase the accessibility of sulphuric acid into the catalyst bulk. This is because more $–SO_3H$ functional groups will be attached to the catalyst with large number of pores to increase the catalytic activity of the catalyst (Shu et al., 2010). However, small pore size will limit the diffusion of oil molecules into the catalytic sites resulted in lower biodiesel yield (Islam et al., 2013).

The morphological structures changes of self-developed catalysts were visualized via SEM with magnification of 10,000. Figure 4.1(a) shows the images of SEM for the aluminum oxide powder. It can be seen that the original aluminium oxide exhibited a compact network structure with a small amount of pores on the

surface in Figure 4.1(a). The structure of aluminium oxide had become loosen and the amount of pores had increased after the sulfonation process as shown in Figure 4.1(b). It also can be observed that the particles had agglomerated after aluminium oxide was sulfonated.

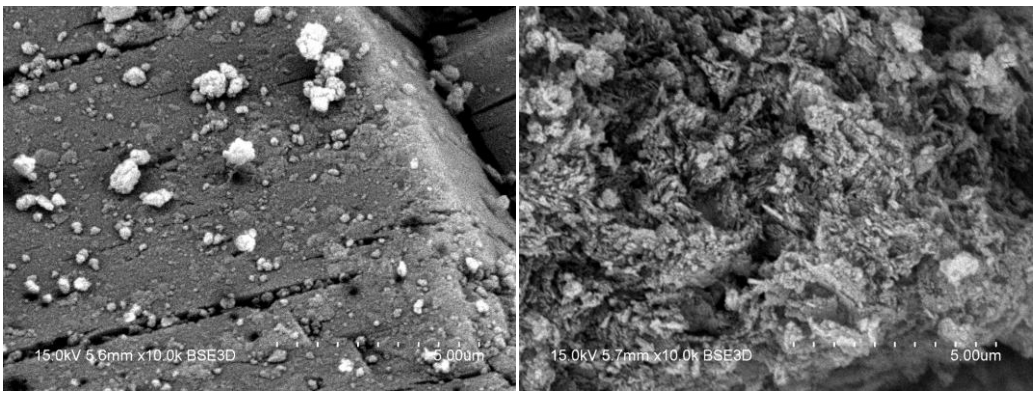

(a) (b)

Figure 4.1: SEM micrographs of (a) original Al_2O_3 and (b) sulfonated Al_2O_3.

Figure 4.2(a) and Figure 4.2(b) depict the structures of silicon dioxide in different forms which were very compact and there was no significant pore can be found on the surface. After undergoing sulfonation process, no noticeable change on the structure of silicon dioxide can be found in Figure 4.2(a). The low porosity of SiO_2-SO_3H did affect the catalytic activity on biodiesel production with low biodiesel yield. This was due to the low accessibility of reactants to the active catalytic sites of sulfonated SiO_2.

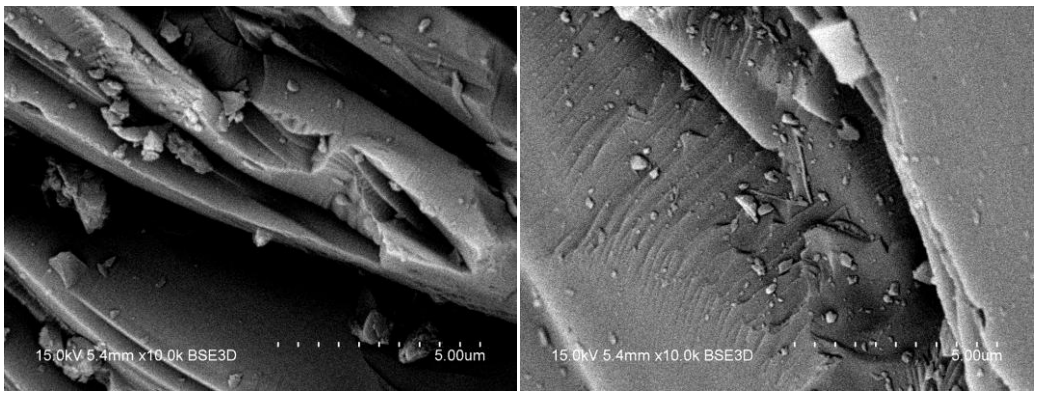

(a) (b)

Figure 4.2: SEM micrographs of (a) original SiO_2 and (b) sulfonated SiO_2.

Figure 4.3(a) and Figure 4.3(b) show the surface morphologies of titanium (IV) oxide before and after sulfonation process. The network structure of titanium (IV) oxide exhibited a less compact form compared to aluminium oxide. The titanium (IV) oxide after sulfonation process in Figure 4.3(b) did not have significant changes in morphology as silicon dioxide whereby the size of pores increased and disintegration of the particles agglomerates can be observed.

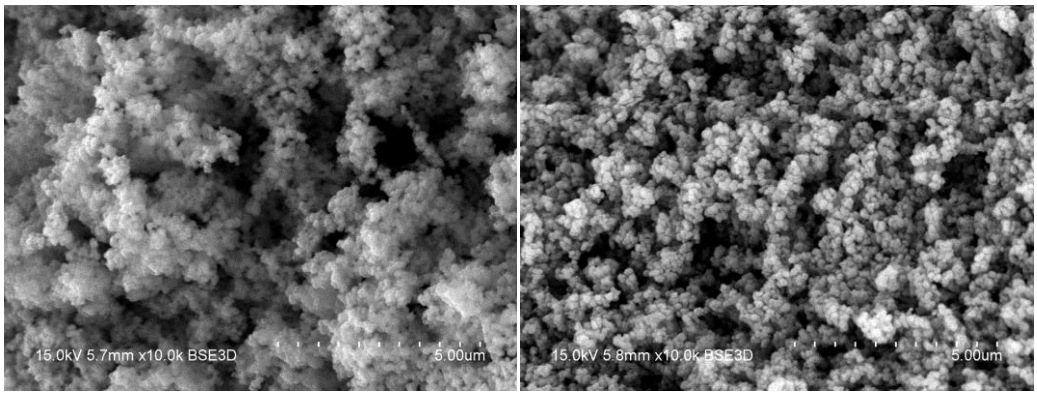

(a) (b)

Figure 4.3: SEM micrographs of (a) original TiO_2 and (b) sulfonated TiO_2.

4.1.2 Energy Dispersive X-ray (EDX) Analysis

The purpose of EDX analysis in this study was to determine the amount of sulphur contents inside each types of catalyst. Based on the EDX analysis, the elemental composition of sulphur present in each type of catalysts was summarized in Table 4.1. Appendix G shows the SEM elemental mapping of Al_2O_3-SO_3H, SiO_2-SO_3H and TiO_2-SO_3H. It was reported that all sulphur atoms in sulfonated material were present as $–SO_3H$ groups (Suganuma et al., 2008). The result showed that Al_2O_3-SO_3H contained the highest sulphur content which is 3.71 wt%. The presence of high sulphur content in Al_2O_3-SO_3H can be due to the existence of large amount of pores with large pore size which increased the accessibility of sulphuric acid into the aluminium oxide powder bulk. This catalyst would be expected to possess a higher catalytic activity for the production of biodiesel from PFAD due to its high acid site density (Shu et al., 2010). SiO_2-SO_3H and TiO_2-SO_3H have low sulphur contents. SiO_2-SO_3H had the lowest sulphur content because its morphological structure was compact and no noticeable pore appeared on the surface of the catalyst. Almeida et al. (2008) reported the specific surface area and pore specific volume of modified TiO_2 ranged from 193 to 266 m^2/g and 0.196 to 0.327 cm^3/g. TiO_2 after modified with sulphate had the low catalytic activity might be due to inadequate amount of sulphuric acid used in catalyst preparation. The pore specific volume of original powder Al_2O_3 is 0.59 cm^3/g. The pore specific volume of Al_2O_3 is larger than SiO_2-SO_3H and TiO_2-SO_3H. Therefore, the accessibility of sulphuric acid into silicon dioxide and titanium (IV) oxide were low compared to aluminium oxide.

Table 4.1: Sulphur content of catalysts examined by EDX analysis.

Types of catalyst	Sulphur content, wt%
Al_2O_3-SO_3H	3.71
SiO_2-SO_3H	0.24
TiO_2-SO_3H	0.42

4.1.3 Fourier Transform Infra-Red (FTIR) Analysis

FTIR spectra of original Al_2O_3 and Al_2O_3-SO_3H are shown in Figure 4.4(a)-(b). An obvious band was detected at 1077 cm^{-1}. The IR peak at 1077 cm^{-1} indicated the presence of SO_3 species (Park et al., 2008).. The band was typical for sulphate ions coordinated to metal oxide. This indicated the sulphuric group bounded on the surface of Al_2O_3. In Figure 4.4(b), a broad band at 3059 cm^{-1} and accompanied by a band at 1647 cm^{-1} indicated the presence of physisorbed and coordinated water (-OH group) (Park et al., 2008). The researchers had reported that the formation of –OH bonds on the surface of solid acid catalyst enhanced the catalytic activities (Chorkendorff and Niemantsverdriet, 2003).

Figure 4.5(a)-(b) and Figure 4.6(a)-(b) show the FTIR spectra of SiO_2-SO_3H and TiO_2-SO_3H. FTIR was not able to detect the bands of –OH group and sulphuric group in both of the catalysts after the sulfonation. For the FTIR analysis, there were no significant change in SiO_2-SO_3H and TiO_2-SO_3H. In conclusion, the strong interaction of sulphuric group occurred mainly with Al_2O_3.

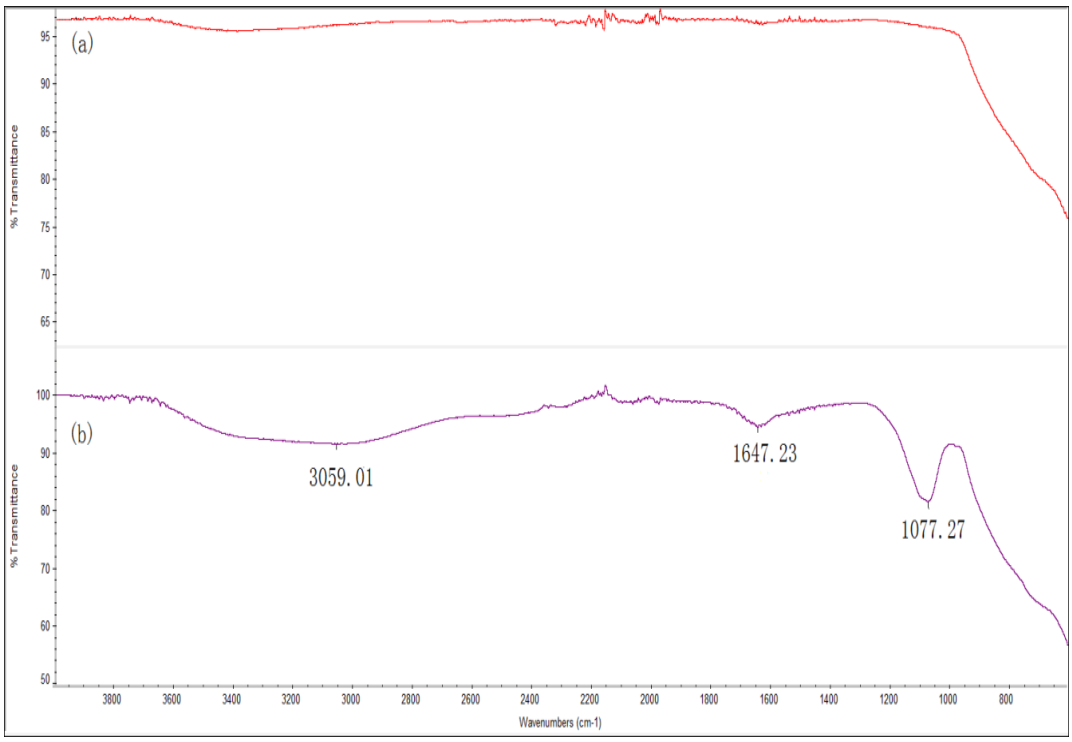

Figure 4.4: FTIR spectra of (a) originalAl_2O_3 and (b) Al_2O_3-SO_3H.

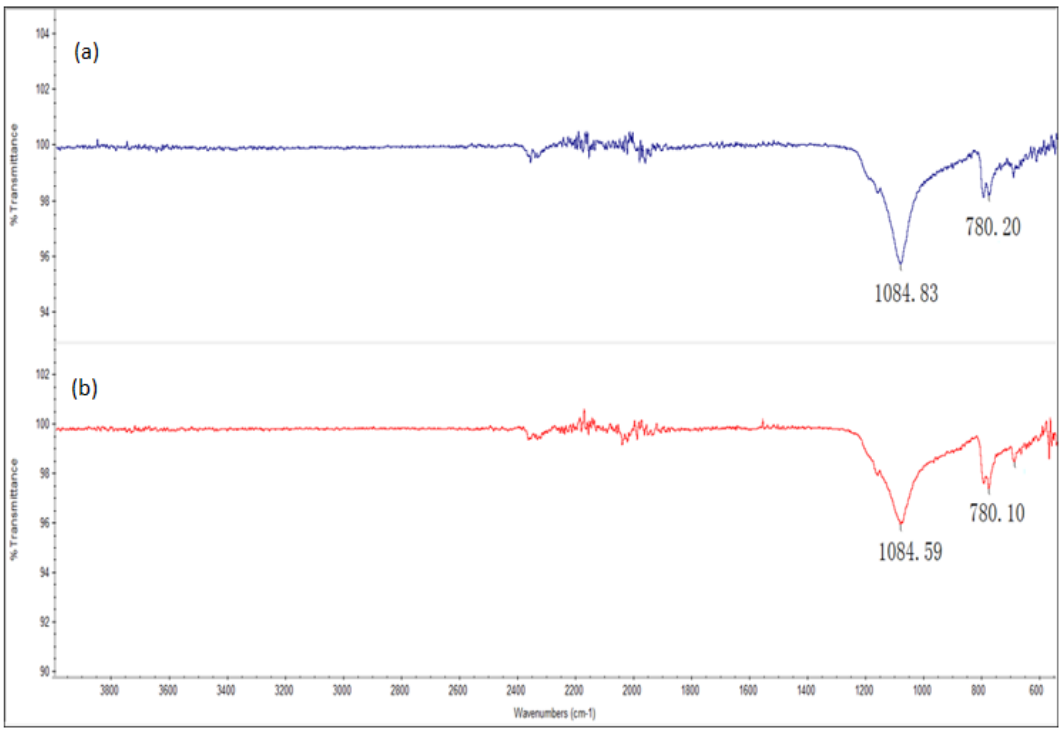

Figure 4.5: FTIR spectra of (a) original SiO_2 and (b) SiO_2-SO_3H.

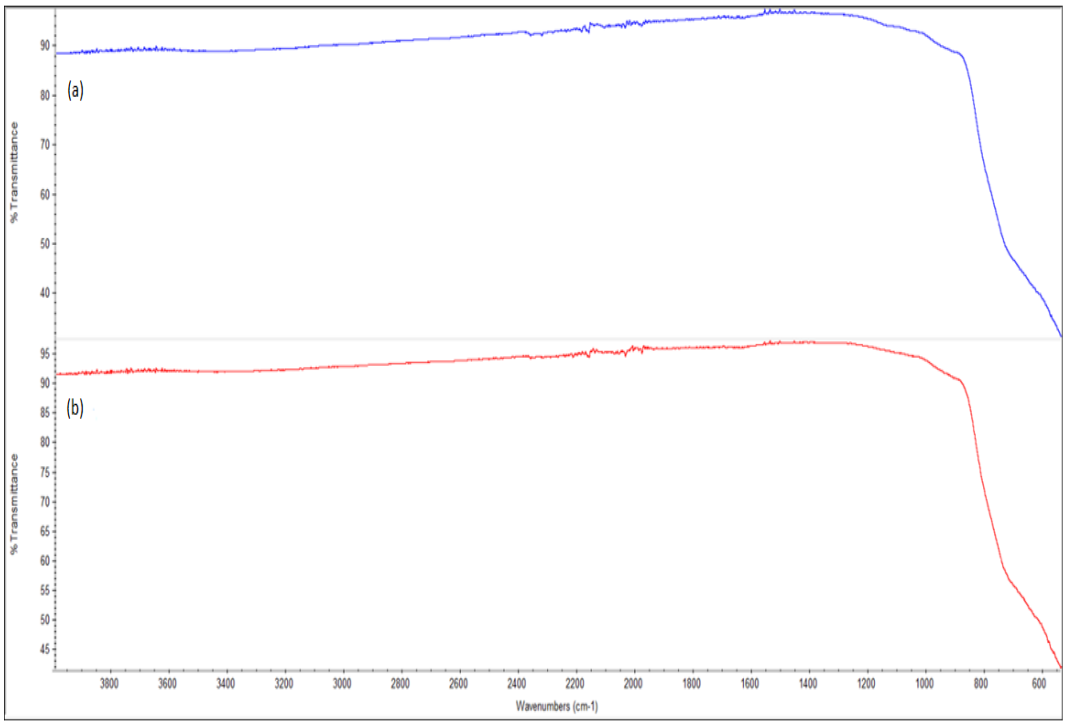

Figure 4.6: FTIR spectra of (a) original TiO_2 and (b) TiO_2-SO_3H.

4.1.4 Catalyst Screening

The catalyst with good catalytic performance was selected with the aids of statistical analysis. In this study, statistical analysis of the experimental results was performed by using Design Expert software version 9. Regression analysis was the approach used to fit the collected response data into empirical model (Montgomery, 2001). Based on the sequential model sum of squares and model summary statistics, it has suggested that cubic model fit the data better compared to linear, 2FI and quadratic models. The suggestion was focus on maximizing the R-Squared (R^2) and the Predicted R-Squared values.

Transformation of the response variable was required in order to stabilize the variance of the response and thus enhance the model fitness to the data. For the response where λ (parameter of the transformation to be determined) was close to unity, transformation was needed (Montgomery, 2001). Based on the Box-Cox diagnostics tool available in Design Expert, the response biodiesel yield was suggested to be transformed in square root form with 0.5749 as the constant k value. By doing transformation, abnormal response problems can be avoided and inequality of variance can be associated (Sim et al., 2007).

Table 4.2: Analysis of Variance for the Regression Model and Respective Model Terms.

Source	Sum of Squares	Degree of Freedom	Mean Square	F-Value	Prob> F	
Model	102.49	9	11.39	36.85	<0.0001	Significant
A	70.82	2	35.41	114.57	<0.0001	
B	18.89	1	18.89	61.12	<0.0001	
B^2	1.30	1	1.30	4.22	0.0645	
AB	6.96	2	3.48	11.25	0.0022	
B^3	1.48	1	1.48	4.78	0.0513	
AB^2	3.05	2	1.52	4.93	0.0296	
Residual	3.40	11	0.31			
Cor Total	105.89	20				

Table 4.2 presents the results of Analysis Of Variance (ANOVA) which show the levels of significance for the model and individual model terms. Based on Table 4.2, the model with Prob > F value less than 0.05 implied the model was significant. In this case, model terms A (catalyst), B (reaction time), AB and AB^2were significant model terms because both "Prob > F" for A and B were <0.0001. Although the "Prob > F" for B^2 and B^3terms were larger than 0.05, but the variables were included in the model to improve its R^2 value from 0.9416 to 0.9679.

Table 4.3: Final empirical models in actual factors.

Types of catalyst	Empirical models
Catalyst Al_2O_3-SO_3H	Sqrt(Biodiesel Yield + 0.57)=1.49894+0.053047 * Reaction Time-1.81785 $x10^{-4}$* ReactionTime^2+2.21010 x 10^{-7}* Reaction Time^3
Catalyst SiO_2-SO_3H	Sqrt(Biodiesel Yield + 0.57)= 0.68757 + 0.021919 * Reaction Time -1.24995 x 10^{-4}* Reaction Time^2 + 2.21010 x 10^{-7} * Reaction Time^3
Catalyst TiO_2-SO_3H	Sqrt(Biodiesel Yield + 0.57)= 0.47159 +0.018068 * Reaction Time -1.11216 x 10^{-4}* Reaction Time^2 +2.21010 $x10^{-7}$ * Reaction Time^3

Table 4.4: Summarization of the ANOVA for the dependent responses.

Types of transformation	Model of Hierarchy	Significant model terms	R^2	Adjusted R^2	Predicted R^2	Adequate precision
Square root	Cubic	A, B, AB, AB^2	0.9679	0.9416	0.6898	17.925

The empirical model in terms of actual factors is shown in Table 4.3. The reliability levels of the generated empirical model for the response could be verified through the values of correlation coefficient (R^2) and adequate precision. Table 4.4 shows the R^2 value of 0.9679 for this cubic model. In term of adequate precision, it measures the signal to noise ratio, a ratio greater than 4 is desirable. In this study, the adequate precision was 17.925, this indicated an adequate signal. Hence, this model can be used to navigate the design space.

The reliability of the model also can be determined from predicted versus actual plot. As shown in Figure 4.7, the experiment results were in well agreement with the predicted biodiesel yields. The normal probability plot of the residuals for the response is presented in Figure 4.8. It can be seen that the residuals were distributed near to the straight line. This indicated the underlying error distribution was normal. All the normal probability plots with sample from a normal distribution centered at zero mean that there was no severe indication of non-normality of the experimental results (Sim et al., 2007).

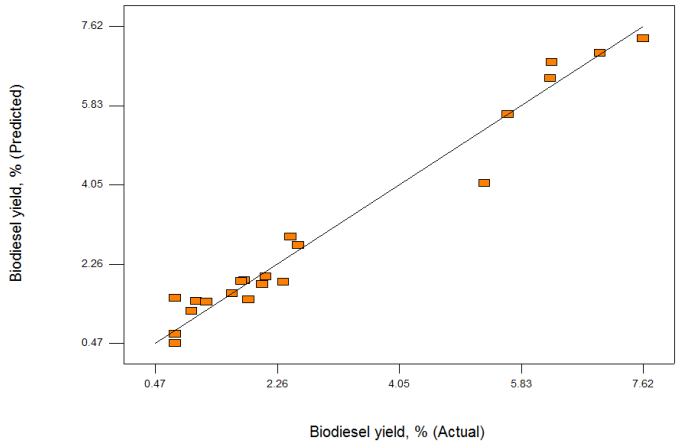

Figure 4.7: Predicted versus actualbiodiesel yield.

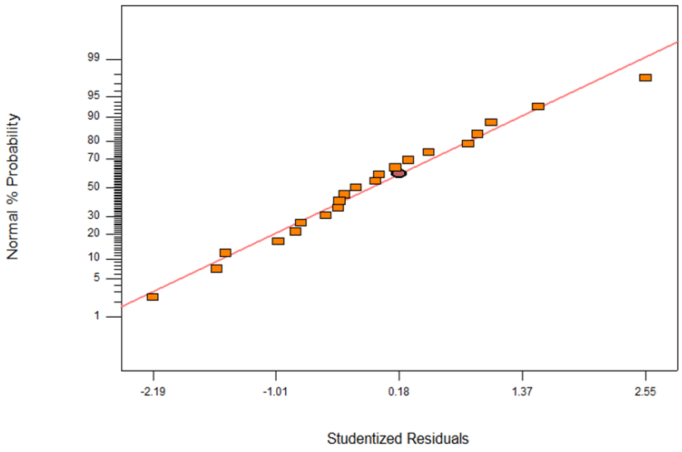

Figure 4.8: Normal probability plot of residuals for biodiesel yield.

In this study, numerical method was carried out to find the optimum catalyst and reaction time which resulted in maximum biodiesel yield using Design Expert software. Criterions set for optimization are shown in Table 4.5. The aim for the screening process was to achieve the highest biodiesel yield in the shortest reaction time using appropriate catalyst. The suggested optimum conditions were achieved by using Al_2O_3-SO_3H as solid acid catalyst with 57.49 % of maximum biodiesel yield achieved in 6 hours reaction time.

Table 4.5: Optimization constraints employed to obtain the optimum yield of biodiesel.

Criteria	Goal	Lower Limit	Upper Limit
Catalyst	Is in range	Al_2O_3-SO_3H	TiO_2-SO_3H
Reaction Time (min)	Minimize	0.00	360.00
Sqrt(Biodiesel Yield+0.57)	Maximize	0.00	1.76

4.1.5 Esterification of PFAD using different uncalcined catalysts

The esterification of PFAD with high FFA was catalyzed by the three different types of uncalcined catalysts, Al_2O_3-SO_3H, SiO_2-SO_3H and TiO_2-SO_3H. Figure 4.9 shows the graph of biodiesel yield versus reaction time under three different types of solid acid catalysts. Overall, the biodiesel yield increased as reaction time increased for all types of catalyst. However, individual catalyst exhibited different catalytic activity. For the SiO_2-SO_3H and TiO_2-SO_3H, the biodiesel yield increased slowly with time. The esterifications with SiO_2-SO_3H and TiO_2-SO_3H have resulted in very low biodiesel yields of less than 6 %. The sulphur contents of SiO_2-SO_3H and TiO_2-SO_3H were only 0.24 % and 0.32 % respectively. These catalysts required a longer reaction time to achieve the saturation point and maximum biodiesel yield. Among the tested catalysts, Al_2O_3-SO_3H achieved the highest biodiesel yield of 57.49 % in 6 hours reaction time. This shows the Al_2O_3-SO_3H possessed the highest catalytic activity compared to SiO_2-SO_3H and TiO_2-SO_3H. This might due to its high sulphur content. The sulphur content of the catalyst was said to directly influence the biodiesel yield

during the esterification process (Abdoulmoumine, 2010; Petchmala et al., 2010). Therefore, the increase in the sulphur content of catalyst resulted in the increase of biodiesel yield.

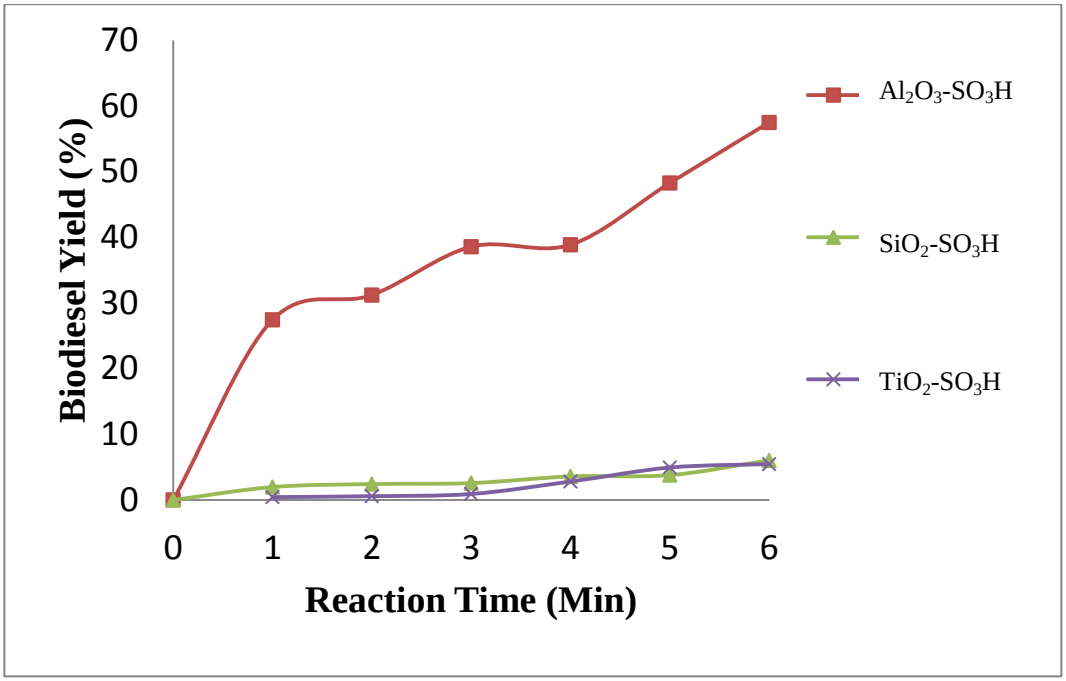

Figure 4.9: Comparison of biodiesel yield achieved by different types of uncalcined catalysts in different reaction time at 18 hours immersion time.

4.2 Effect of different types of calcined catalysts (with calcination treatment)

The catalytic activities of different types of catalyst (Al_2O_3-SO_3H, TiO2-SO3H, and SiO_2-SO_3H) that undergo calcinations treatment on biodiesel production were investigated. The catalysts were prepared according to catalyst preparation conditions as stated in Section 3.4. All the prepared catalysts were calcined at 550 ^oC for duration of 4 hours prior to be used in the esterification reaction for biodiesel production. These catalysts were analyzed by SEM, EDX and FTIR to determine the physical and chemical properties that would directly and indirectly affect the catalyst activity. The esterification of PFAD were carried out at 80 ºC reaction temperature, 2 wt% catalyst to PFAD mass ratio, 20:1 methanol to PFAD molar ratio and 360 minutes reaction time.

4.2.1 Scanning Electron Microscopy (SEM) Analysis

Figure 4.10, Figure 4.11 and Figure 4.12 compared the images of SEM for the catalysts: Al_2O_3-SO_3H, SiO_2-SO_3H, and TiO_2-SO_3H with calcinations treatment and without calcinations treatment. The morphological structures of original powders and sulfonated catalysts were described in Section 4.1.1. From Figure 4.10, it can be observed that the particles tend to agglomerate onto each other after Al_2O_3-SO_3H undergoing calcination treatment. Apparently, there was a significant difference in terms of number of pore and pore sizes of Al_2O_3-SO_3H before and after the calcinations process. The structure of SiO_2-SO_3H and TiO_2-SO_3H after undergoing

calcinations treatment showed no significant changes on the structure and arrangement of the particles before and after the calcinations treatment.

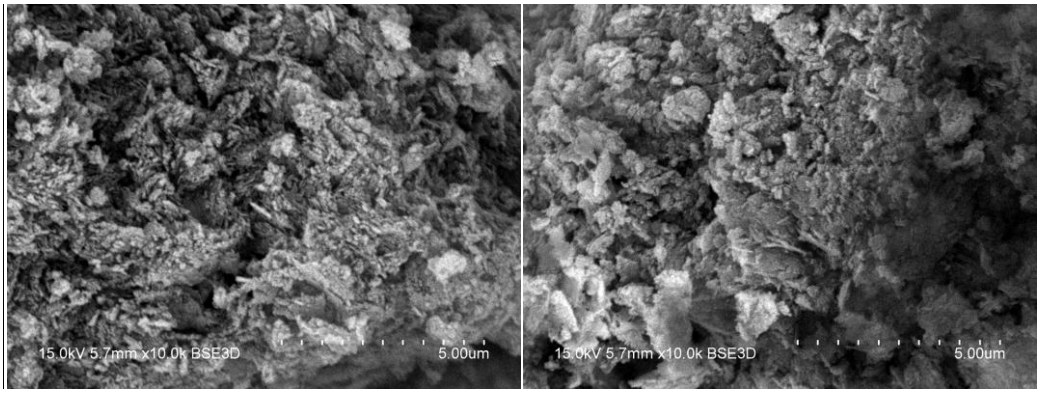

(a) (b)

Figure 4.10: SEM micrographs of (a) sulfonated Al_2O_3 and (b) calcined sulfonated Al_2O_3.

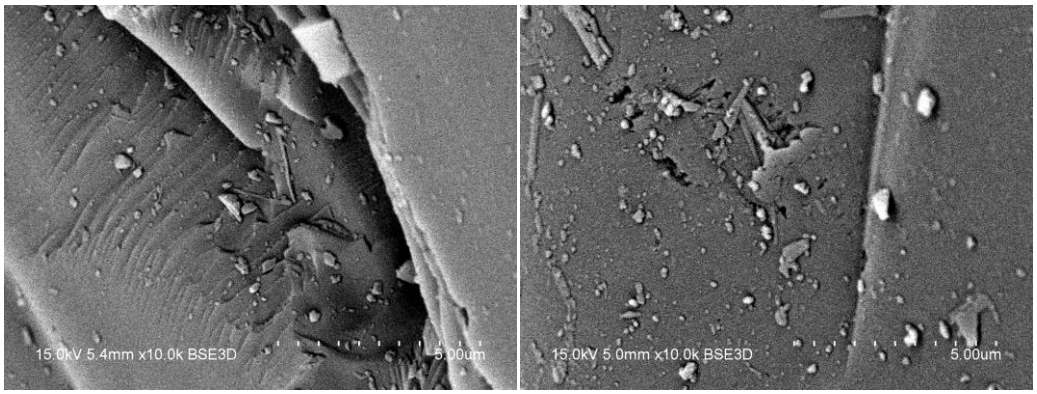

(a) (b)

Figure 4.11: SEM micrographs of (a) sulfonated SiO_2 and (c) calcined sulfonated SiO_2.

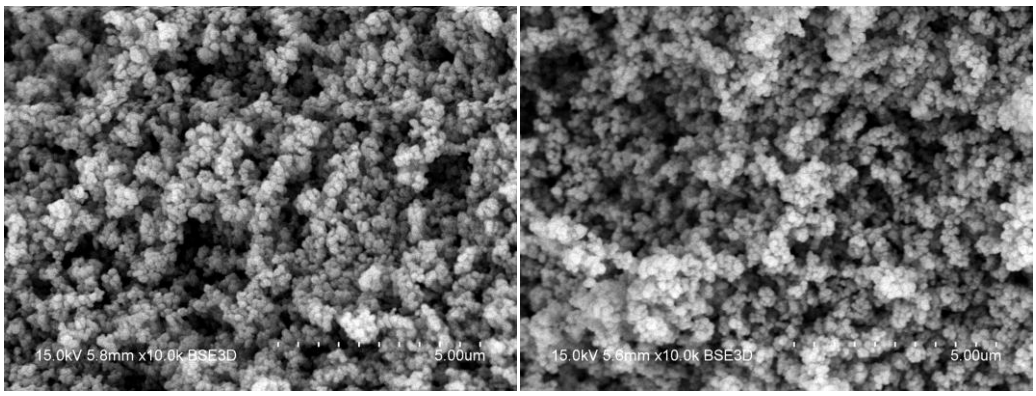

Figure 4.12: SEM micrographs of (a) sulfonated TiO_2 and (c) calcined sulfonated TiO_2.

4.2.2 Energy Dispersive X-ray (EDX) Analysis

Table 4.6 compared the sulphur contents of all catalysts with and without calcinations treatments. It was clearly shown that among the tested catalysts. Al_2O_3-SO_3H contained the highest sulphur content either with calcinations treatment or without calcinations treatment. The sulphur content of Al_2O_3-SO_3H without calcinations treatment was 3.71 wt% and with calcinations treatments was 2.60 wt%. In contrast, the sulphur content of SiO_2-SO_3H and TiO_2-SO_3H either with calcinations treatment or without calcinations treatment were relatively low with the range of 0.17 wt% to 0.42 wt%, which were 80 % lower than the sulphur content of Al_2O_3-SO_3H. When all the catalysts undergo calcinations treatment, the sulphur contents of Al_2O_3-SO_3H, SiO_2-SO_3H and TiO_2-SO_3H were reduced compared to the catalysts without the calcinations treatment. Al_2O_3-SO_3H lost 30% of its sulphur content after the calcinations treatment.

Several researchers (Benjapornkulaphong et al., 2009; Wan et al., 2009) have carried out the study on the effect of calcinations treatment. They claimed that the calcinations treatment will affect the sulphur content of the catalyst used. The researcher found out that the uncalcined catalyst had the higher sulphur content compared to the calcined catalyst that contained lower sulphur content (Abdoulmoumine, 2010).

Table 4.6: Sulphur content of catalysts examined by EDX analysis.

Types of catalyst	Sulphur content, wt% (without calcination)	Sulphur content, wt% (with calcination)
Al_2O_3-SO_3H	3.71	2.60
SiO_2-SO_3H	0.24	0.17
TiO_2-SO_3H	0.42	0.29

4.2.3 Fourier Transform Infra-Red (FTIR) Analysis

FTIR spectra of Al_2O_3-SO_3H with calcination and without calcinations are shown in Figure 4.13. As mentioned in Section 4.1.3, the obvious band was detected at 1077 and 1102 cm^{-1}. The IR peaks at 1077 and 1102 cm^{-1} indicated the presence of SO_3 species. The broad band at 3381 cm^{-1} accompanied by a band at 1640cm^{-1} indicated the presence of -OH group (Park et al., 2008). In comparison between calcined and uncalcined of Al_2O_3-SO_3H, the intensity for all the IR peaks (SO_3 species) and –OH group were reduced after the calcination process.

Figure 4.14 and Figure 4.15 show the FTIR spectra of SiO_2-SO_3H (with and without calcination) and TiO_2-SO_3H (with and without calcination). FTIR was not able to detect the bands of –OH group and sulphuric group in both of the catalysts either before or after calcination process. This is in agreement of EDX results as the sulphur contents for SiO_2-SO_3H and TiO_2-SO_3H were very low of less than 0.5 % only. For the FTIR analysis, there were no significant changes in the IR peaks intensity for SiO_2-SO_3H and the calcined SiO_2-SO_3H, TiO_2-SO_3H and the calcined TiO_2-SO_3H.

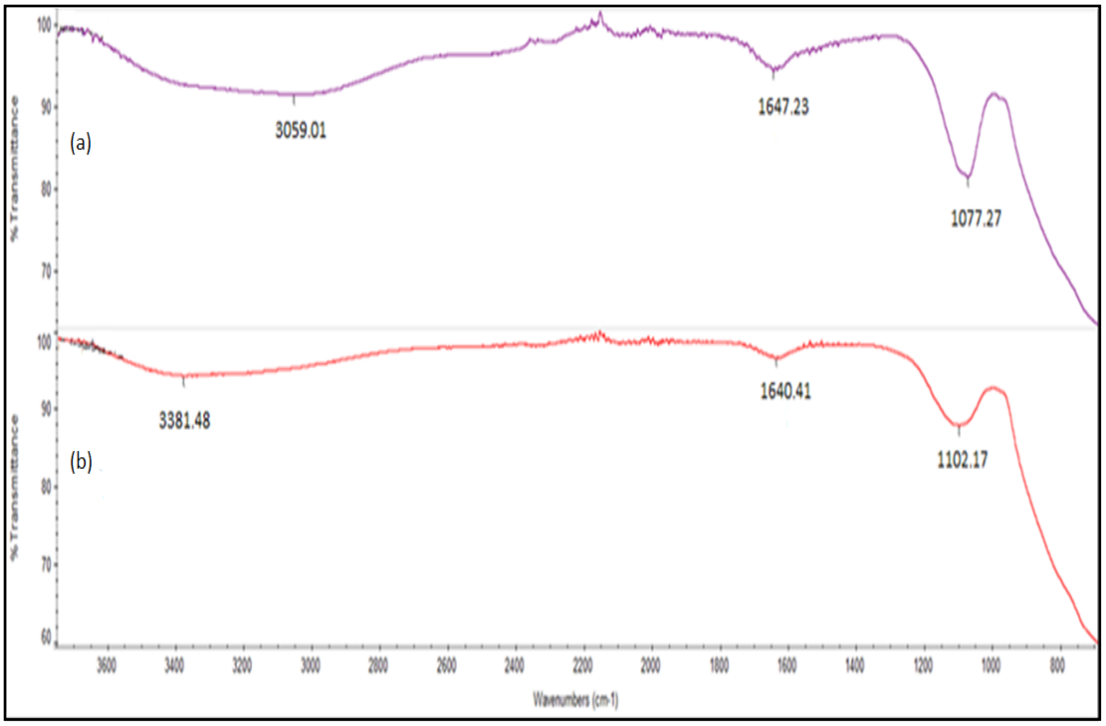

Figure 4.13: FTIR spectra of (a) Al_2O_3-SO_3H and (b) calcined Al_2O_3-SO_3H.

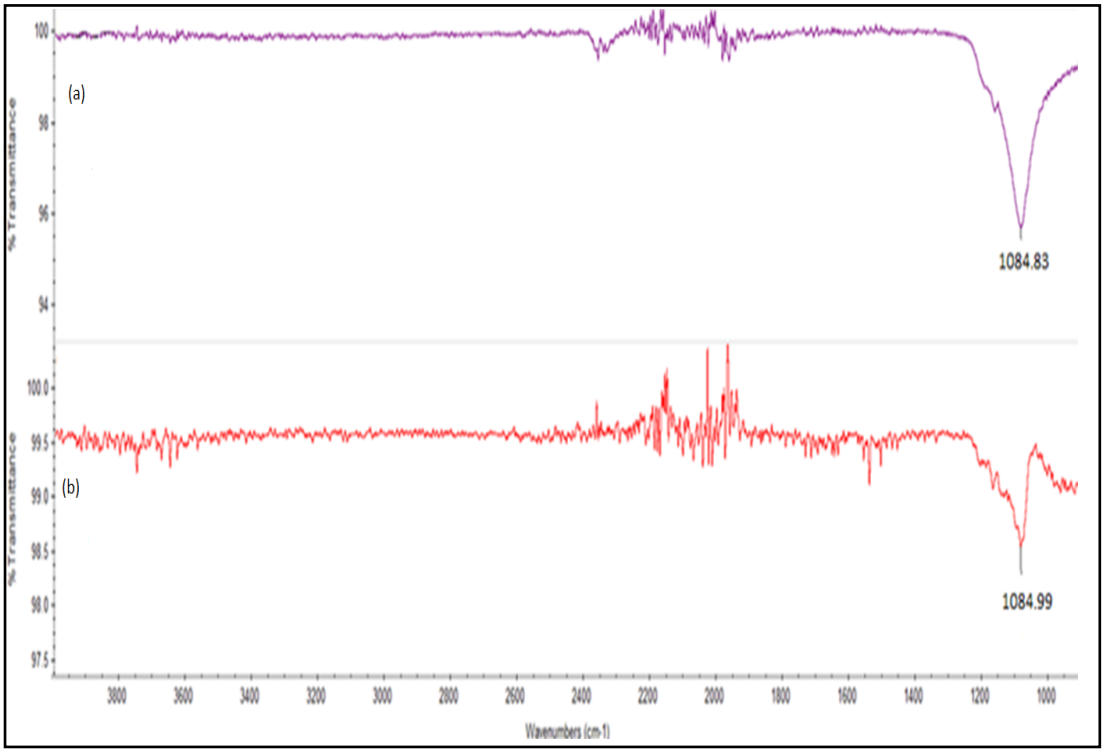

Figure 4.14: FTIR spectra of (a) SiO_2-SO_3H and (b) calcined SiO_2-SO_3H.

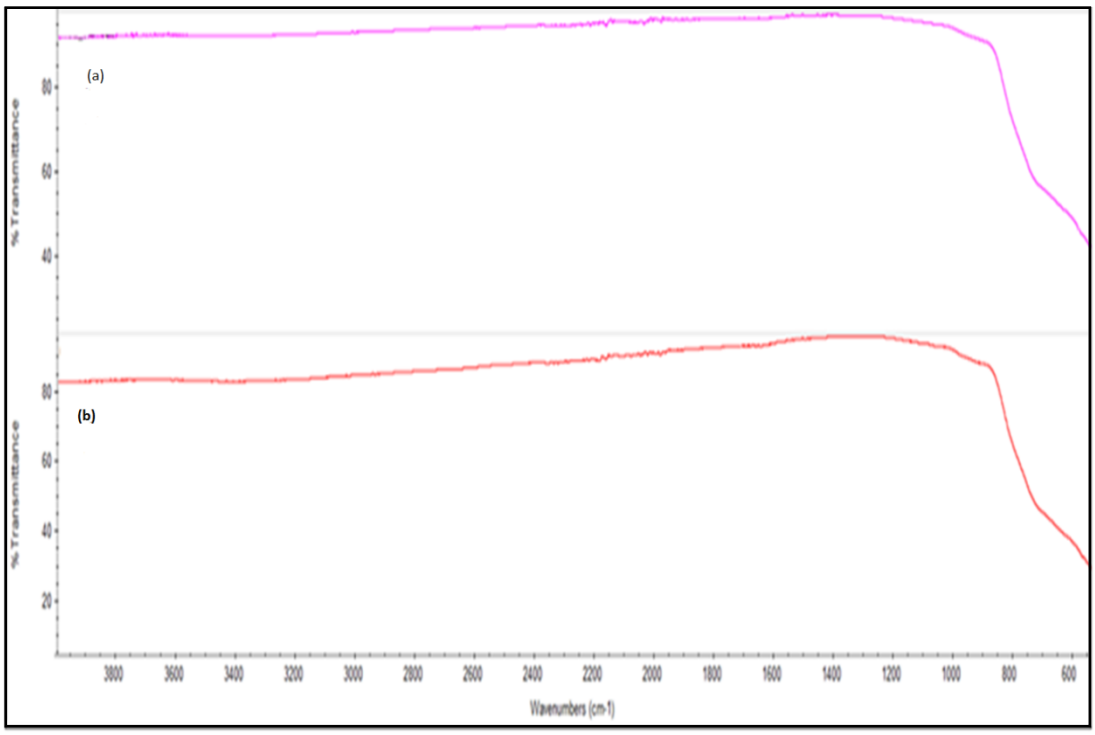

Figure 4.15: FTIR spectra of (a) TiO_2-SO_3H and (b) calcined TiO_2-SO_3H.

4.2.4 Catalyst Screening: Catalysts with calcinations treatment

Among the tested catalysts, catalyst with good catalytic activity was selected using statistical analysis. Based on the Box-Cox diagnostics tool available in Design Expert, the response biodiesel yield was suggested to be transformed in square root form and 0.5749 was the constant k value. By doing transformation, abnormal response problems can be avoided and inequality of variance can be associated (Sim et al., 2007).

Table 4.7 presents the results of Analysis Of Variance (ANOVA) which show the levels of significance for the model and individual model terms. Based on the Table 4.7, the model with Prob > F value less than 0.05 implied the model was significant. In this case, model terms A (catalyst), B (reaction time), B^2, B^3, AB were significant model terms because both "Prob > F" for A and B were <0.0001. Although the "Prob > F" for AB^2terms were larger than 0.05, but the variables were included in the model to improve its R^2 value from 0.9771 to 0.9861.

Table 4.7: Analysis of Variance for the Regression Model and Respective Model Terms.

Source	Sum of Squares	Degree of Freedom	Mean Square	F-Value	Prob > F	
Model	60.50	9	6.72	86.61	< 0.0001	Significant
A	40.02	2	20.01	257.80	<0.0001	
B	10.95	1	10.95	141.13	< 0.0001	
B^2	0.40	1	0.40	5.14	0.0445	
AB	7.93	2	3.96	51.07	< 0.0001	
B^3	0.65	1	0.65	8.37	0.0146	
AB^2	0.55	2	0.28	3.56	0.0643	
Residual	0.85	11	0.078			
Cor Total	61.36	20				

The empirical model in terms of actual factors is shown in Table 4.8. The reliability levels of the generated empirical model for the response could be verified through the values of correlation coefficient (R^2) and adequate precision. Table 4.9 shows the R^2 value of 0.9861 for this cubic model. In term of adequate precision, it measures the signal to noise ratio, a ratio greater than 4 is desirable. In this study, the adequate precision was 29.371, this indicated an adequate signal. Hence, this model can be used to navigate the design space.

The reliability of the model also can be determined from predicted versus actual plot. As shown in Figure 4.16, the experiment results were in good agreement with the predicted biodiesel yields. The normal probability plot of the residuals for the response is presented in Figure 4.17. It can be seen that the residuals were

distributed near to the straight line. This indicated the underlying error distribution was normal. All the normal probability plots with sample from a normal distribution centered at zero mean that there was no severe indication of non-normality of the experimental results (Sim et al., 2007).

Table 4.8: Final empirical models in actual factors.

	Empirical models
Generalized (Coded factors)	Sqrt(Biodiesel Yield (Calcined) + 0.41) =2.39+2.25 * A[1]-1.04 * A[2]+0.42 * B-0.39 * B^2+1.31 * A[1]B
Actual factors	
Catalyst Calcined Al_2O_3-SO_3H	Sqrt(Biodiesel Yield (Calcined) + 0.41) =1.01271+0.035701 * Reaction Time -1.14118E-004 * Reaction $Time^2$+1.53936E-007 * Reaction $Time^3$
Catalyst Calcined SiO_2-SO_3H	Sqrt(Biodiesel Yield (Calcined) + 0.41)=0.54385+0.015068 * Reaction Time-8.65152E-005 * Reaction $Time^2$+1.53936E-007 * Reaction $Time^3$
Catalyst Calcined TiO_2-SO_3H	Sqrt(Biodiesel Yield (Calcined) + 0.41) =0.50310+0.014002 * Reaction Time-8.46879E-005 * Reaction $Time^2$+1.53936E-007 * Reaction $Time^3$

Table 4.9: Summarization of the ANOVA for the dependent responses.

Type of transformation	**Model Hierarchy**	**Significant model terms**	**R^2**	**Adjusted R^2**	**Predicted R^2**	**Adequate precision**
Square root	Cubic	A, B, B^2, B^3, AB	0.9861	0.9747	0.8698	29.371

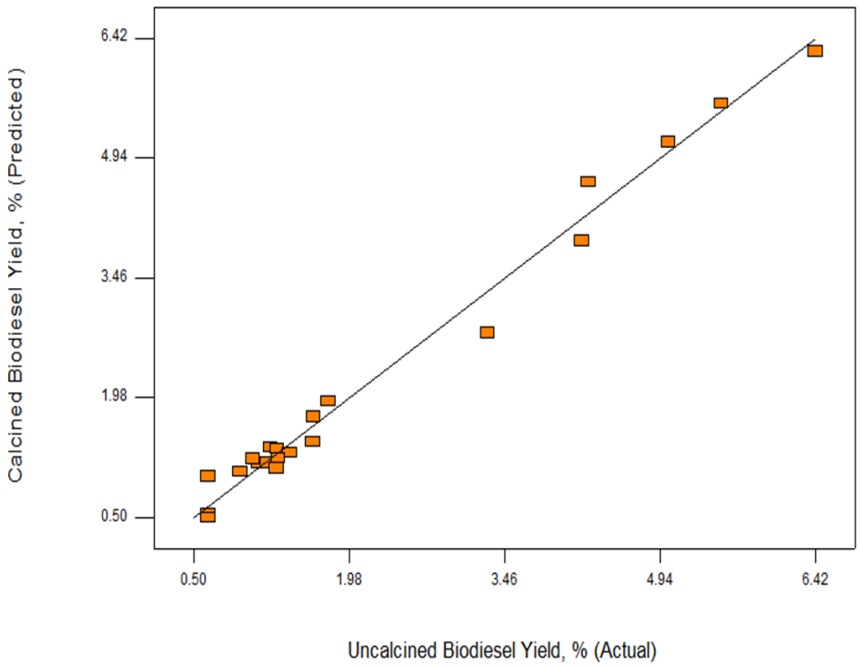

Figure 4.16: Predicted versus actualbiodiesel yield.

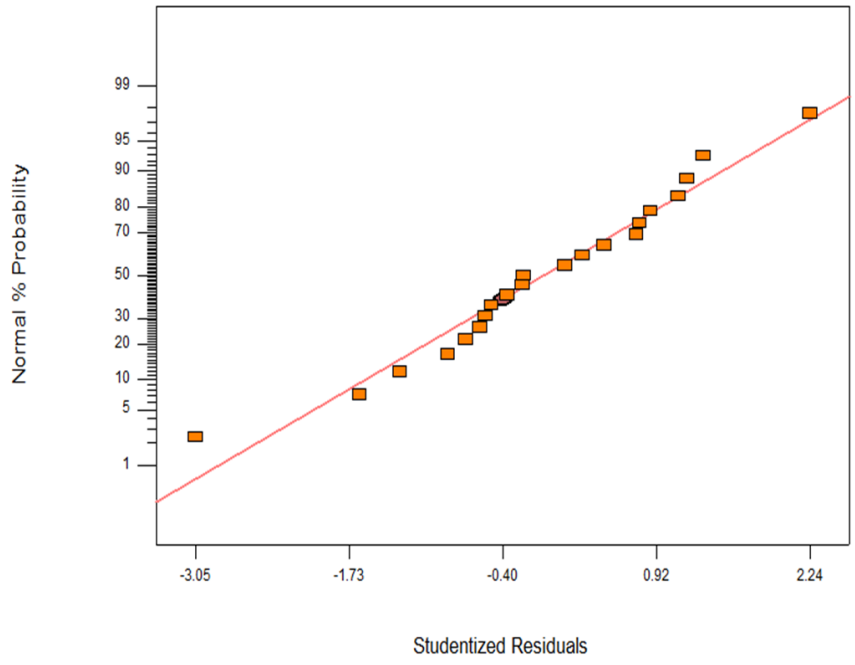

Figure 4.17: Normal probability plot of residuals for biodiesel yield.

4.2.5 Esterification of PFAD using different types of calcined catalysts

Figure 4.18 shows the graph of biodiesel yield versus reaction time under three different types of calcined catalysts. In overall, the biodiesel yield increased as reaction time increased for all types of catalyst. However, individual catalyst exhibited different catalytic activity. For the calcined SiO_2-SO_3H and calcined TiO_2-SO_3H, the biodiesel yield increased slowly with time. The esterifications with calcined SiO_2-SO_3H and calcined TiO_2-SO_3H have resulted in very low biodiesel yields of less than 6 %. The sulphur contents of calcined SiO_2-SO_3H and calcined TiO_2-SO_3H were only 0.17 % and 0.29 % respectively. These catalysts required a longer reaction time to achieve the saturation point and maximum biodiesel yield. Among the tested catalysts, the calcined Al_2O_3-SO_3-H achieved the highest biodiesel yield of 40.80 % at 6 hours of reaction time. After undergoing calcination process, the sulphur content of each types of catalyst was reduced. The calcination temperature at 550 ^oC might cause the loss of sulphur content as proven by EDX anaylsis. Thus, the catalytic activities which is measured by biodiesel yield were affected by the calcinations treatment. The sulfonated catalyst support without calcinations contained high sulphur content whereas the sulphur content of sulfonated catalyst was reduced after undergoing the calcination process.

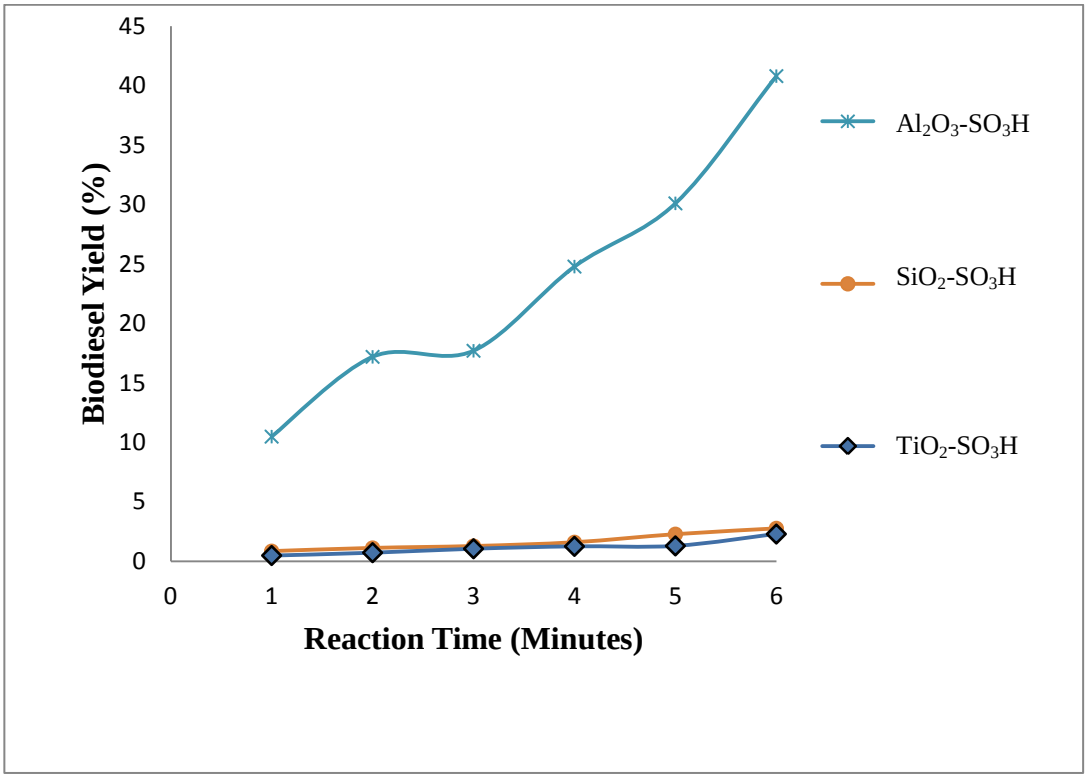

Figure 4.18: Comparison of biodiesel yield achieved by different types of calcined catalysts in different reaction time.

4.3 Comparison between calcined catalysts and uncalcined catalysts

The effects of different types of uncalcined and calcined catalysts had been studied in Section 4.1 and 4.2. Based on the maximum biodiesel yield obtained at the shortest reaction time, Al_2O_3-SO_3H without calcinations treatment was selected as a best catalyst for the subsequent studies.

In Figure 4.19, the biodiesel yield achieved by uncalcined Al_2O_3-SO_3H was compared with the biodiesel yield achieved with the calcined Al_2O_3-SO_3H. It was

found that the uncalcined Al_2O_3-SO_3H achieved the highest biodiesel yield of 57.49 % in 6 hours. Whereas, the calcined Al_2O_3-SO_3H reached the lower biodiesel yield of 40.80 % in 6 hours. This was due to the higher sulphur content of uncalcined Al_2O_3-SO_3H, 3.71 wt% compared to the sulphur content of calcined Al_2O_3-SO_3H which was only 2.60 wt%.

Both the calcined and uncalcined SiO_2-SO_3H and TiO_2-SO_3H achieved the undesired biodiesel yields. From Figure 4.19, all the catalysts (SiO_2-SO_3H and TiO_2-SO_3H) with low sulphur content produced the low biodiesel yield with the range of 0 % to 6 %.

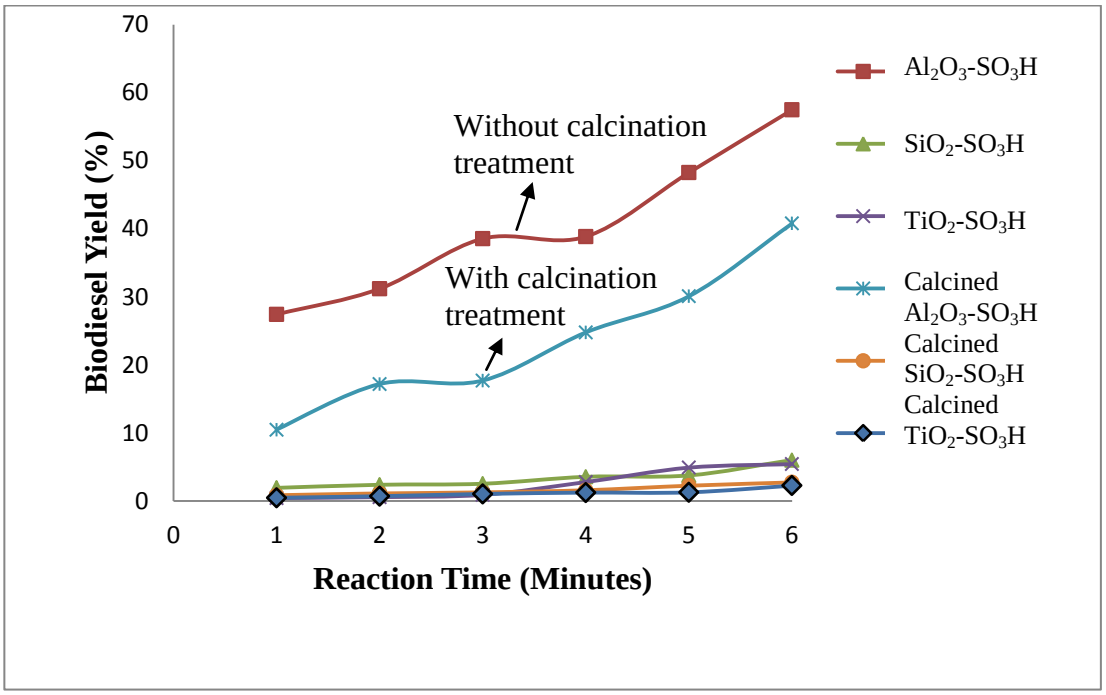

Figure 4.19: Comparison of biodiesel yield achieved by uncalcined Al_2O_3-SO_3H and calcined Al_2O_3-SO_3H in different reaction time.

4.4 Effect of acid concentration and immersion time

Al_2O_3-SO_3H determined earlier as best catalyst was used as the catalyst in the subsequent study. The catalytic activities of catalysts immersed at different immersion time (6, 12 and 18 hours) and acid concentration (2M, 3M, 4M and 5M) were investigated. The effects of acid concentration and immersion time on catalyst activity were studied based on the biodiesel yield obtained. The esterification of PFAD were carried out at 80 ºC reaction temperature, 2 wt% catalyst to PFAD mass ratio, 20:1 methanol to PFAD molar ratio and 360 minutes reaction time. The catalysts were characterized by BET, SEM, EDX, ICP-OES, FTIR and XRD.

4.4.1 Brunauer-Emmett-Teller (BET) Surface Area Analysis

Alumina catalyst immersed at 2M, 3M, 4M and 5M acid concentration were named as 2M-Al_2O_3-SO_3H, 3M-Al_2O_3-SO_3H, 4M-Al_2O_3-SO_3H and 5M-Al_2O_3-SO_3H respectively. As tabulated in Table 4.10, catalyst sulfonated at 2M acid concentration regardless of immersion time had the highest specific surface areas. The specific surface area for 2M-Al_2O_3-SO_3H at 6 hours, 12 hours and 18 hours were 154.95, 152.09, 149.80 m^2/g, respectively. All catalysts (6 hours, 12 hours and 18 hours) at low acid concentration (2M) tend to have similar specific surface area. The specific surface areas of catalysts were not affected by the increasing immersion time when 2M acid concentration was used. The high acid concentration of 5M regardless of immersion time had the lowest specific surface areas. The specific surface area for 5M-Al_2O_3-SO_3H at 6 hours, 12 hours and 18 hours were 25.87, 18.65 , 7.64 m^2/g

respectively. Apparently, the catalysts (2M-Al_2O_3-SO_3H, 3M-Al_2O_3-SO_3H, 4M-Al_2O_3-SO_3H and 5M-Al_2O_3-SO_3H) immersed in increasing acid concentration at 18 hours had the decreasing specific surface area (149.80 , 57.72 , 36.39 and 7.64 m^2/g).

It can be concluded that the increase of acid concentration used for the catalysts in sulfonation process has caused the reduction in the specific surface area of Al_2O_3-SO_3H. The results showed that the acid concentration used did affect the specific surface area of the catalysts. The researcher claimed that the specific surface area for synthesized catalyst ($NaAlO_2$) was found to be lower than pure alumina. The reduction of the specific surface area of the support was observed when a catalyst was promoted with alkali metals (Taufiq-Yap et al., 2011). Surface and pores of alumina were covered by higher sulphur compounds during the impregnation step when the supports were immersed at higher acid concentration (Mross, 1983). Further analysis by SEM micrographs (Figure 4.21 to Figure 4.23) proved that sulfonation process carried out at different acid concentration had altered the surface structural of the catalysts.

The specific surface area and pore specific volume of original powder Al_2O_3 are 167.51 m^2/g and 0.59 cm^3/g. Catalyst consists of a large number of pores and large pore sizes would increase the accessibility of sulphuric acid into the catalyst bulk. This was because more $–SO_3H$ functional groups will be attached to the catalyst with large number of pores to increase the catalytic activity of the catalyst (Shu et al., 2010). Catalyst 5M-Al_2O_3-SO_3H obtained the lowest specific surface area (7.64 m^2/g), pore volume (0.0987 cm^3/g) and high density of sulphur content which

indicated most of the $–SO_3H$ groups of the catalyst were in the interior of the powder (Shu et al., 2010). The surface of 5M-Al_2O_3-SO_3H was covered by sulphur element which is shown at Appendix A.

Table 4.10: BET surface area measurement on the effect of acid concentration.

Immersion time (hours)	Types of catalyst	Specific Surface area (m^2/g)	Pore specific volume, cm^3/g
-	Pure Al_2O_3	167.51	0.5900
6	2M-Al_2O_3-SO_3H	154.95	0.4626
	3M-Al_2O_3-SO_3H	81.47	0.5752
	4M-Al_2O_3-SO_3H	47.84	0.3377
	5M-Al_2O_3-SO_3H	25.87	0.5791
12	2M-Al_2O_3-SO_3H	152.09	0.4541
	3M-Al_2O_3-SO_3H	67.89	0.4793
	4M-Al_2O_3-SO_3H	42.88	0.4799
	5M-Al_2O_3-SO_3H	18.65	0.4174
18	2M-Al_2O_3-SO_3H	149.80	0.5249
	3M-Al_2O_3-SO_3H	57.72	0.6548
	4M-Al_2O_3-SO_3H	36.39	0.2110
	5M-Al_2O_3-SO_3H	7.64	0.0987

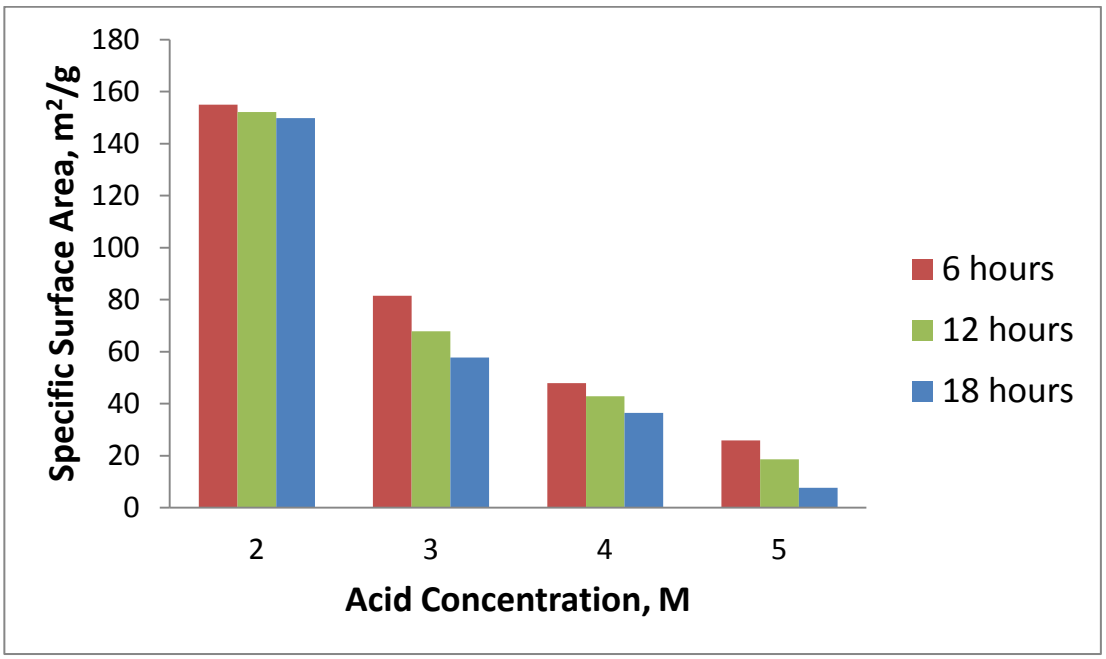

Figure 4.20: Specific surface area versus acid concentration at different immersion time of 6, 12 and 18 hours.

4.4.2 Scanning Electron Microscopy (SEM) Analysis

The morphological structures of synthesized catalysts were visualized via SEM with magnification of 10,000. Figure 4.21 to Figure 4.23 showed the SEM images of sulfonated catalysts (2M-Al_2O_3-SO_3H, 3M-Al_2O_3-SO_3H, 4M-Al_2O_3-SO_3H and 5M-Al_2O_3-SO_3H) at different immersion time of 6 h, 12 h and 18 h. The specific surface areas of Al_2O_3-SO_3H viewed by SEM were in good agreement with the BET surface measurement.

As observed in Figure 4.21(a)-(b), the 2M-Al_2O_3-SO_3H and 3M-Al_2O_3-SO_3H catalysts consisted different sizes of plate like form of catalysts. The 4M-Al_2O_3-SO_3H and 5M-Al_2O_3-SO_3H catalysts in Figure 4.21(c)-(d) were in bulky form. Thus, the specific surface areas of catalysts immersed in high acid concentration 4M and

5M were reduced compared to catalysts immersed in low acid concentration (2M-Al_2O_3-SO_3H and 3M-Al_2O_3-SO_3H).

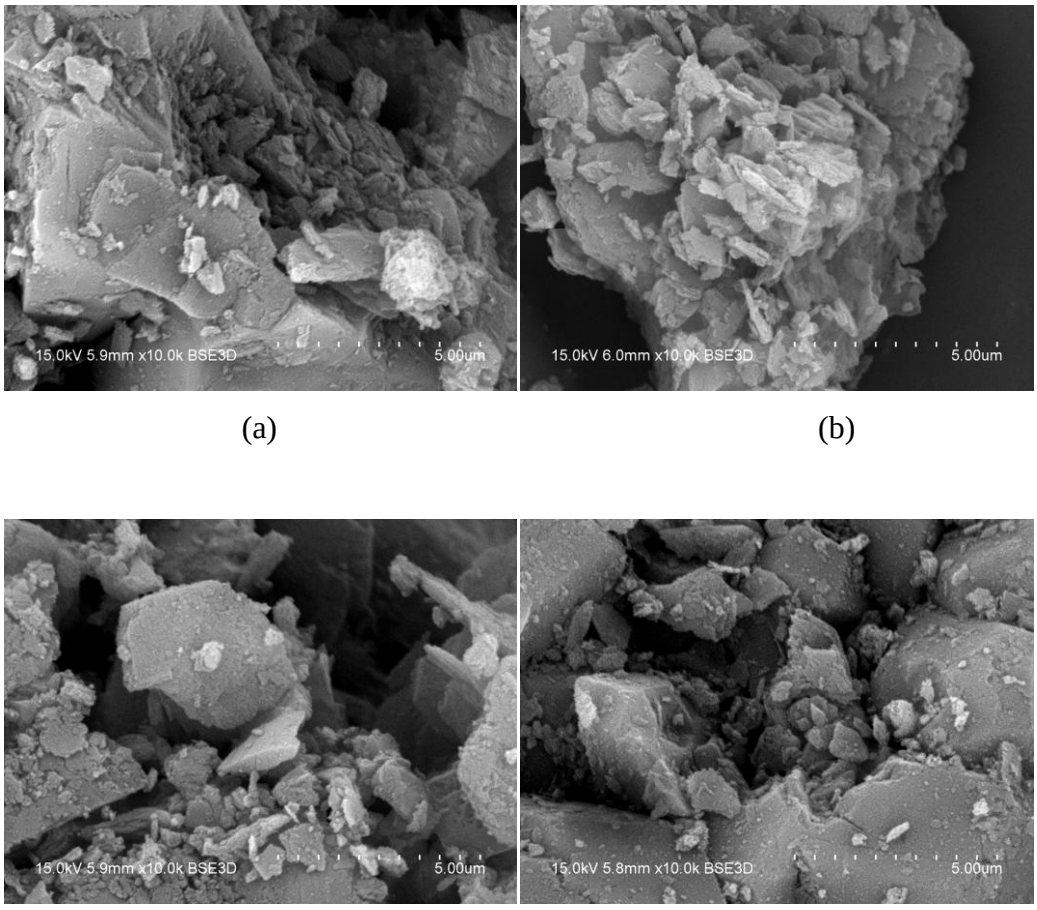

Figure 4.21: SEM micrographs of Al_2O_3-SO_3H at 6 hours immersion time and at acid concentration of (a) 2M, (b) 3M, (c) 4M, (d) 5M.

Figure 4.22 showed the surface morphologies of 2M-Al_2O_3-SO_3H, 3M-Al_2O_3-SO_3H, 4M-Al_2O_3-SO_3H and 5M-Al_2O_3-SO_3H at 12 hours immersion time. When the acid concentration was increased from 2M to 5M, the specific surface area of the catalysts had been substantially reduced from 152.09 m^2/g (2M-Al_2O_3-SO_3H) to 18.65 m^2/g (5M-Al_2O_3-SO_3H). The structure of 4M-Al_2O_3-SO_3H and 5M-Al_2O_3-

SO_3H had become loosen and become a plate-like form of catalyst with agglomeration of small particles on the catalyst surface when immersed in high acid concentration of 4M and 5M (Figure 4.22(c)-(d)). On the contrary, the catalysts (2M-Al_2O_3-SO_3H and 3M-Al_2O_3-SO_3H) were still in bulky form with less agglomeration of fine particles on the catalyst surface. It was said that the shape of a catalyst can affect the surface area (Taufiq-Yap et al., 2011).

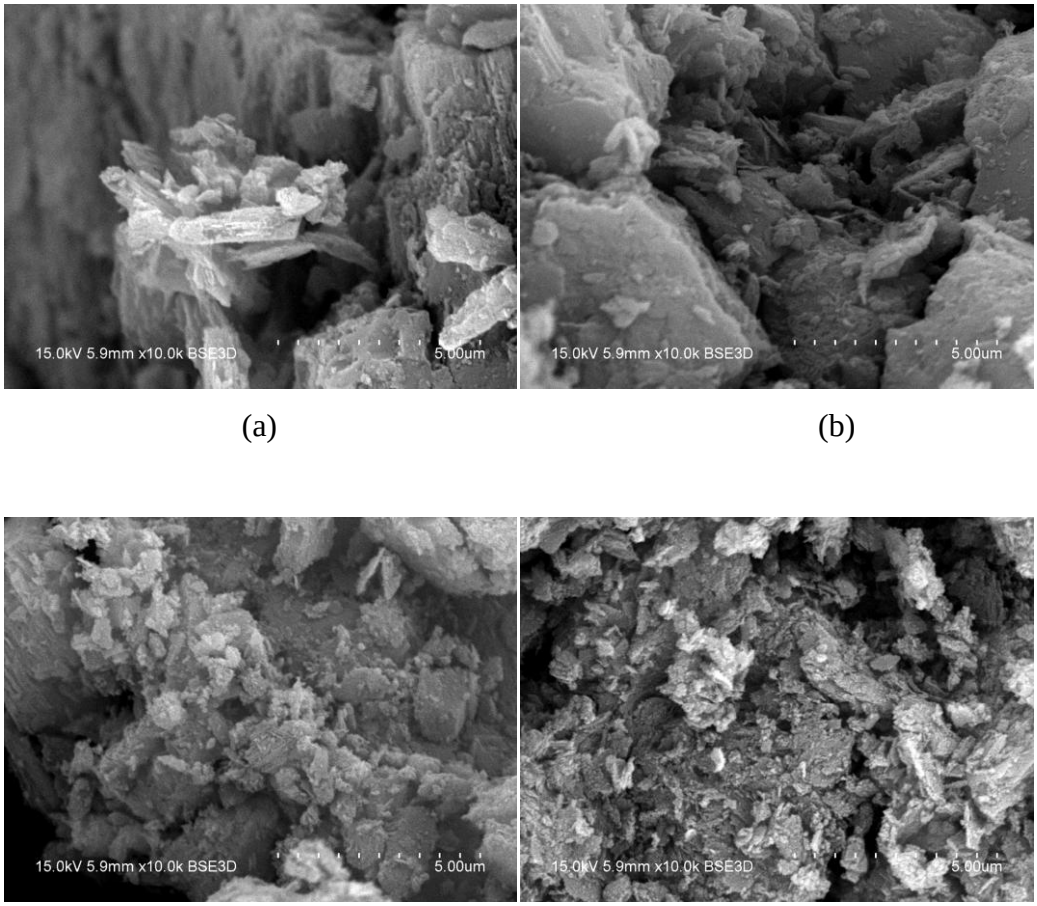

Figure 4.22: SEM micrographs of Al_2O_3-SO_3H at 12 hours immersion time and at acid concentration of (a) 2M, (b) 3M, (c) 4M, (d) 5M.

Figure 4.23(a)-(d) depicts the surface morphology of 2M-Al_2O_3-SO_3H, 3M-Al_2O_3-SO_3H, 4M-Al_2O_3-SO_3H and 5M-Al_2O_3-SO_3H at 18 hours immersion time. When the acid concentration was increased from 2M to 5M, the specific surface area on the catalyst had been reduced from 149.80 m^2/g (2M-Al_2O_3-SO_3H) to 7.64 m^2/g (5M-Al_2O_3-SO_3H). From the Figure 4.23(c)-(d), the higher acid concentration of 4M-Al_2O_3-SO_3H and 5M-Al_2O_3-SO_3H catalysts had formed smaller clusters and mostly all the catalyst surface were attached with fine particles. Whereas from Figure 4.23(a)-(b), the pore sizes and pore volumes were apparently larger than the 4M-Al_2O_3-SO_3H and 5M-Al_2O_3-SO_3H catalysts. This might indicate that most of the catalyst surfaces have yet to be covered by active group of sulfonic compounds.

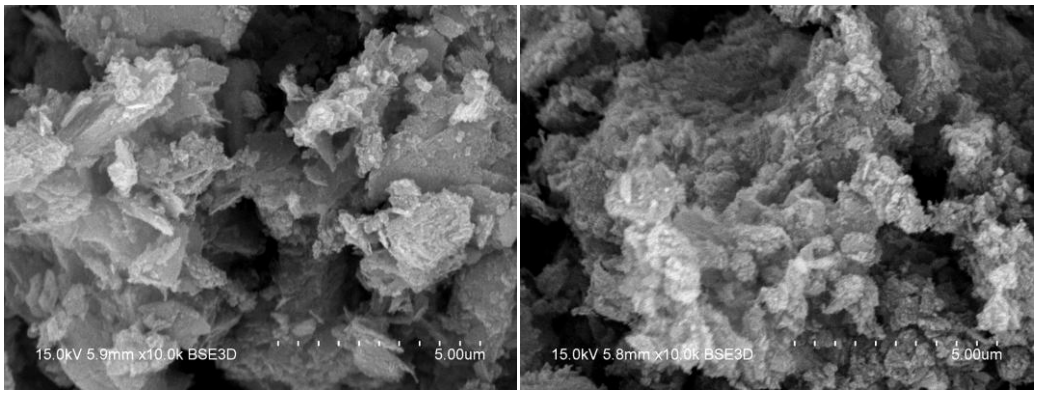

(a) (b)

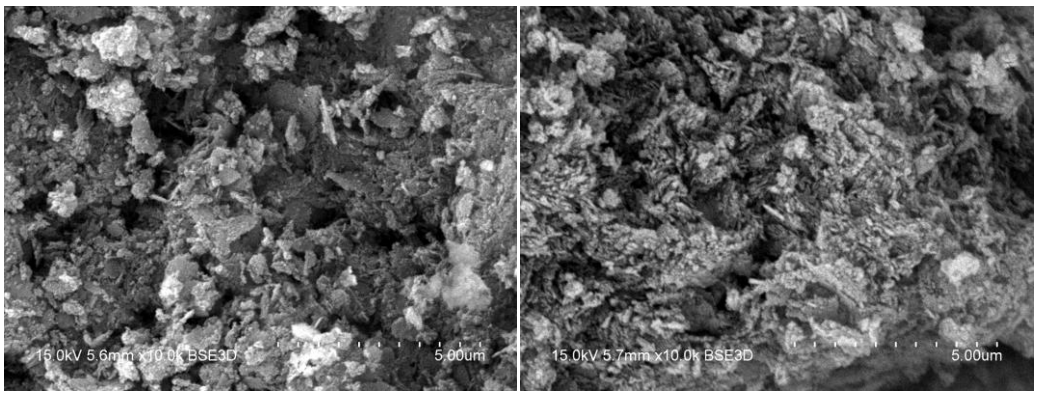

(c) (d)

Figure 4.23: SEM micrographs of Al_2O_3-SO_3H at 18 hours immersion time and at acid concentration of (a) 2M, (b) 3M, (c) 4M, (d) 5M.

4.4.3 Energy Dispersive X-ray Spectroscopy (EDX) Analysis

Table 4.11 showed the sulphur content of Al_2O_3-SO_3H immersed at 2M, 3M, 4M and 5M of acid concentration and at different immersion time (6 hours – 18hours). In Figure 4.24, it displayed the effect of acid concentration on the sulphur content of catalyst. At low immersion time of 6 hours, the increase of acid concentration did not have significant effect on sulphur content of catalysts from 2M to 5M (sulphur content: 1.14 wt% to 1.36 wt%). However, at longer immersion time of 12 hours and 18 hours, the increase in acid concentration for sulfonation process would lead to the increasing trend of the catalyst sulphur content. At immersion time of 18 h, 5M-Al_2O_3-SO_3H achieved the highest sulphur content of 3.71 wt%. It dropped to 2.49 wt% sulphur content at 4 M acid concentration. The sulphur contents of 2M-Al_2O_3-SO_3H and 3M-Al_2O_3-SO_3H were 1.67 wt % and 1.64 wt %, respectively.

At 18 hours immersion time, the sulphur contents of 2M, 3M, 4M and 5M were 1.67 wt%, 1.64 wt%, 2.49 wt%, 3.71 wt% respectively. Table 4.11 shows the sulphur contents of Al_2O_3-SO_3H immersed at 6 hours, 12 hours and 18 hours immersion time. The effect of immersion time on sulphur content was pronounced at the acid concentration of 4M and 5M. At 4M and 5M acid concentration, the increase in the immersion time to 18 hours led to the increment in the sulphur content. The sulphur content of catalysts at 4M and 18 hours was 2.49 wt% and at 5M and 18 hours was 3.71 wt%. The effects of immersion time on sulphur content can be neglected when the catalysts were immersed at low acid concentration of 2M and 3M. The sulphur contents of catalysts 2M-Al_2O_3-SO_3H and 3M-Al_2O_3-SO_3H at 6, 12 18 hours immersion time were less than 2 wt%. The increasing in the immersion time would lead to the increase in the sulphur contents of catalysts only at 4M and 5M acid concentration.

The operating principle of EDX analysis might have the incomplete content analysis of EDX as EDX analysis is based on surface technique by penetrating X-ray beam into a depth of 0.1 to 0.2 nm (5 -10 atomic layers) (Hafner, 2006). There might be more –SO_3H groups active catalytic sites that are attached to the interior of Al_2O_3 particles. Therefore, the ICP-OES analysis was used to verify the results obtained by the EDX analysis.

Table 4.11: Sulphur contents of Al_2O_3-SO_3H at different acid concentration.

	Sulphur content, wt %		
Acid Concentration, M	**6 h**	**12 h**	**18h**
2	1.30	1.16	1.67
3	1.36	1.22	1.64
4	1.23	1.23	2.49
5	1.14	1.75	3.71

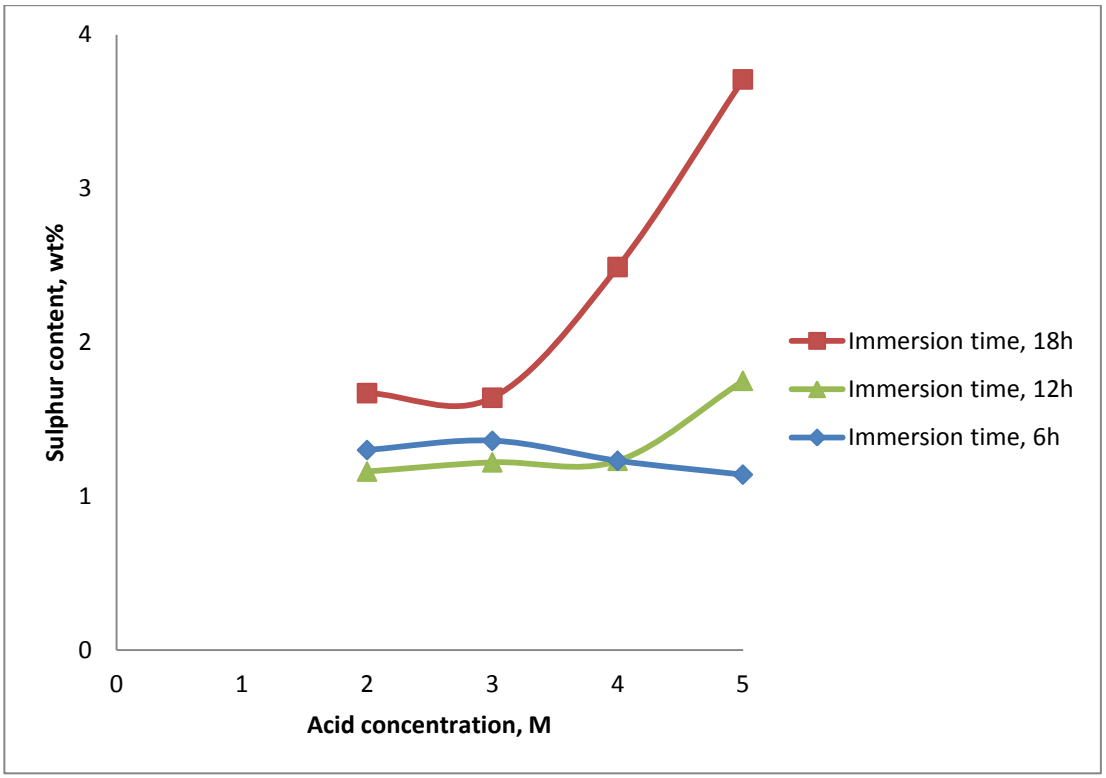

Figure 4.24: Sulphur contents of Al_2O_3-SO_3H at different acid concentration.

4.4.4 Inductively Coupled Plasma-Optical Emission Spectrometer (ICP-OES) Analysis

The elemental composition of sulphur for Al_2O_3-SO_3H was measured by ICP and the results were tabulated in Table 4.12. The sulphur contents of Al_2O_3-SO_3H immersed at different acid concentration were in good agreement with EDX analysis.

The compositions of sulphur for 2M-Al_2O_3-SO_3H, 3M-Al_2O_3-SO_3H, 4M-Al_2O_3-SO_3H and 5M-Al_2O_3-SO_3H at 6 hours and 12 hours immersion time were 1.26 mg/L and 1.91 mg/L. For the immersion time of 18 hours, the sulphur contents of the catalyst immersed in low acid concentration of 2M and 3 M were 1.50 mg/L and 1.57 mg/L respectively. The Al_2O_3-SO_3H immersed in 5M acid concentration contained the highest sulphur content which is 3.02 mg/L. The sulphur content of Al_2O_3-SO_3H immersed in 4M acid concentration was 2.47 mg/L.

Table 4.12: Sulphur contents of Al_2O_3-SO_3H at different acid concentration.

	Sulphur content, mg/L		
Acid Concentration, M	**6 h**	**12 h**	**18h**
2	1.26	1.50	1.50
3	1.41	1.36	1.57
4	1.32	1.64	2.47
5	1.88	1.91	3.02

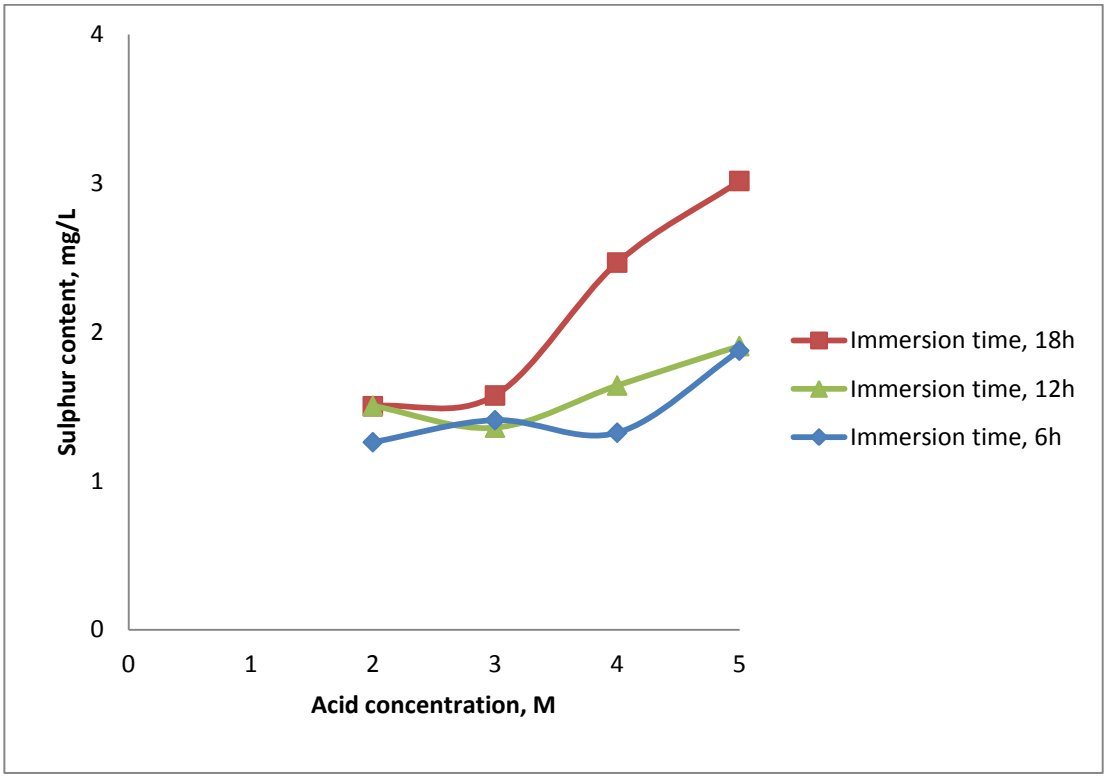

Figure 4.25: Sulphur contents of Al_2O_3-SO_3H at different acid concentration.

4.4.5 Fourier Transform Infra-Red (FTIR) Analysis

FTIR spectra of 2M-Al_2O_3-SO_3H, 3M-Al_2O_3-SO_3H, 4M-Al_2O_3-SO_3H and 5M-Al_2O_3-SO_3H catalysts at 6 hours, 12 hours and 18 hours immersion time are shown in Figure 4.26, Figure 4.27 and Figure 4.28. In general, FTIR spectra for all the catalysts at 2M, 3M, 4M and 5M acid concentration and at 6 hours, 12 hours and 18 hours immersion time showed the similar obvious peaks at the same wavelength. As mentioned earlier in Section 4.1.3, obvious bands were detected at 1103.99 cm^{-1} to 1117.42 cm^{-1}. These IR peaks denote the presence of SO_3 species. The broad bands at 3379.50 cm^{-1} to 3447.29 cm^{-1} accompanied by the bands at 1633.50 cm^{-1} to 1647.09 cm^{-1} indicate the presence of physisorbed and coordinated water (-OH group)

(Park et al., 2008). However, the intensity for these IR peaks tends to increase with high acid concentration used especially at long immersion time of 18 hours. The IR peaks intensity remained almost the same for catalysts 2M-Al_2O_3-SO_3H, 3M-Al_2O_3-SO_3H, 4M-Al_2O_3-SO_3H and 5M-Al_2O_3-SO_3H when sulfonated at relatively short immersion time of 6 hours. As observed in Figure 4.27, the magnitudes of these bands for 2M-Al_2O_3-SO_3H, 3M-Al_2O_3-SO_3H, 4M-Al_2O_3-SO_3H and 5M-Al_2O_3-SO_3H at 6 hours immersion time were found to be similar to each other. As discussed in Section 4.4.3, the sulphur contents of 2M-Al_2O_3-SO_3H, 3M-Al_2O_3-SO_3H, 4M-Al_2O_3-SO_3H and 5M-Al_2O_3-SO_3H at 6 hours immersion time catalysts were in the range of 1.14 wt % to 1.36 wt %. This indicated that numbers of active phase (-SO_3H) present on the catalysts were mildly affected by acid concentration.

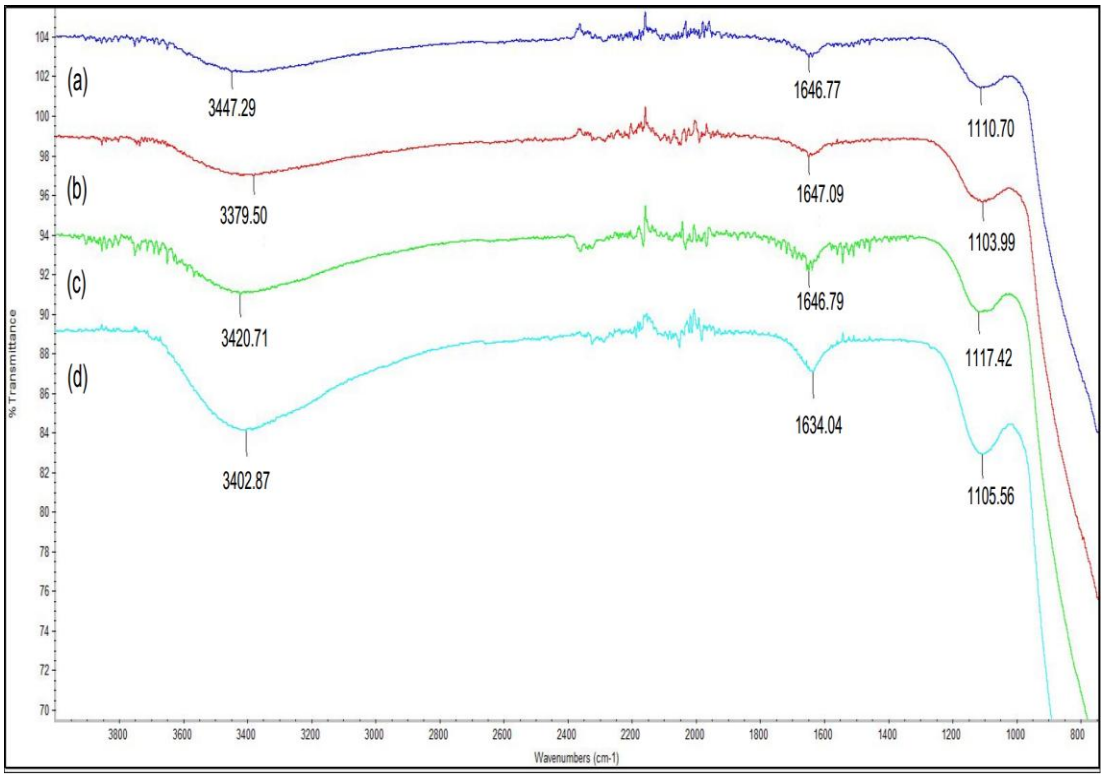

Figure 4.26: FTIR spectra of the effect of acid concentration (a) 2M-Al_2O_3-SO_3H, (c) 3M-Al_2O_3-SO_3H, (d) 4M-Al_2O_3-SO_3H and (e) 5M-Al_2O_3-SO_3H at the immersion time of 6 hours.

FTIR spectra of 2M-Al_2O_3-SO_3H, 3M-Al_2O_3-SO_3H, 4M-Al_2O_3-SO_3H and 5M-Al_2O_3-SO_3H catalysts at 12 hours immersion time are shown in Figure 4.27. From Figure 4.27, the magnitudes of the IR peak for catalysts 2M-Al_2O_3-SO_3H, 3M-Al_2O_3-SO_3H and 4M-Al_2O_3-SO_3H were similar to each other. The IR peaks for catalysts become wider and more intense at 5M acid concentration. As tabulated in Table 4.8, the sulphur contents of 2M-Al_2O_3-SO_3H, 3M-Al_2O_3-SO_3H, 4M-Al_2O_3-SO_3H and 5M-Al_2O_3-SO_3H catalysts as analyzed by EDX increased from 1.16 wt % to 1.75 wt %.

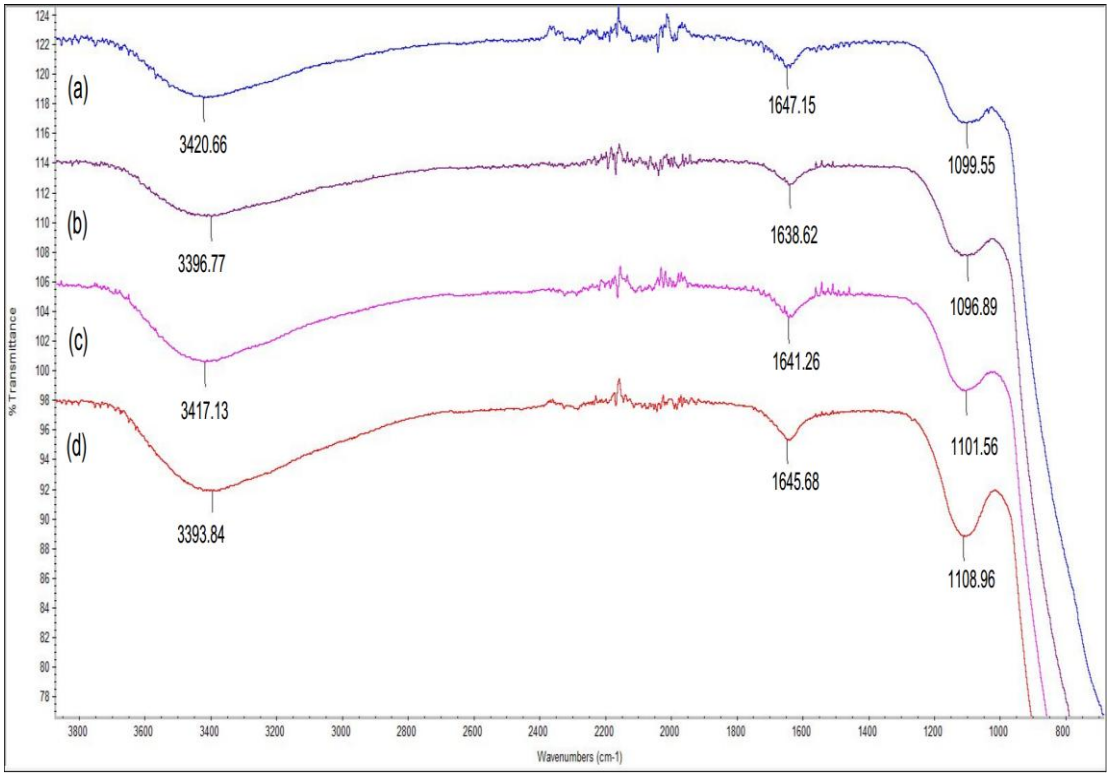

Figure 4.27: FTIR spectra of the effect of acid concentration (a) 2M-Al_2O_3-SO_3H, (c) 3M-Al_2O_3-SO_3H, (d) 4M-Al_2O_3-SO_3H and (e) 5M-Al_2O_3-SO_3H at the immersion time of 12 hours.

Figure 4.28 depicts the FTIR spectra of 2M-Al_2O_3-SO_3H, 3M-Al_2O_3-SO_3H, 4M-Al_2O_3-SO_3H and 5M-Al_2O_3-SO_3H catalysts at 18 hours immersion time. It was found that the 5M-Al_2O_3-SO_3H catalyst has the highest intensity of IR peak at 1077.27 cm^{-1}. As analyzed by EDX, the sulphur content of 5M-Al_2O_3-SO_3H was 3.71 wt%. The higher the IR peaks indicated the higher the sulphur content. High sulphuric groups were active sites bounded on the surface of Al_2O_3. It was expected that 5M-Al_2O_3-SO_3H at 18 hours immersion time had the highest catalytic activity. The effects of acid concentration on catalyst sulphur contents become significant when the catalysts were sulfonated at longer immersion time of more than 12 hours. The catalyst at longest immersion time paired with the highest acid concentration of 5M were contained the highest –SO_3H functional groups in the catalyst.

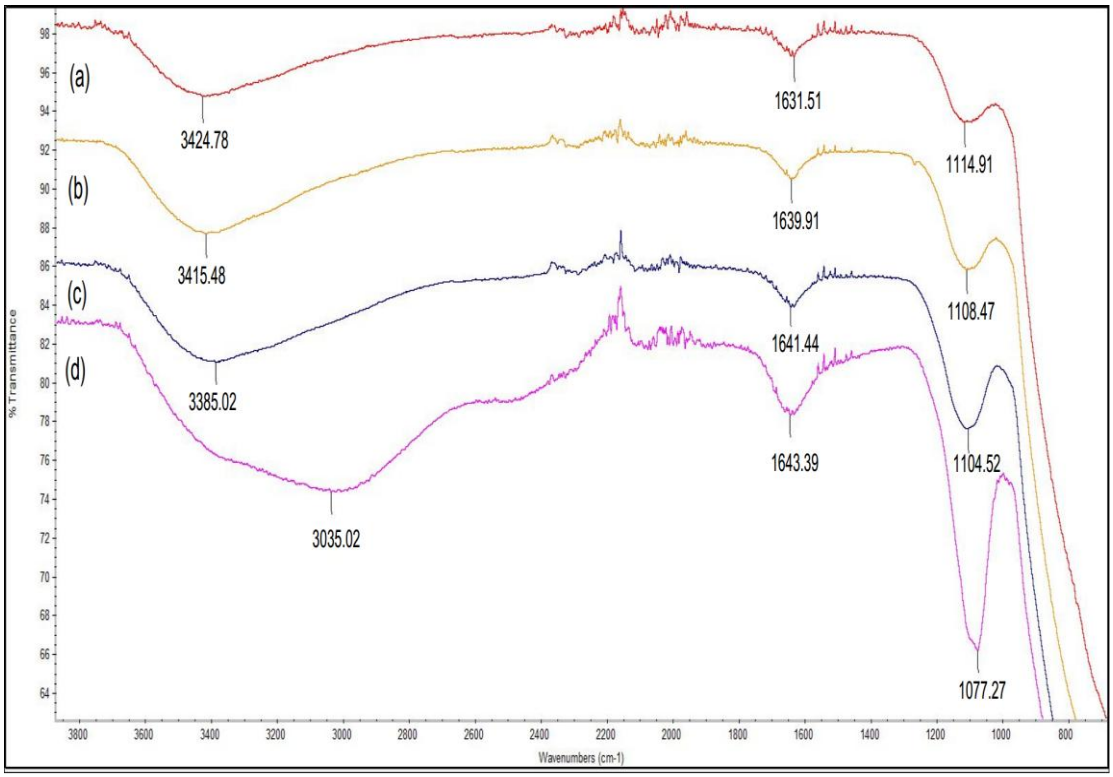

Figure 4.28: FTIR spectra of the effect of acid concentration (a) 2M-Al_2O_3-SO_3H, (c) 3M-Al_2O_3-SO_3H, (d) 4M-Al_2O_3-SO_3H and (e) 5M-Al_2O_3-SO_3H at the immersion time of 18 hours.

4.4.6 X-ray Diffraction (XRD) Analysis

XRD analysis was performed to obtain more information about the catalyst structure. Compared to XRD patterns of original Al_2O_3, the peak intensities for all the sulfonated catalysts of Al_2O_3-SO_3H decreased after the sulfonation process in Figure 4.29, Figure 4.30 and Figure 4,31. XRD patterns showed that all the sulfonated catalysts Al_2O_3-SO_3H had formed of semi amorphous and almost identical to the support. The decrease in the peak intensity indicated a good dispersion of sulphuric acid on alumina (Taufiq-yap et al., 2011). According to Derman et al. (2009), XRD peaks were decreased with the increase of acid concentration. These indicate that H_2SO_4 has reacted with the support Al_2O_3 that originated the stronger acid sites of the catalysts (Taufiq-yap et al., 2011). The typical diffraction peak of Al_2O_3 were at (111), (311), (440) and (400) with a cubic structure (Jian-hong et al., 2009). The three wide peaks of original Al_2O_3 at $2\theta = 37^o$, 45^o and 67^o correspond to diffraction peak of (311), (440) and (400) planes. A single wide peak appeared at $2\theta = 20^o$ was observed for 5M-Al_2O_3-SO_3H catalyst at 18 hours immersion time. This results agrees with Changyou et al. (2015) which claims that a certain regular structure may exist in the Al_2O_3-SO_3H.

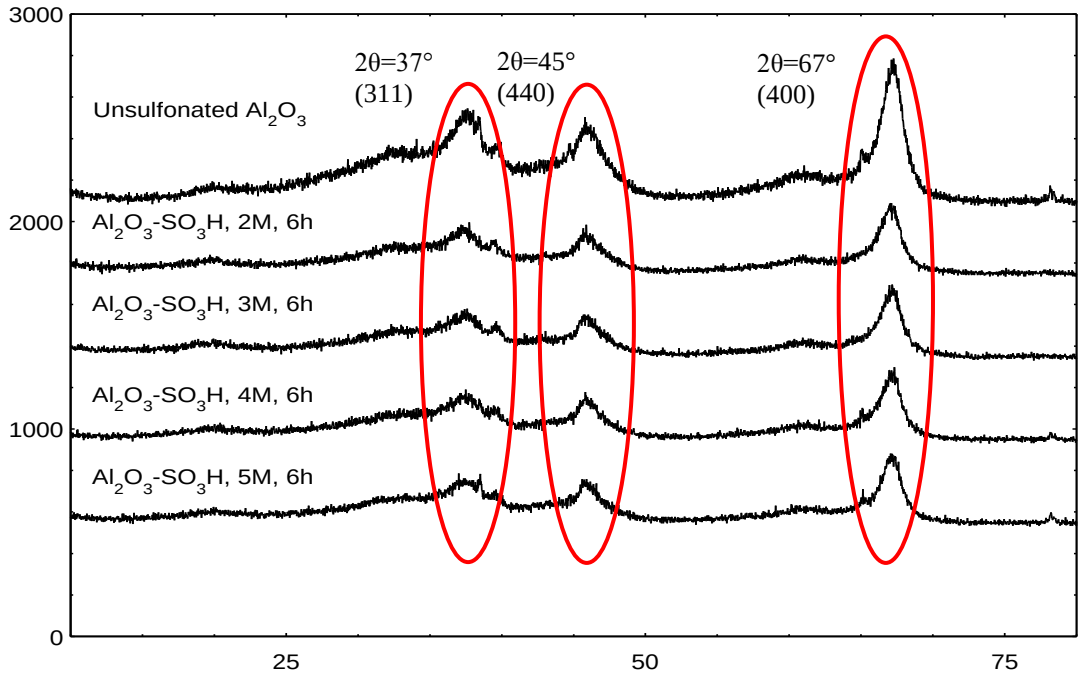

Figure 4.29: XRD patterns of 2M-Al_2O_3-SO_3H, 3M-Al_2O_3-SO_3H, 4M-Al_2O_3-SO_3H and 5M-Al_2O_3-SO_3H at immersion time of 6 hours.

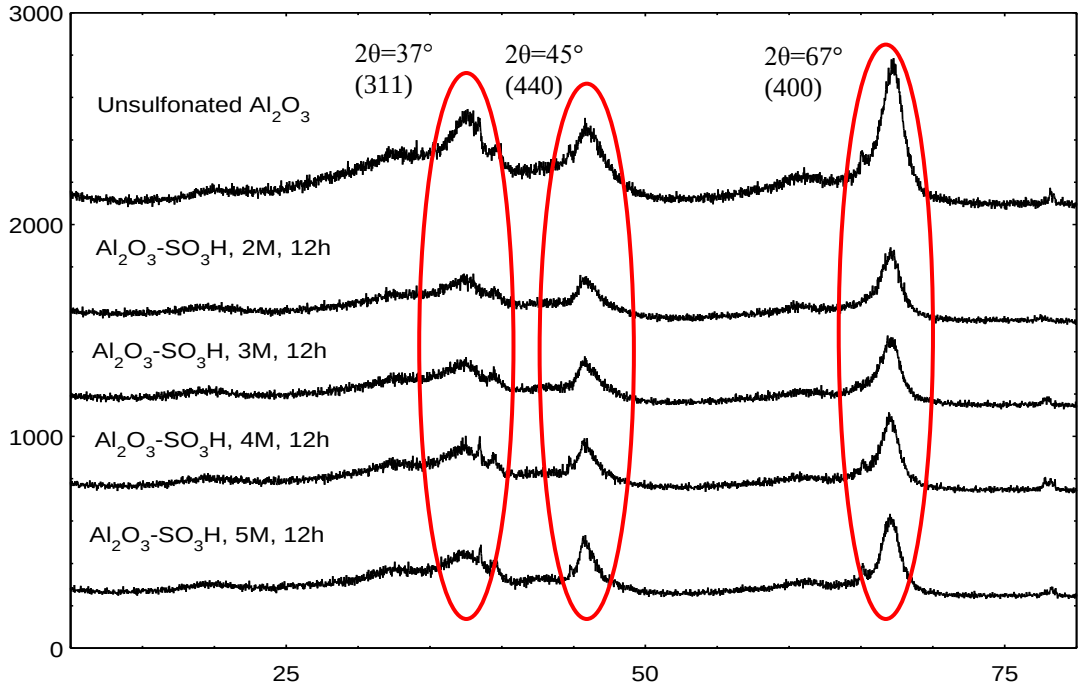

Figure 4.30: XRD patterns of 2M-Al_2O_3-SO_3H, 3M-Al_2O_3-SO_3H, 4M-Al_2O_3-SO_3H and 5M-Al_2O_3-SO_3H at immersion time of 12 hours.

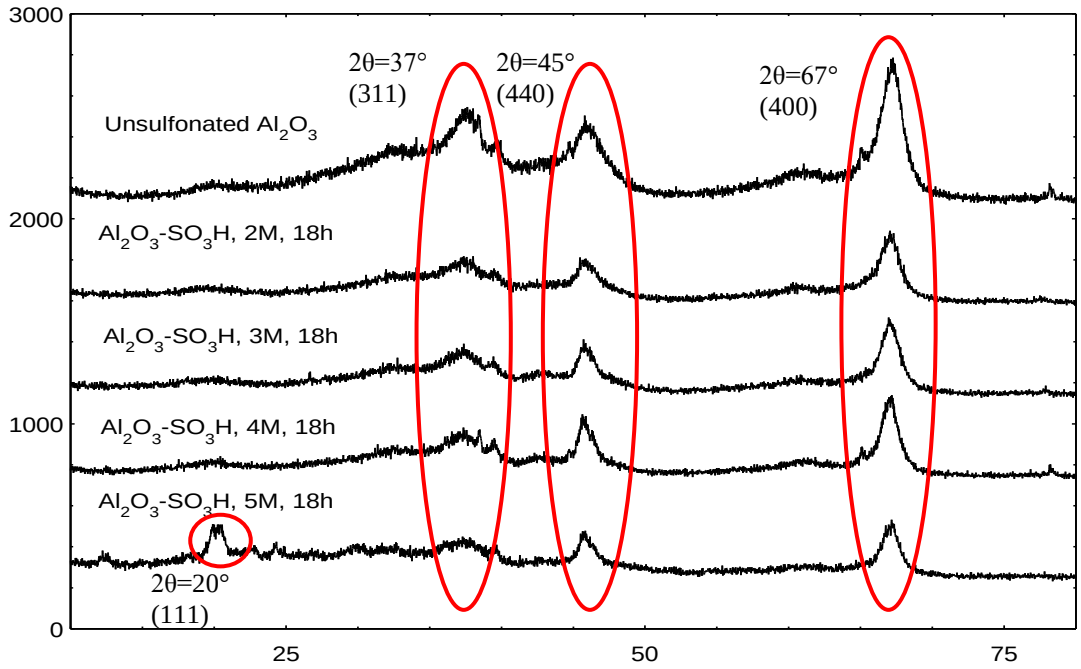

Figure 4.31: XRD patterns of 2M-Al_2O_3-SO_3H, 3M-Al_2O_3-SO_3H, 4M-Al_2O_3-SO_3H and 5M-Al_2O_3-SO_3H at immersion time of 18 hours.

4.4.7 Catalytic activity: Biodiesel yield

Four levels of acid concentration (2M, 3M, 4M and 5M) were used to sulfonate the alumina support and the catalyst activities were tested through esterification of PFAD. Figure 4.32 shows the effect of acid concentration on biodiesel yield at 6 hours immersion time. In general, the acid concentration did not generate significant impact on catalytic activity as can be seen from biodiesel yield. The biodiesel yield ranges from 0.71 % to 4.68 % after 6 hours reaction time which was rather low. This may be caused by the low sulphur content of the catalysts. As mentioned earlier in Section 4.4.1, specific surface areas for the catalyst were drastically reduced when the catalyst has immersed in high acid concentration. However, biodiesel yield obtained were not affected by the specific surface area of the catalysts. Apparently,

the catalytic activity was affected by sulphur content rather than the surface area. It was reported that higher sulphur content corresponded to higher catalyst acidity and thus higher catalytic activity in biodiesel production (Kiss et al., 2006).

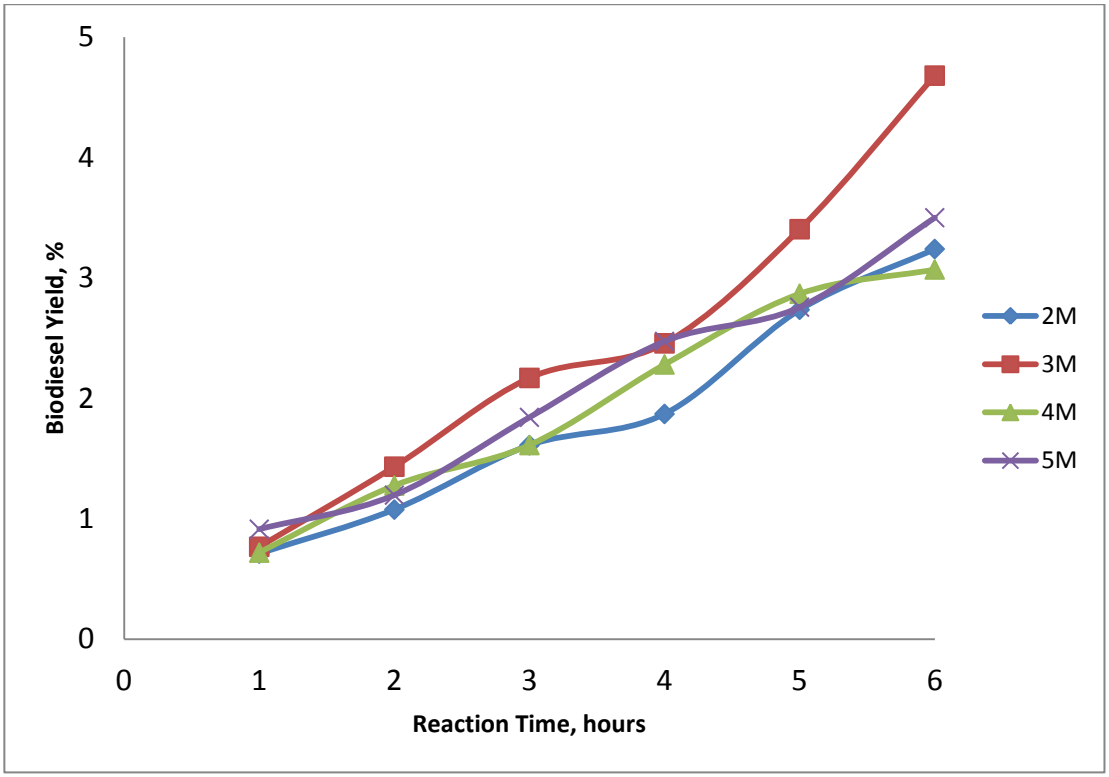

Figure 4.32: Biodiesel yield at 6 hours immersion time.

From Figure 4.33, for the catalysts 2M-Al_2O_3-SO_3H, 3M-Al_2O_3-SO_3H and 4M-Al_2O_3-SO_3H at 12 hours immersion time, the biodiesel yield of the catalysts were very low, ranging from 0.58 % to 4.02 %. There was a slight increment on the biodiesel yield for catalyst 5M-Al_2O_3-SO_3H, it produced the highest biodiesel yield, 7.44 %. Compared to other catalysts, the sulphur content of 5M-Al_2O_3-SO_3H was 1.75 wt% and it was the highest sulphur content. The increase in sulphur content has led to the increase in biodiesel yield. The specific surface area for 2M-Al_2O_3-SO_3H,

3M-Al_2O_3-SO_3H, 4M-Al_2O_3-SO_3H and 5M-Al_2O_3-SO_3H were 152.09 m^2/g, 67.89 m^2/g, 42.88 m^2/g and 18.65 m^2/g respectively. In view of that, the specific surface area of the catalyst did not affect the biodiesel yield obtained.

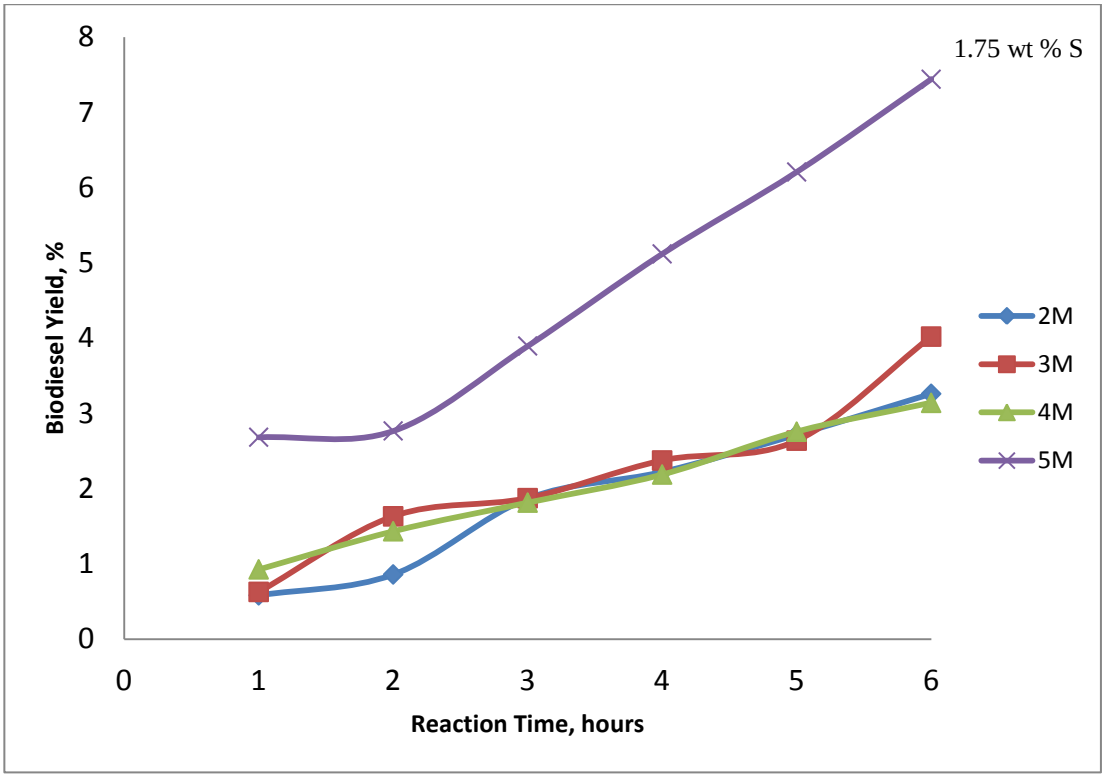

Figure 4.33: Biodiesel yield at 12 hours immersion time.

The catalytic performances of sulfonated catalysts 2M-Al_2O_3-SO_3H, 3M-Al_2O_3-SO_3H, 4M-Al_2O_3-SO_3H and 5M-Al_2O_3-SO_3H at 18 hours immersion time were displayed in Figure 4.34. The biodiesel yield for catalysts 2M-Al_2O_3-SO_3H, 3M-Al_2O_3-SO_3H, 4M-Al_2O_3-SO_3H and 5M-Al_2O_3-SO_3H were 12.47 %, 8.31 %, 25.68 % and 57.49 % respectively.

In conclusion, the increase in acid concentration used in sulfonation process would increase the biodiesel yield when the catalyst sulfonated at sufficient long

immersion time of 18 hours. More sulphur compounds were able to attach on the catalyst when the catalysts were allowed to contact with concentrated sulphuric acid at sufficient time. Thus, biodiesel yield increased due to the high contents of active sites in the catalyst. High acid concentration of 5M was designed to be used to sulfonate alumina support during the catalyst preparation stage. In general, biodiesel yield at 18 hours immersion time were quite low at 2M and 3M regardless of the reaction time. However, 5M acid concentration paired with 18 hours obtained the biodiesel yield from 20% to 60 %. The longer immersion time and higher acid concentration had significantly enhanced the sulphur content (3.71 wt %), and thus increased the biodiesel yield. The lowest specific surface area of 5M-Al_2O_3-SO_3H at 18 hours immersion time (7.64 m^2/g) did not affect the biodiesel yield. In conclusion, the sulphur content of the catalyst was more essential than the specific surface area.

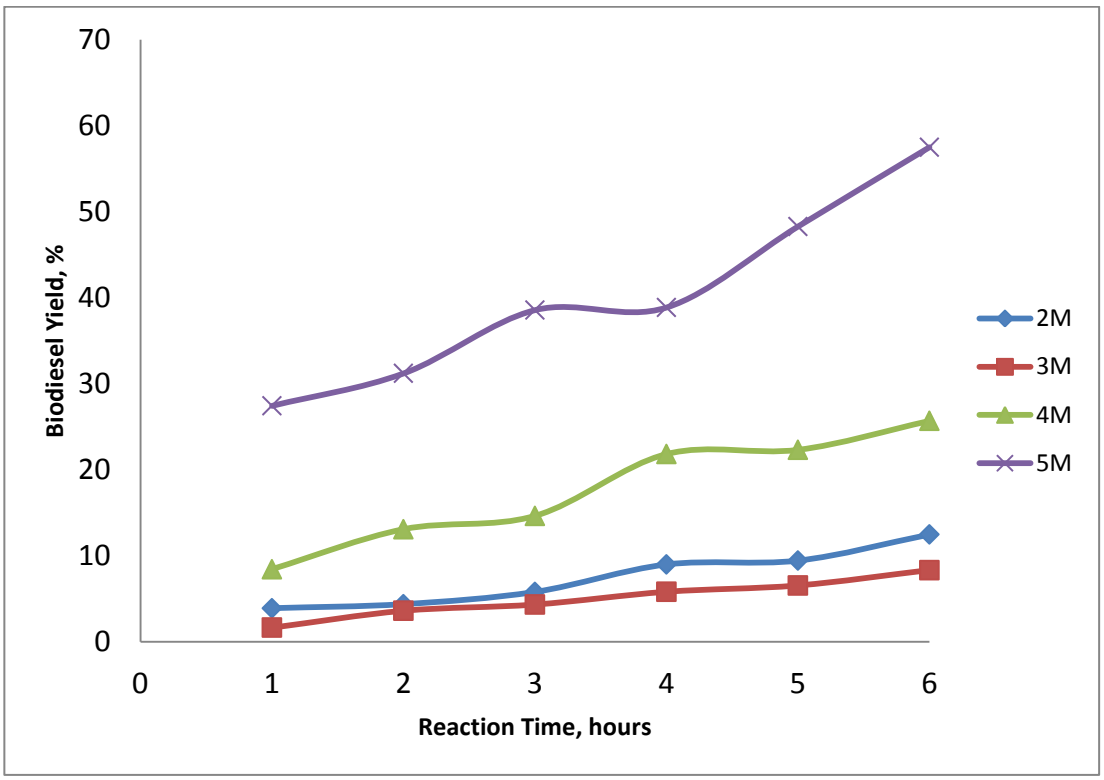

Figure 4.34: Biodiesel yield at 18 hours immersion time.

4.5 Statistical Study

Table 4.13 presents the results of analysis of variance (ANOVA) which show the levels of significance for the model and individual model terms. Based on Table 4.13, the model with Prob > F value less than 0.05 implied the model was significant. In this case, A (acid concentration), B (immersion time), A^2, B^2, C^2, AB, BC, C^3, A^2B, AC^2 and BC^2 were significant model terms because 'Prob > F' were <0.0001. Although the 'Prob > F' for C (reaction time), AC, ABC, A^2C, AB^2, B^2C and A3 terms were larger than 0.05, but the variables were included in the model to improve its R^2 value from 0.9281 to 0.9426.

The empirical model in terms of actual factors is shown in Table 4.14. The reliability levels of the generated empirical model for the response could be verified through the values of correlation coefficient (R^2) and adequate precision. Table 4.15 shows the R^2 value of 0.9426 for this cubic model. In term of adequate precision, it measures the signal to noise ratio, a ratio greater than 4 is desirable. In this study, the adequate precision was 33.483, this indicated an adequate signal. Hence, this model can be used to navigate the design space.

Table 4.13: Analysis of variance (ANOVA) of the variable

Source	Sum of Squares	df	Mean Square	F Value	p-value Prob > F
Model	19.57	18	1.09	59.35	< 0.0001
A-Acid concentration	0.13	1	0.13	7.36	0.0085
B-Immersion time	1.41	1	1.41	77.02	< 0.0001
C-Reaction time	0.024	1	0.024	1.32	0.2555
AB	0.89	1	0.89	48.66	< 0.0001
AC	0.027	1	0.027	1.49	0.2266
BC	0.28	1	0.28	15.45	0.0002
A^2	0.22	1	0.22	11.99	0.0010
B^2	1.11	1	1.11	60.65	< 0.0001
C^2	1.41	1	1.41	77.03	< 0.0001
ABC	0.035	1	0.035	1.90	0.1725
A^2B	0.22	1	0.22	12.21	0.0009
A^2C	6.390×10^{-3}	1	6.390×10^{-3}	0.35	0.5568
AB^2	0.025	1	0.025	1.35	0.2489
AC^2	0.094	1	0.094	5.13	0.0269
B^2C	0.071	1	0.071	3.88	0.0533
BC^2	0.33	1	0.33	18.28	< 0.0001
A^3	4.748×10^{-3}	1	4.748×10^{-3}	0.26	0.6124
B^3	0.000	0			
C^3	0.53	1	0.53	28.77	< 0.0001
Residual	1.19	65	0.018		
Cor Total	20.76	83			

Table 4.14: Final empirical models in coded factors

Types of catalyst	Empirical models
Catalyst Al_2O_3-SO_3H	Log_{10} (Biodiesel Yield + 0.57)= 0.45 + 0.22 * A + 0.31 * B + 0.084 * C + 0.17 * AB + 0.036 * AC + 0.11 * BC + 0.12 A^2 + 0.24 * B^2 – 0.34 C^2 + 0.05 * ABC + 0.14 * A^2B + 0.029 * A^2C + 0.049 * A B^2 – 0.12 A C^2 + 0.092 B^2C – 0.2 *B C^2 – 0.038 A^3 + B^3 + 0.38 C^3

Table 4.15: Summarization of the ANOVA for the Dependent Responses

Types of transformation	Model of Hierarchy	Significant model terms	R^2	Adjusted R^2	Predicted R^2	Adequate precision
Base 10 Log	Cubic	A, B, A^2, B^2, C^2, AB, BC, C^3, A^2B, AC^2, BC^2	0.9426	0.9268	0.8822	33.483

The reliability of the model also can be determined from predicted versus actual plot. As shown in Figure 4.36, the experiment results were in well agreement with the predicted biodiesel yields. The normal probability plot of the residuals for the response is presented in Figure 4.35. It can be seen that the residuals were distributed near to the straight line. This indicated the underlying error distribution was normal. All the normal probability plots with sample from a normal distribution centred at zero mean that there was no severe indication of non-normality of the experimental results (Sim et al., 2007).

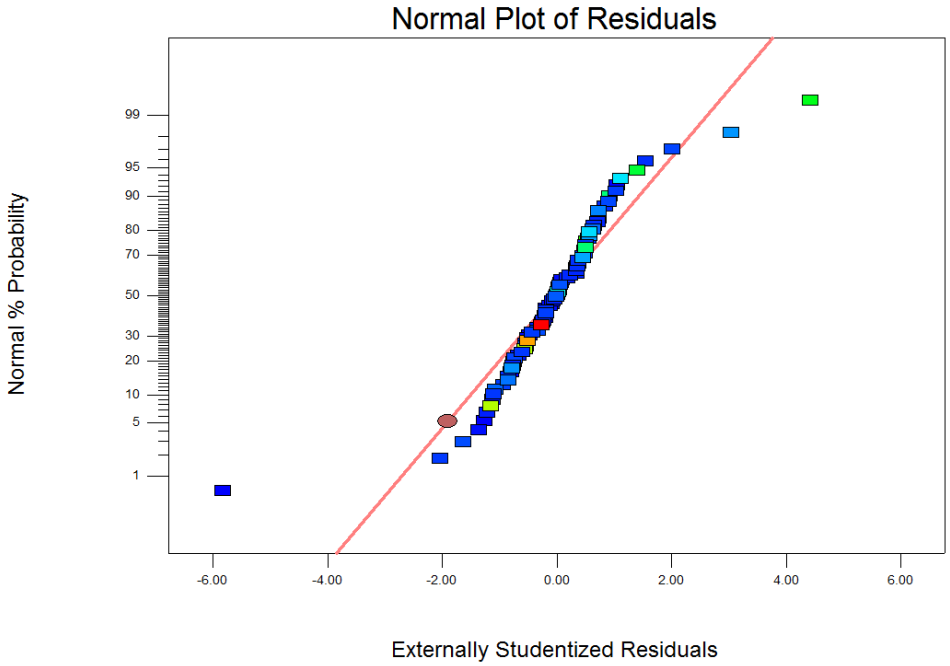

Figure 4.35: Normal probability plot of residuals for biodiesel response

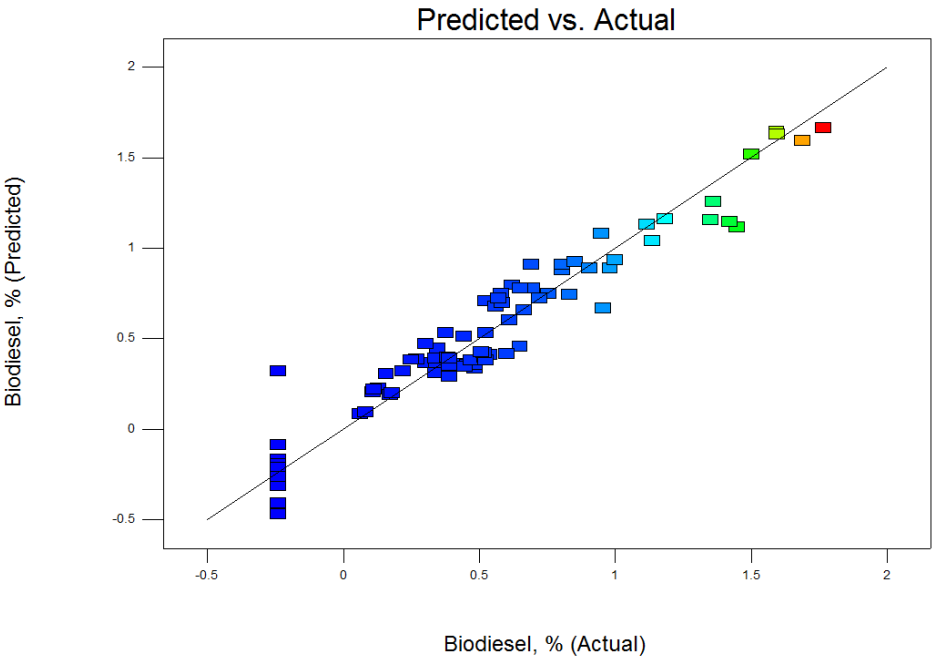

Figure 4.36: Predicted versus actual biodiesel yield

Figure 4.37-4.39 shows the interaction between acid concentration and immersion time on the biodiesel at different reaction time. At the beginning, the interaction between the acid concentration and immersion time was very low as displayed in Figure 4.37 with 3-D surface and 2-D contour plots. The 3-D surface and 2-D contour plots appeared in dark blue. The contour occurred in light blue when the biodiesel yield was increased at 5 M acid concentration and 18 hours immersion time.

In general, higher acid concentration used for catalyst treatment combined with longer immersion time would result in higher biodiesel yield regardless of reaction time. All the response surface plots at 1 hour, 3 hours and 6 hours reaction time (Figure 4.37, Figure 4.38 and Figure 4.39) displayed nearly the same surface curvature. Non productive areas for biodiesel were detected at short immersion time of 6 hours paired with low acid concentration of 2M for all the response surface plots.

Immersion time used to achieve high biodiesel yield can be shorten by using high acid concentration (5M). Thus, it was advisable to immerse the catalyst in sulphuric acid at high concentration of 5M and at minimum18 hours immersion time. This was to ensure sufficient time of contact between active phases of sulfonic groups to attach on the alumina support. Thus, the influences of factors of acid concentration and immersion time on biodiesel yield were more pronounced compared to reaction time as verified in ANOVA test in Section 4.5. Besides, there was an interaction between immersion time and acid concentration. Highest acid concentration used but paired with low immersion time (6 hours and 12 hours) would

also result in low biodiesel yield. For 3 hours reaction time, yellow colour indicates the highest biodiesel yield of 47.39 % obtained at higher acid concentration (5M) and longer immersion time (18 hours). For 6 hours reaction time, red colour indicates the highest biodiesel yield of 64.11 % obtained at higher acid concentration (5M) and longer immersion time (18 hours).

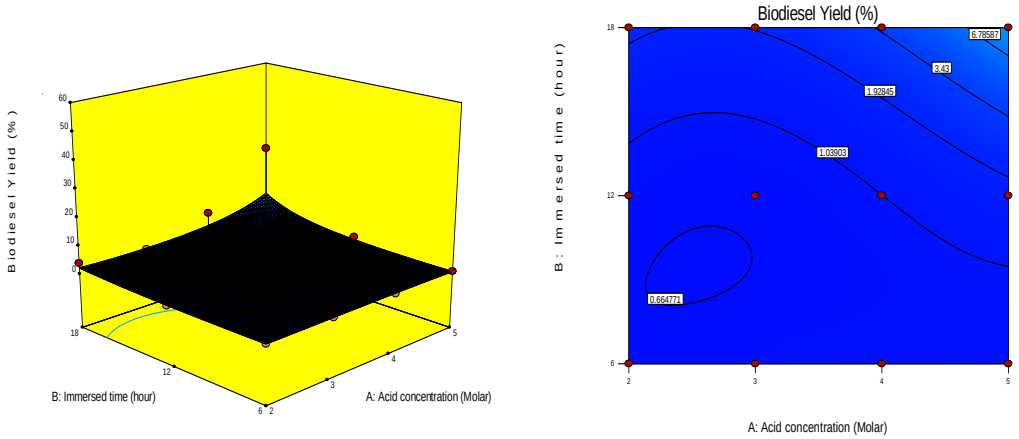

(a) (b)

Figure 4.37: Response surface plot of the interaction between acid concentration and immersion time on biodiesel yield at 1 hour reaction time.

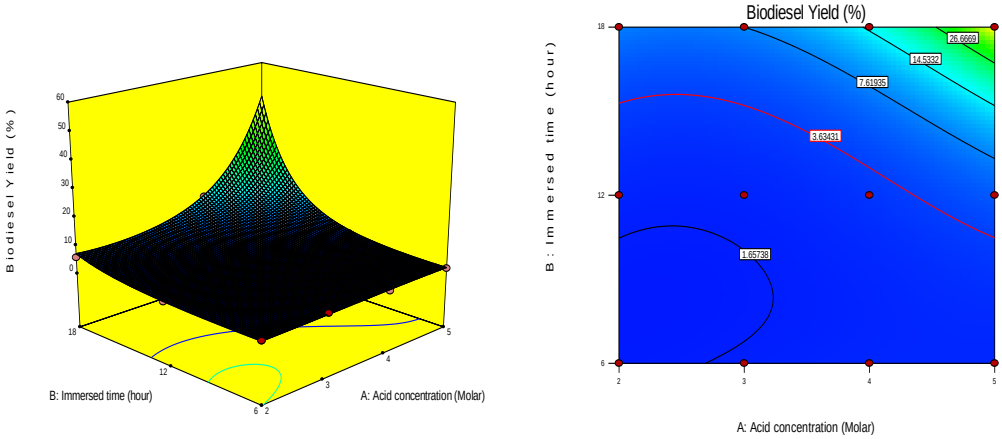

(a) (b)

Figure 4.38: Response surface plot of the interaction between acid concentration and immersion time on biodiesel yield at 3 hours reaction time.

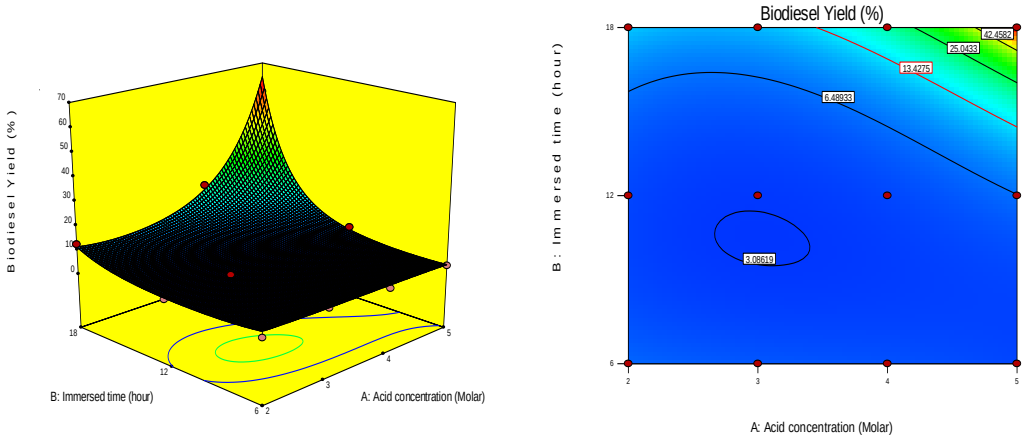

(a) (b)

Figure 4.39: Response surface plot of the interaction between acid concentration and immersion time on biodiesel yield at 6 hours reaction time.

4.6 Optimization Study

In this study, numerical optimization was carried out to find the optimum acid concentration and immersion time which resulted in maximum biodiesel yield using Design Expert 9.0 software. Criterions set for optimization are shown in Table 4.16. The aim for the optimization process was to achieve the highest biodiesel yield in the shortest reaction time.

Table 4.16: Constraint for optimization solution

Factor	Criteria	Goal	Lower Limit	Upper Limit
A	Acid concentration	in range	2	5
B	Immersion time	in range	6	18
C	Reaction time	minimum	0	360
	Biodiesel Yield	maximum	0	57.49

The optimum condition was suggested by Design Expert 9.0 based on the criteria set in Table 4.16. The estimated of 56.25 % of biodiesel yield was obtained at 6 hours by using Al_2O_3-SO_3H as solid acid catalyst immersed in 5 M of acid concentration and 18 hours of immersion time.

The experimental work was performed by using the optimum conditions suggested in Table 4.17. The biodiesel yield of 57.49 % was obtained with 2.2 % error compared to the predicted value (56.25 %). The predicted biodiesel yield based on empirical model was in well agreement with experimental data with error about ±5 %.

Table 4.17: Numerical Optimization

Acid concentration	Immersion time	Reaction time	Biodiesel yield	Desirability
5	18	360	56.252	0.979

4.7 Biodiesel purification using polymeric membrane

The biodiesel mixture was produced from the esterification of PFAD at 80 ºC reaction temperature, 2 wt% of sulfonated 5M-18h catalyst to PFAD mass ratio, 20:1 methanol to PFAD molar ratio and 6 hours reaction time. The biodiesel mixture was purified using the 5 kD and 20 kD polyethersulfone (PES) and 30 kD and 100 kD polyvinylidene fluoride (PVDF) membranes.

4.7.1 Effects of transmembrane pressure and molecular weight cut-off (MWCO)

Figure 4.40 presents the permeate flux obtained at different transmembrane pressure and at different molecular cut-off (MWCO) of PES and PVDF membranes. Biodiesel mixtures were filtered through 5 kD and 20 KD MWCO and at 5 bar and 3 bar respectively. For PVDF membranes, biodiesel mixtures were passed through 30 kD and 100 kD MWCO and at 2 bar and 1 bar transmembrane pressures respectively. Based on the preliminary study, smaller MWCO of PES membranes required higher transmembrane pressure of 3-5 bar to allow the biodiesel mixture passing through the membrane. On the contrary, PVDF membranes with higher MWCO required low transmembrane pressure (1-2 bar) for the separation.

For the tested transmembrane pressure, the flux decreases were observed for each evaluated membranes, showing that longer separation time resulted in a drop in permeate fluxes at the end of separation time. At the first 10 minutes of separation time, filtration with 30 kD PVDF membrane resulted in the highest permeate flux

compared to the others. For the 20 kD PES membrane at 3 bar transmembrane pressure, permeate flux declined drastically for the first 40 minutes, from 16.45 $x10^{-6}$ to 9.87 $x10^{-6}$ m^3/m^2s. On the contrary, low MWCO of 5 kD PES membrane at 5 bar resulted in slow decline of permeate flux from 10.75 $x10^{-6}$ to 6.03 $x10^{-6}m^3/m^2s$ at 60 minutes separation time. The membrane with higher MWCO exhibited higher permeates flux at the end of separation. Table 4.18 shows the observed final flux of 5 kD and 20 kD PES membranes and 30 kD and 100 kD PVDF membranes. The final permeate flux achieved at the ascending order as PES 5 kD< PVDF 30 kD< PES 20 kD< PVDF 100 kD.

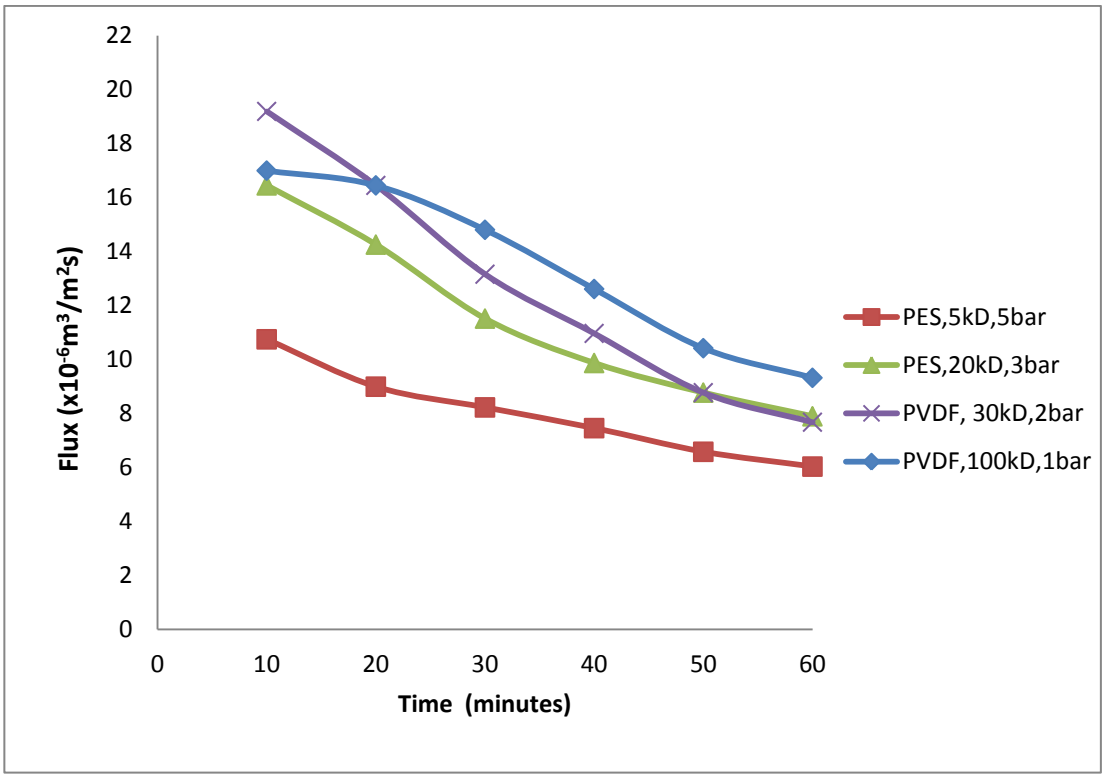

Figure 4.40: Permeate fluxes of biodiesel at 5, 3, 2 and 1 bar of transmembrane pressures throughout 5 kD and 20 kD PES membranes and 30 kD and 100 kD PVDF membranes.

Table 4.18: Final flux throughout PES and PVDF membranes.

Molecular cut-off (MWCO)	PES 5 kD	PES 20 kD	PVDF 30 kD	PVDF 100 kD
Pressure (bar)	5	3	2	1
Final flux ($x10^{-6}m^3/m^2s$)	6.03	7.89	7.68	9.32

4.7.2 Permeate composition: palmitic acid

Figure 4.41 and Table 4.19 show the percentage reduction of palmitic acid at 10, 30 and 60 minutes of separation time. For all types of polymeric membranes, the increase in separation time tends to decrease the percentage of palmitic acid in permeate. PES 5 kD at 10 and 30 minutes gave the highest percentage reduction of palmitic acid, followed by PVDF 30 kD, PES 20 kD and PVDF 100 kD. The PVDF 100 kD obtained the lowest percentage reduction at 10 and 30 minutes. This 100 kD PVDF membrane did not show promising values for biodiesel purification due to the relatively large pore size that allowed fast flow of palmitic acid permeate through the membrane easily.

Although PES and PVDF membranes exhibited flux decline throughout the separation process, 5 kD of PES membrane had the good percentage reduction of palmitic acid (78.76 % at 10 minutes) in overall. Previous study reported that PES membrane showed high rejections of palm oils based fatty acids and had poor

permeate flux. Nonetheless, PVDF membrane exhibited higher flux and resulted in low fatty acid rejections (Amin et al., 2010).

Table 4.19: Percentage reduction of palmitic acid at 10 and 30 minutes of separation time.

	Palmitic acid	
	Percentage reduction at 10 minutes	**Percentage reduction at 30 minutes**
PES 5 kD	78.76	45.19
PES 20 kD	45.14	27.01
PVDF 30 kD	46.95	35.51
PVDF 100 kD	24.69	16.52

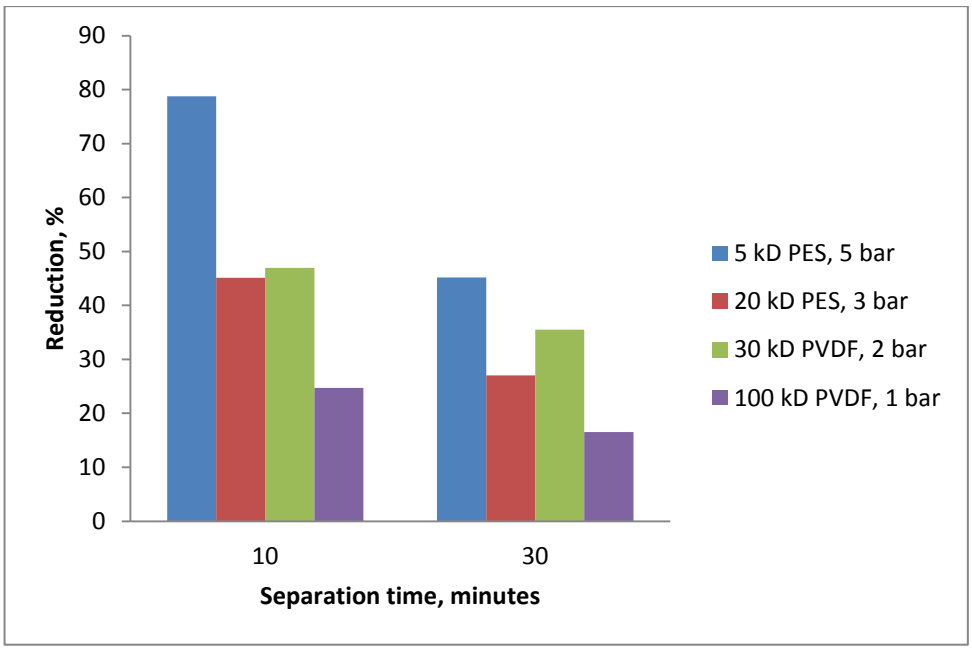

Figure 4.41: Percentage reductions of palmitic acid at 10 and 30 minutes separation time.

4.7.3 Permeate composition: oleic acid

Percentage reduction of oleic acid at 10 and 30 minutes of separation are shown in Table 4.20 and Figure 4.42. For all types of polymeric membranes, the increased in separation time tends to decrease the percentage of oleic acid in permeate. PES 5 kD at 10 and 30 minutes gave the highest percentage reduction of oleic acid, followed by PES 20 kD, PVDF 30 kD and PVDF 100 kD. The PVDF 100 kD obtained the lowest percentage reduction at 10 and 30 minutes. This 100 kD PVDF membrane did not show promising values for biodiesel purification due to the relatively large pore size that allowed fast flow of oleic acid permeate through the membrane easily.

Although PES and PVDF membranes exhibited flux decline throughout the separation process, 5 kD of PES membrane had the good percentage reduction of oleic acid (93.73 % at 10 minutes) in overall. The percentage reduction in oleic acid is higher than the palmitic acid reduction. This was due to the long hydrocarbon chain length of oleic acid compared to palmitic acid (Amin et al., 2010). Therefore, the reduction value for each type of fatty acids can be determined according to the sequence of hydrocarbon chain length (oleic acid > palmitic acid) (Amin et al., 2010).

Table 4.20: Reduction of oleic acid at 10, 30 and 60 minutes of separation time.

	Oleic acid	
	Percentage reduction at 10 minutes	**Percentage reduction at 30 minutes**
PES 5 kD	93.73	52.16
PES 20 kD	71.16	53.60
PVDF 30 kD	58.93	37.44
PVDF 100 kD	41.87	23.93

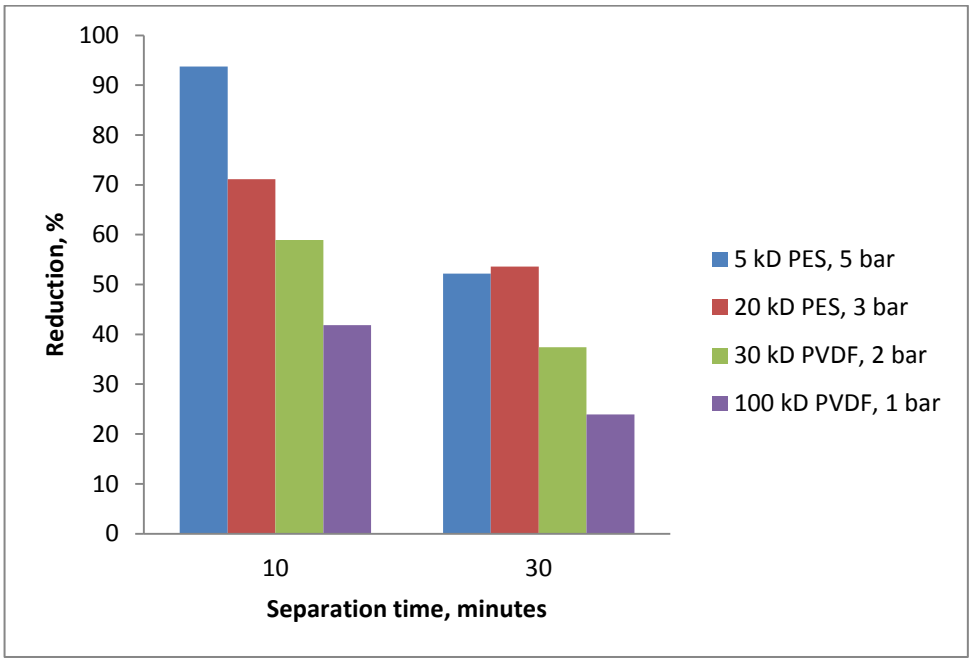

Figure 4.42: Percentage reductions of oleic acid at 10 and 30 minutes separation time.

Biodiesel mixture obtained through esterification reaction was recommended to be purified using 5 kD of PES membrane and at 5 bar transmembrane pressure. The permeate flux obtained with this membrane was quite stable with final flux of 6.03 $x10^{-6}m^3/m^2s$. Besides, the biodiesel purification results obtained with this membrane was quite promising with 78.76 % reduction of palmitic acid and 93.73 % reduction of oleic acid.

CHAPTER 5

CONCLUSION AND RECOMMENDATION

5.1 Conclusion

Among the tested catalysts (Al_2O_3-SO_3H, SiO_2-SO_3H and TiO_2-SO_3H), Al_2O_3-SO_3H possessed the desired criteria of a good catalyst with high sulphur content of 3.71 wt %. In term of the catalytic activity which based on the biodiesel yield, Al_2O_3-SO_3H was found to be the most promising catalyst. Esterification with Al_2O_3-SO_3H had achieved the maximum biodiesel yield of 57.49 % at 6 hours reaction time. At longer immersion time of 12 hours and 18 hours, the increase in acid concentration for sulfonation process would lead to the increasing trend of the catalyst sulphur content. However, at shorter immersion time of 6 hours, the increased in acid concentration did not have significant effect on sulphur content of catalysts from 2M to 5M. The longest immersion time (18h) paired with the highest acid concentration (5M) gave the most promising catalyst performance with 57.49 % biodiesel yield at 6 hours reaction time. For the membrane purification process, biodiesel mixture obtained through esterification reaction was recommended to be purified using 5 kD of PES membrane and at 5 bar transmembrane pressure. Besides, the biodiesel purification results obtained with this membrane was quite promising with 78.76 % reduction of palmitic acid and 93.73 % reduction of oleic acid.

5.2 Recommendation

The recommendations are proposed in the further research as stated below:

1. Other low cost feedstocks such as recycled oils (waste cooking oil and waste engine oils) are proposed to be carried out in esterification reaction by using Al_2O_3-SO_3H.
2. The other operating parameters of esterification of PFAD such as amount of catalyst, methanol to oil molar ratio, reaction temperature should be studied in order to obtain the optimum conditions.
3. The esterifiction of PFAD can be carried out at a higher reaction temperature to produce higher biodiesel yield.
4. The other operating parameters of the biodiesel purification via membrane process such as temperature and pH should be studied in order to obtain the optimum conditions.

REFERENCES

Abdoulmoumine, N., 2010. *Sulfate and Hydroxide Supported on Zirconium Oxide Catalysts for Biodiesel Production Sulfate and Hydroxide Supported on Zirconium Oxide Catalysts for Biodiesel Production*. Thesis, Virginia Polytechnic Institute and State University.

Agarwal, A.K., 2007. Biofuels (alcohols and biodiesel) applications as fuels for internal combustion engines. *Process in energy and combustion science*, 33, pp.233–271.

Almeida, R.M., Noda, L.K., Goncalves, N.S., Meneghetti, S.M.P. and Meneghetti, M.R., 2008. Transesterification reaction of vegetable oils , using superacid sulfated TiO 2 – base catalysts. *Applied Catalysis A : General*, 347(3), pp.100–105.

Amin, I.N.H.M., Mohammad, A.W., Markom, M. and Leo, C.P, 2010. Effects of palm oil-based fatty acids on fouling of ultrafiltration membranes during the clarification of glycerin-rich solution. *Journal of Food Engineering*, 101(3), pp.264–272.

Atabani, a. E. et al., 2012. A comprehensive review on biodiesel as an alternative energy resource and its characteristics. *Renewable and Sustainable Energy Reviews*, 16(4), pp.2070–2093.

Atadashi, I.M., Aroua, M.K., Aziz, A.R.A. and Sulaiman N.M.N., 2012. Production of biodiesel using high free fatty acid feedstocks. *Renewable and Sustainable Energy Reviews*, 16(5), pp.3275–3285..

Atadashi, I.M., Aroua, M.K., Aziz, A.R.A. and Sulaiman N.M.N., 2011. Refining technologies for the purification of crude biodiesel. *Applied Energy*, 88(12), pp.4239–4251.

Atadashi, I.M., Aroua, M.K. and Aziz, a. A., 2010. Biodiesel separation and purification: A review. *Renewable Energy*, 36(2), pp.437–443.

Awalludin, M.F., Sulaiman, O., Hashim, R. and Nadhari, W.N.A.W., 2015. An overview of the oil palm industry in Malaysia and its waste utilization through thermochemical conversion, specifically via liquefaction. *Renewable and Sustainable Energy Reviews*, 50, pp.1469–1484.

Balat, M. and Balat, H., 2009. Recent trends in global production and utilization of bio-ethanol fuel. *Applied Energy*, 86(11), pp.2273–2282.

Banga, S. and Varshney, P.K., 2010. Effect of impurities on performance of biodiesel : A review. *Scientific & Industrial Research*.

Benjapornkulaphong, S., Ngamcharussrivichai, C. and Bunyakiat, K., 2009. Al2O3-supported alkali and alkali earth metal oxides for transesterification of palm kernel oil and coconut oil. *Chemical Engineering Journal*, 145(3), pp.468–474.

Berrios, M., Martín, M. A. and Martín, A., 2010. Study of esterification and transesterification in biodiesel production from used frying oils in a closed system. *Chemical Engineering Journal*, 160(2), pp.473–479.

Berrios, M. and Skelton, R.L., 2008. Comparison of purification methods for biodiesel. *Chemical Engineering Journal*, 144, pp.459–465.

Borges, M.E. and Díaz, L., 2012. Recent developments on heterogeneous catalysts for biodiesel production by oil esterification and transesterification reactions: A review. *Renewable and Sustainable Energy Reviews*, 16(5), pp.2839–2849.

Bp, 2012. *BP Statistical Review of World Energy June 2012*, BP. Available at: www.bp.com/statisticalreview.

Brunauer, S., Emmett, P.H. and Teller, E., 1938. Adsorption of gases in multimolecular layers. *Journal of the American Chemical Society*, 60(2), pp. 309-319.

Changyou, G., Zhiqi, S., Shaojun, W. and Fengxiang, L., 2015. The solvothermal synthesis , structure and properties of Al_2O_3 & TiO_2 mesoporous material. *Materials Chemistry and Physics journal*, 151, pp.288–294.

Cheah, K.Y., Toh, T.S. and Koh, P.M., 2008. Palm fatty acid distillate biodiesel : Next-generation palm biodiesel. *AmericanOil Chemistry' Society* , pp.264–266.

Cho, H.J., Kim, J.K., Hong, S.W. and Yeo, Y.K., 2012. Development of a novel process for biodiesel production from palm fatty acid distillate (PFAD). *Fuel Processing Technology*. 104, pp.271–280.

Chorkendorff, I. and Niemantsverdriet, J.W., 2007. *Concepts of Modern Catalysis and Kinetics*,

Corro, G. et al., 2011. Biodiesel from waste frying oil. Two step process using acidified SiO2 for esterification step. *Catalysis Today*, 166(1), pp.116–122.

Derman, M.N., Nasuha, M., Halim, A. and Shamsudin, S.R., 2009. The Influence of Sulphuric Acid Concentration on Hard Anodising Process of Powder Metallurgy Al-Mg. *Journal of Nuclear And Related Technologies*, 6(1), pp.224–229.

Encinar, J.M., González, J.K., Pardal, A. and Martinez, G., 2010. Rape oil transesterification over heterogeneous catalysts. *Fuel Processing Technology*, 91(11), pp.1530–1536.

Eterigho, E.J., Lee, J.G.M. and Harvey, A.P., 2011. Triglyceride cracking for biofuel production using a directly synthesised sulphated zirconia catalyst. *Bioresource Technology*, 102(10), pp.6313–6316.

Ferrero, G.O., Almeida, M.F., Alvim-Ferraz, M.C.M. and Dias, J.M., 2014. Water-free process for eco-friendly puri fi cation of biodiesel obtained using a heterogeneous Ca-based catalyst. *Fuel Processing Technology*, 121, pp.114–118.

Fillières, R. and Bouchra Benjelloun-Mlayah, M.D., 1995. Ethanolysis of rapeseed oil: Quantitation of ethyl esters, mono-, di-, and triglycerides and glycerol by high-performance size-exclusion chromatography. *Journal of the American Oil Chemists' Society*, 72(4), pp.427–432.

Garcia, C.M., Teixeira, S., Marciniuk, L.L., and Schuchardt, U., 2008. Transesterification of soybean oil catalyzed by sulfated zirconia. *Bioresource technology*, 99(14), pp.6608–13.

Goldstein, J., Newbury, D.E., Joy, D.C., Lyman, C.E., Echlin, P., Lifshin, E., Sawyer, L. and Michael, J.R., 2003. *Scanning Electron Microscopy and X-ray Micronalysis*, pp.690.

Gopal, K.N., et al., 2014. Investigation of emissions and combustion characteristics of a CI engine fueled with waste cooking oil methyl ester and diesel blends. *Alexandria Engineering Journal*, 53(2), pp.281–287.

Hafner, B., 2006. Energy Dispersive Spectroscopy on the SEM: A Primer, *Characterization Facility*, University of Minnesota.

Hassan, S.Z., Chopade, S.A. and Vinjamur, M., 2013. Study of Parametric Effects and Kinetic Modeling of Trans-esterification Reaction for Biodiesel Synthesis. , 2, pp.67–75.

He, C., Baoxiang, P., et al., 2007. Biodiesel production by the transesterification of cottonseed oil by solid acid catalysts. *Frontiers of Chemical Engineering in China*, 1(1), pp.11–15.

Hossein, M. et al., 2014. A source of renewable energy in Malaysia , why biodiesel ? *Renewable and Sustainable Energy Reviews*, 35, pp.244–257.

Hossein, M., Ashnani, M., Johari, A. and Hashim, H., 2014. A source of renewable energy in Malaysia , why biodiesel ? *Renewable and Sustainable Energy Reviews*, 35, pp.244–257.

Hou, X. and Jones, B.T., 2000. Inductively Coupled Plasma / Optical Emission Spectrometry. *Encyclopedia of Analytical Chemistry*, pp.9468–9485.

Huang, G., Chen, F., Wei, D., Zhang, X. and Chen, G., 2010. Biodiesel production by microalgal biotechnology. *Applied Energy*, 87(1), pp.38–46.

Islam, A., Taufiq-Yap, Y.H., Chu, C.-M., Chan, E.-S. and Ravindra, P., 2013. Studies on design of heterogeneous catalysts for biodiesel production. *Process Safety and Environment Protection*, 91(1-2), pp.91, 131–144.

Jaichandar, S. and Annamalai, K., 2011. The Status of Biodiesel as an Alternative Fuel for Diesel Engine – An Overview. *Sustainable energy and environment*, 2, pp.71–75.

Jian-hong, Y.I., You-yi, S.U.N., Jian-feng, G.A.O. and Chun-yan, X.U., 2009. Synthesis of crystalline γ -Al 2 O 3 with high purity. *Transactions of Nonferrous Metals Society of China*, 19, pp.1237–1242.

Joshi, R.M. and Pegg, M.J., 2007. Flow properties of biodiesel fuel blends at low temperatures. *Fuel*, 86(1-2), pp.143–151.

Kaijun, L., 2013. *Biodiesel Synthesis Via Solid Acid Catalyst by Using Palm Fatty Acid Distillate (PFAD) as Feedstock*. Thesis, Universiti Tunku Abdul Rahman.

Kartika, I.A., Yani, M., Ariono, D., Evon, P. and Rigal, L., 2013. Biodiesel production from jatropha seeds: Solvent extraction and in situ transesterification in a single step. *Fuel*, 106, pp.111–117.

Kim, H. et al., 2004. Development of heterogeneous catalyst system for esterification of free fatty acid contained in used vegetable oil. *Studies in Surface Science and Catalysis* , 153, pp.201–204.

Kim, H.-J. et al., 2004. Transesterification of vegetable oil to biodiesel using heterogeneous base catalyst. *Catalysis Today*, 93-95, pp.315–320.

Kim, M., Dimaggio, C., Steven, O.S. and Simon Ng, K.Y., 2012. A new generation of zirconia supported metal oxide catalysts for converting low grade renewable feedstocks to biodiesel. *Bioresource technology*, 118, pp.37–42.

Kiss, A.A., Omota, F., Dimian, A. and Rothenberg, G., 2006. The heterogeneous advantage: biodiesel by catalytic reactive distillation. *Topics in Catalysis*, 40(1-4), pp.141–150.

Klug, P.H. and Alexander, L.E., 1974. *X-ray diffraction procedures for polycrystalline and amorphous materials.* In: X-ray diffraction procedures. 2nd Edition, New York: John Wiley and Sons, pp. 177-424.

Kontorovich, A. E., Epov, M.I. and Eder, L.V., 2014. Long-term and medium-term scenarios and factors in world energy perspectives for the 21st century. *Russian Geology and Geophysics*, 55(5-6), pp.534–543.

Ladavos, K. et al., 2012. The BET equation, the inflection points of N2 adsorption isotherms and the estimation of specific surface area of porous solids. *Microporous and Mesoporous Materials*, 151, pp.126–133.

Lam, M.K., Lee, K.T. and Mohamed, A.R., 2010. Homogeneous, heterogeneous and enzymatic catalysis for transesterification of high free fatty acid oil (waste cooking oil) to biodiesel: a review. *Biotechnology advances*, 28(4), pp.500–18.

Lam, M.K., Lee, K.T. and Mohamed, A.R., 2009. Sulfated tin oxide as solid superacid catalyst for transesterification of waste cooking oil: An optimization study. *Applied Catalysis B: Environmental*, 93(1-2), pp.134–139.

Lee, J.-S. and Saka, S., 2010. Biodiesel production by heterogeneous catalysts and supercritical technologies. *Bioresource technology*, 101(19), pp.7191–200.

Liu, X., He, H., Wang, Y., Zhu, S. and Piao, X., 2008. Transesterification of soybean oil to biodiesel using CaO as a solid base catalyst. *Fuel*, 87(2), pp.216–221.

Lokman, I.M., Rashid, U. and Taufiq-Yap, Y.H., 2015a. Meso- and macroporous sulfonated starch solid acid catalyst for esterification of palm fatty acid distillate. *Arabian Journal of Chemistry*, 9(2), pp.179-189.

Lokman, I.M., Rashid, U. and Taufiq-Yap, Y.H., 2015b. Production of Biodiesel from Palm Fatty Acid Distillate using Sulfonated-Glucose Solid Acid Catalyst: ssCharacterization and Optimization. *Chinese Journal of Chemical Engineering*, 23, pp.1857–1864.

Lopez, D., Suwannakam, K., Bruce, D.A. and Goodwin Jr, J.G., 2007. Esterification and transesterification on tungstated zirconia: Effect of calcination temperature. *Journal of Catalysis*, 247(1), pp.43–50.

Low, S L and Cheong, K.T., 2009. Polymeric Membrane Application for Bio-diesel Transesterification. In Bandung: 1st AUN/ SEED-Net Regional Workshop.

Macario, A. et al., 2010. Biodiesel production process by homogeneous/heterogeneous catalytic system using an acid–base catalyst. *Applied Catalysis A: General*, 378(2), pp.160–168.

Marchetti, J.M., Miguel, V.U. and Errazu, a. F., 2007. Heterogeneous esterification of oil with high amount of free fatty acids. *Fuel*, 86(5-6), pp.906–910.

Mat, R., Samsudin, R.A., Mohamed, M. and Johari, A., 2012. Solid Catalysts and theirs Application in Biodiesel Production. *Bulletin of Chemical Reaction Engineering & Catalysis*, 7(2), pp.142–149.

Mello, V.M., Pousa, G.P.A.G., Pereira, M.S.C., Dias, I.M. and Suarez, P.A.Z., 2011. Metal oxides as heterogeneous catalysts for esterification of fatty acids obtained from soybean oil. *Fuel Processing Technology*, 92(1), pp.53–57.

Mo, M. et al., 2013. A study on the effects of promising edible and non-edible biodiesel feedstocks on engine performance and emissions production : A comparative evaluation. *Renewable and Sustainable Energy Reviews*, 23, pp.391–404.

Mohan, M., Kandasamy, K. and Thangavelu, M., 1991. Investigation on the Performance of Diesel Engine Using Various Bio Fuels and the Effect of Temperature Variation. *Sustainable development*, 2(3), pp.176–182.

Mongkolbovornkij, P. et al., 2010. Esterification of industrial-grade palm fatty acid distillate over modified ZrO2 (with WO3–, SO4 –and TiO2–): Effects of co-solvent adding and water removal. *Fuel Processing Technology*, 91(11), pp.1510–1516.

Montgomery, D., 2001. *Design and analysis of experiments* 5th edition., Willey.

Mross, W.-D. 1983. Alkali doping in heterogeneous catalysis. *Catalysis Reviews, Science and Engineering* 25: 591-637.

Nixon, W.C., 1971. The General Principles of Scanning Electron Microscopy. *Philosophical Transactions of the Royal Society of London. Series B, Biological Sciences,* 261(837), pp.45–50.

Nyambuu, U. and Semmler, W., 2014. Trends in the extraction of non-renewable resources : The case of fossil energy. *Economic Modelling*, 37, pp.271–279.

Othman, R., Mohammad, A.W., Ismail, M. and Salimon, J., 2010. Application of polymeric solvent resistant nanofiltration membranes for biodiesel production. *Journal of Membrane Science*, 348(1-2), pp.287–297.

Park, Y.-M., Lee, D.-W., Kim, D.-K., Lee, J.-S. and Lee, K.-Y., 2008. The heterogeneous catalyst system for the continuous conversion of free fatty acids in used vegetable oils for the production of biodiesel. *Catalysis Today*, 131(1-4), pp.238–243.

Peng, B.-X. et al., 2008. Biodiesel production from waste oil feedstocks by solid acid catalysis. *Process Safety and Environmental Protection*, 86(6), pp.441–447.

Petchmala, A. et al., 2010. Transesterification of palm oil and esterification of palm fatty acid in near- and super-critical methanol with SO4–ZrO2 catalysts. *Fuel*, 89(9), pp.2387–2392.

Rasimoglu, N. and Temur, H., 2014. Cold flow properties of biodiesel obtained from corn oil. *Energy*, 68, pp.57–60.

Saleh, J., Tremblay, A.Y. and Dubé, M. a., 2010. Glycerol removal from biodiesel using membrane separation technology. *Fuel*, 89(9), pp.2260–2266.

Shu, Q. et al., 2010. Synthesis of biodiesel from waste vegetable oil with large amounts of free fatty acids using a carbon-based solid acid catalyst. *Applied Energy*, 87(8), pp.2589–2596.

Shuit, S.H., Ong, Y.T., Lee, K.T., Subhash, B. and Tan, S.H., 2012. Membrane technology as a promising alternative in biodiesel production: A review. *Biotechnology advances*,30(6), pp.1364-1380.

Silitonga, S. et al., 2013. Production of biodiesel from Sterculia foetida and its process optimization. *Fuel*, 111, pp.478–484.

Sim, J.H., Kamaruddin, A.H., Long, W.S. and Najafpour, G., 2007. Clostridium aceticum—A potential organism in catalyzing carbon monoxide to acetic acid: Application of response surface methodology. *Enzyme and Microbial Technology*, 40(5), pp.1234–1243.

Srivastava, A. and Prasad, R., 2000. Triglycerides-based diesel fuels. *Renewable and Sustainable Energy Reviews*, 4(2), pp.111–133.

Suganuma, S. et al., 2008. Hydrolysis of cellulose by amorphous carbon bearing SO3H, COOH, and OH groups. *Journal of the American Chemical Society*, 130(38), pp.12787–93.

Suwannakarn, K., 2008. Biodiesel production from high free fatty acid content feedstocks. Thesis, University of Clemson.

Tao, M.-L., Guan H,-Y., Wang, X.-H, Liu, Y,-C. and Louh, R.-F., 2015. Fabrication of sulfonated carbon catalyst from biomass waste and its use for glycerol esterification. *Fuel Processing Technology*, 138, pp.355–360.

Taufiq-Yap, Y.H., Fitriyah Abdullah, N. and Basri, M., 2011. Biodiesel Production via Transesterification of Palm Oil Using NaOH/Al 2 O 3 Catalysts (Pengeluaran Biodiesel Melalui Pengtransesteran Minyak Sawit dengan Menggunakan Mangkin NaOH/Al 2 O 3). *Sains Malaysiana*, 40(6), pp.587–594.

Tay, B., Ping, Y. and Yusof, M., 2009. Characteristics and Properties of Fatty Acid Distillates from Palm Oil. *Oil Palm Bulletin*, 59, pp.5–11.

Wan, T. et al., 2009. Application of Sodium Aluminate As a Heterogeneous Base Catalyst for Biodiesel Production from Soybean Oil. *Energy fuels*, 23, pp.1089–1092.

Wellner, N., 2013. *Fourier transform infrared (FTIR) and Raman microscopy: principles and applications to food microstructures*, Elsevier.

Xie, W. and Li, H., 2006. Alumina-supported potassium iodide as a heterogeneous catalyst for biodiesel production from soybean oil. *Journal of Molecular Catalysis A: Chemical*, 255(1-2), pp.1–9.

Yan, S., Lu, H. and Liang, B., 2008. Supported CaO Catalysts Used in the Transesterification of Rapeseed Oil for the Purpose of Biodiesel Production. *Energy fuels*, 22, pp.646–651.

Zhu, M. et al., 2010. Preparation and characterization of PSSA/PVA catalytic membrane for biodiesel production. *Fuel*, 89(9), pp.2299–2304.

APPENDICES

APPENDIX A

Biodiesel Yield Sample Calculation

The following sample calculation shown is done based on the result obtained by esterification reaction catalyzed by Al_2O_3-SO_3H at 6 hour reaction time.

1. Determine the response factor, R_a of each component corresponding to the FAME calibration standard

$$R_s = \frac{Area\ of\ component}{Area\ of\ internal\ standard\ in\ the\ calibration\ curve}$$

For methyl palmitate standard:

$$R_s = \frac{10889.39}{20188.31} = 0.5394$$

For methyl sterate standard:

$$R_s = \frac{12125.44}{19032.67} = 0.6371$$

For methyl oleate standard:

$$R_s = \frac{12967.84}{6052.51} = 2.1426$$

For methyl linoleate standard:

$$R_s = \frac{12705.69}{17589.13} = 0.7224$$

2. Determine the response factor R_a of each component corresponding to the FAME sample

$$R_a = \frac{Area\ of\ component}{Area\ of\ internal\ standard\ in\ the\ calibration\ curve}$$

For methyl palmitate standard:

$$R_a = \frac{11674.8}{8063.21} = 1.4479$$

For methyl sterate standard:

$$R_a = \frac{664.5}{8063.21} = 0.0824$$

For methyl oleate standard:

$$R_a = \frac{7273.68}{8063.21} = 0.9021$$

For methyl linoleate standard:

$$R_a = \frac{1626.75}{8063.21} = 0.9021$$

Note: The area of each respective component can be determined from the GC results.

3. Determine the concentration of each component in the FAME sample

$$C = \frac{R_a}{R_s} \times 1\,\frac{g}{L}$$

For methyl palmitate:

$$c = \frac{1.4479}{0.5394} \text{ x } 1 \text{ g/L} = 2.6843 \text{ g/L}$$

For methyl sterate:

$$c = \frac{0.0824}{0.6371} \text{ x } 1 \text{ g/L} = 0.1294 \text{ g/L}$$

For methyl oleate:

$c = \frac{0.9021}{2.1426}$ x 1 g/L = 0.4210 g/L

For methyl linoleate:

$c = \frac{0.2017}{0.7224}$ x 1 g/L = 0.2793 g/L

4. Determine the biodiesel yield

$$Yield = \frac{\sum Conc\ of\ each\ types\ of\ FAME\ in\ sample}{Total\ conc\ of\ FAME\ theoretically} \times Dilution\ Factor$$

For Al_2O_3-SO_3H catalyzed reaction at 6 hour reaction time:

$$\sum Concentration\ of\ each\ types\ of\ FAME\ in\ sample = 3.5140\ \frac{g}{L}$$

In the reaction, 25 g of PFAD is mixed with methanol. Based on the molecular weight of PFAD (287.54g/L), the number of mole of PFAD is equal to 0.09 moles.

$$Total\ conc.of\ FAME\ theoretically = \frac{Number\ of\ moles \times MW_{FAME}}{Total\ Volume}$$

$$Total\ conc.of\ FAME\ theoretically = \frac{0.09\ mol \times 283.89\ \frac{g}{mol}}{0.11\ L} = 232.2731\ g/L$$

The dilution factor in this study is calculated as follow:

$$Dilution\ Factor = \frac{Final\ Volume}{Aliquot\ Volume}$$

$$Dilution\ Factor\ I = \frac{9500\ \mu L}{500\ \mu L} = 19$$

$$Dilution\ Factor\ II = \frac{1000\ \mu L}{500\ \mu L} = 2$$

$$Total\ Dilution\ Factor = 19 \times 2 = 38$$

Hence,

$$Yield(\%) = \frac{3.5140\,\frac{g}{L}}{232.2731\,\frac{g}{L}} \times 38 = 57.49\,\%$$

APPENDIX B

Percentage reduction of palmitic acid sample calculation

The following sample calculation shown is done based on the result obtained by biodiesel purification using PES 5 kD at 10 minutes of separation time.

1. Determine the response factor, R_a of each component corresponding to the palmitic acid calibration standard

$$R_s = \frac{Area\ of\ component}{Area\ of\ internal\ standard\ in\ the\ calibration\ curve}$$

For palmitic acid:

$$R_s = \frac{4302.05}{19959.85} = 0.2155$$

2. Determine the response factor R_a of each component corresponding to the palmitic acid sample

$$R_a = \frac{Area\ of\ component}{Area\ of\ internal\ standard\ in\ the\ calibration\ curve}$$

For palmitic acid:

$$R_a = \frac{1229.18}{25292.22} = 0.0486$$

3. Determine the concentration of each component in the FAME sample

$$C = \frac{R_a}{R_s} \times 1\,\frac{g}{L}$$

For palmitic acid:

$$c = \frac{0.0486}{0.2155} \text{ x } 1 \text{ g/L} = 0.2255 \text{ g/L}$$

4. Determine the reduction of palmitic acid

   The concentration of palmic acid before permeation experiment: 1.0617 g/L

   Palmitic acid reduction, % = $(1 - \frac{\text{Ci,p}}{\text{Ci,f}}) \times 100\ \%$

   where $C_{i,p}$ is the permeate concentration and $C_{i,f}$ is the feed concentration.

   Palmitic acid reduction, % = 1- $\frac{0.2255}{1.0617} X\ 100\ \%$

$$= 78.76\ \%$$

APPENDIX C

GC Analysis

Sulphuric acid concentration: 5M-Al_2O_3	Immersion time: 18 hours					
	1	**2**	**3**	**4**	**5**	**6**
13	4815.10	9648.96	8845.77	10252.41	5554.40	11674.80
15	6939.82	12090.52	9119.58	10548.33	4608.70	8063.21
18	238.77	618.37	508.65	596.26	403.69	664.50
19	3113.15	6731.99	5618.90	6648.20	5246.36	7273.68
21	635.33	1461.92	1209.10	1452.08	156.80	1626.75
yield	27.43	31.20	38.56	39.86	47.58	57.49

Sulphuric acid concentration: 5M-Al_2O_3	Immersion time: 18 hours					
	1	**2**	**3**	**4**	**5**	**6**
13	1305.25	6890.61	7276.13	5950.88	6535.28	3014.25
15	4321.78	1305.25	3138.71	3280.47	3785.23	5618.37
18	0	6890.61	7276.13	5950.88	6535.28	3014.25
19	748.65	6890.61	7276.13	5950.88	6535.28	3014.25
21	0	6890.61	7276.13	5950.88	6535.28	3014.25
yield	10.48	17.19	17.70	24.78	24.78	40.80

Sulphuric acid concentration:5M-SiO_2	Immersion time: 18 hours					
	1	**2**	**3**	**4**	**5**	**6**
13	1907.20	484.07	273.84	528.93	6518.80	1108.02
15	3795.18	6499.09	3446.38	5081.23	532.27	6518.80
18	650.19	0.00	0.00	0.00	6518.80	0
19	0.00	258.23	0.00	275.32	6518.80	733.73
21	0	0.00	0.00	0.00	6518.80	0.00
yield	1.96	2.41	2.56	3.57	3.77	6.01

Sulphuric acid concentration: 5M- SiO_2	Immersion time: 18 hours					
	1	**2**	**3**	**4**	**5**	**6**
13	284.29	339.49	259.52	463.42	10128.83	774.49
15	10250.49	10646.13	6193.08	10292.32	748.48	10128.83
18	0	0.00	0.00	0.00	10128.83	0
19	0.00	204.20	0.00	308.10	10128.83	581.32
21	0	0.00	0.00	0.00	10128.83	0.00
yield	0.84	2.41	2.56	1.59	2.27	2.76

Sulphuric acid concentration: 5M-TiO_2	Immersion time: 18 hours					
	1	**2**	**3**	**4**	**5**	**6**
13	87.89	129.27	143.44	486.85	4350.00	429.33
15	6157.83	6845.24	4760.27	5988.35	663.97	4350.00
18	0	0.00	0.00	0.00	4350.00	0
19	0.00	0.00	0.00	264.06	4350.00	178.66
21	0	0.00	0.00	0.00	4350.00	408.99
yield	0.43	0.57	0.91	2.80	4.93	5.44

Sulphuric acid concentration: 5M-TiO_2	Immersion time: 18 hours					
	1	**2**	**3**	**4**	**5**	**6**
13	98.84	113.81	244.64	310.48	5441.43	379.88
15	6232.03	4806.88	7073.80	7525.06	261.00	5441.43
18	0	0.00	0.00	0.00	5441.43	0
19	0.00	0.00	0.00	0.00	5441.43	122.98
21	0	0.00	0.00	0.00	5441.43	0.00
yield	0.48	0.72	1.05	1.25	1.29	2.29

Sulphuric acid concentration: 2M-Al_2O_3	Immersion time: 6 hours					
	1	**2**	**3**	**4**	**5**	**6**
13	96.52	273.87	424.29	376.36	7919.16	728.18
15	4122.88	7724.28	7812.34	7797.01	706.65	7919.16
18	0	0.00	0.00	0.00	7919.16	0
19	0.00	0.00	226.93	153.63	7919.16	466.40
21	0	0.00	0.00	0.00	7919.16	0.00
yield	0.71	1.08	1.87	1.61	2.74	3.24

Sulphuric acid concentration: 3M-Al_2O_3	Immersion time: 6 hours					
	1	**2**	**3**	**4**	**5**	**6**
13	183.51	457.71	651.43	696.51	6257.99	844.14
15	7259.45	11360.02	10666.72	10199.70	1154.50	6257.99
18	0	0.00	0.00	0.00	6257.99	0
19	0.00	312.03	442.57	514.46	6257.99	482.40
21	0	0.00	0.00	0.00	6257.99	0.00
yield	0.77	1.43	2.17	2.46	3.40	4.68

Sulphuric acid concentration: 4M-Al_2O_3			Immersion time: 6 hours			
	1	**2**	**3**	**4**	**5**	**6**
13	259.16	300.80	394.22	610.72	7149.36	621.96
15	10939.13	8431.51	8403.13	9581.94	749.14	7149.36
18	0	0.00	0.00	0.00	7149.36	0
19	0.00	213.55	207.72	436.66	7149.36	402.95
21	0	0.00	0.00	0.00	7149.36	0.00
yield	0.72	1.28	1.61	2.28	2.87	3.07

Sulphuric acid concentration: 5M-Al_2O_3			Immersion time: 6 hours			
	1	**2**	**3**	**4**	**5**	**6**
13	290.46	370.62	534.98	683.95	8168.05	771.78
15	10722.70	10375.84	10148.92	9812.07	675.15	8168.05
18	0	0.00	0.00	0.00	8168.05	0
19	128.71	152.51	323.24	461.18	8168.05	681.24
21	0	0.00	0.00	0.00	8168.05	0.00
yield	0.91	1.20	1.84	2.47	2.76	3.50

Sulphuric acid concentration:2M-Al_2O_3			Immersion time:12 hours			
	1	**2**	**3**	**4**	**5**	**6**
13	219.73	281.93	424.29	598.25	10224.54	928.58
15	11452.30	9949.81	7812.34	9645.45	838.11	10224.54
18	0	0.00	0.00	0.00	10224.54	0
19	0.00	0.00	226.93	429.67	10224.54	676.72
21	0	0.00	0.00	0.00	10224.54	0.00
yield	0.58	0.86	1.87	2.22	2.72	3.26

Sulphuric acid concentration:3M-Al_2O_3			Immersion time: 12 hours			
	1	**2**	**3**	**4**	**5**	**6**
13	203.51	400.51	491.46	585.44	8288.32	944.01
15	9841.96	9921.85	9030.65	8559.03	691.03	8288.32
18	0	0.00	0.00	0.00	8288.32	0
19	0.00	528.72	262.83	334.91	8288.32	618.18
21	0	0.00	0.00	0.00	8288.32	0.00
yield	0.63	1.63	1.87	2.37	2.64	4.02

Sulphuric acid concentration: 4M-Al_2O_3	Immersion time: 12 hours					
	1	**2**	**3**	**4**	**5**	**6**
13	269.04	379.52	516.14	438.94	10013.90	866.72
15	8801.37	9223.52	10076.70	7138.67	675.15	10013.90
18	0	0.00	0.00	0.00	10013.90	0
19	0.00	224.35	343.93	301.50	10013.90	681.50
21	0	0.00	0.00	0.00	10013.90	0.00
yield	0.93	1.43	1.81	2.19	2.76	3.14

Sulphuric acid concentration: 5M-Al_2O_3	Immersion time: 12 hours					
	1	**2**	**3**	**4**	**5**	**6**
13	280.13	640.89	1163.99	1637.24	6349.56	1375.13
15	4243.48	7830.33	10311.17	11231.88	2068.59	6349.56
18	0	0.00	0.00	0.00	6349.56	0
19	378.29	328.61	637.07	1027.00	6349.56	723.98
21	0	0.00	0.00	0.00	6349.56	0.00
yield	2.68	2.77	3.90	5.12	6.21	7.44

Sulphuric acid concentration: 2M-Al_2O_3	Immersion time: 18 hours					
	1	**2**	**3**	**4**	**5**	**6**
13	1532.74	1440.69	1692.03	2864.17	11723.38	3511.73
15	14183.56	8819.54	13824.01	12969.78	3365.92	11723.38
18	0	0.00	0.00	160.30	11723.38	326.18
19	1124.67	951.06	1155.81	2157.16	11723.38	2676.56
21	0	0.00	0.00	399.34	11723.38	481.74
yield	3.88	5.78	4.35	8.98	9.43	12.47

Sulphuric acid concentration: 3M-Al_2O_3	Immersion time: 18 hours					
	1	**2**	**3**	**4**	**5**	**6**
13	545.28	1117.05	997.36	1842.52	11740.62	2667.83
15	11824.88	11731.37	8174.22	11476.54	2136.07	11740.62
18	0	0.00	0.00	0.00	11740.62	0
19	379.84	824.88	664.68	1400.95	11740.62	1972.78
21	0	0.00	0.00	0.00	11740.62	71.32
yield	1.64	3.60	4.32	5.80	6.53	8.31

Sulphuric acid concentration: 4M-Al_2O_3	Immersion time: 18 hours					
	1	**2**	**3**	**4**	**5**	**6**
13	2411.10	2911.67	4241.25	5413.02	12418.62	7608.17
15	11168.03	8902.78	11577.77	10298.49	5911.38	12418.62
18	0	91.40	245.35	359.07	12418.62	547.74
19	1787.48	2080.90	3320.34	4070.51	12418.62	5900.64
21	320.62	423.44	675.98	891.51	12418.62	1281.22
yield	8.42	13.07	14.62	21.82	22.31	25.68

MWCO: PES 5 kD, Palmitic acid		
	10	**30**
13	5924.78	3600.27
15	25890.48	28703.71
Reduction	78.76	45.19

MWCO: PES 20 kD, Palmitic acid		
	10	**30**
13	5223.23	3487.86
15	23534.22	21540.35
Reduction	45.14	27.04

MWCO: PVDF 30 kD, Palmitic acid		
	10	**30**
13	10023.78	3487.86
15	48745.44	26272.35
Reduction	46.95	35.44

MWCO: PES 5 kD, Oleic acid		
	10	**30**
13	4461.38	1706.63
15	25890.48	20703.71
Reduction	93.73	52.16

MWCO: PES 20 kD, Oleic acid		
	10	**30**
13	5672.90	1487.86
15	35267.82	19872.35
Reduction	71.23	53.45

MWCO: PVDF 30 kD, Oleic acid		
	10	**30**
13	8654.53	3434.86
15	48354.22	30562.77
Reduction	58.56	37.21

MWCO: PVDF 100 kD, Palmitic acid		
	10	**30**
13	8023.78	2787.86
15	39095.44	16249.35
Reduction	24.58	16.40

MWCO: PVDF 100 kD, Oleic acid		
	10	**30**
13	10023.78	3487.86
15	48745.44	20309.35
Reduction	24.71	16.48

Software Version	: 6.3.1.0504	Date	: 3/26/2013 12:49:57 PM
Operator	: FES	Sample Name	:
Sample Number	:	Study	:
AutoSampler	: NONE	Rack/Vial	: 0/0
Instrument Name	: Clarus500	Channel	: A
Instrument Serial #	: 650N7041802	A/D mV Range	: 1000
Delay Time	: 0.00 min	End Time	: 26.89 min
Sampling Rate	: 12.5000 pts/s		
Sample Volume	: 1.000000 ul		
Sample Amount	: 1.0000	Area Reject	: 0.000000
Data Acquisition Time	: 3/23/2013 3:05:04 PM	Dilution Factor	: 1.00
		Cycle	: 1

Raw Data File : C:\Documents and Settings\FES\Desktop\Yong Sheng\methylpalmitate.raw
Result File : C:\Documents and Settings\FES\Desktop\Yong Sheng\methylpalmitate.rst [Editing in Progress]
Inst Method : C:\GC\Method\0_Biodiesel (20130308) from C:\Documents and Settings\FES\Desktop\Yong Sheng\methylpalmitate.raw
Proc Method : C:\GC\Method\0_Biodiesel (20130308) from C:\Documents and Settings\FES\Desktop\Yong Sheng\methylpalmitate.rst [Editing in Progress]
Calib Method : C:\GC\Method\0_Biodiesel (20130308) from C:\Documents and Settings\FES\Desktop\Yong Sheng\methylpalmitate.rst [Editing in Progress]
Report Format File: C:\GC\Method\0_Biodiesel (20130308).rpt
Sequence File : C:\GC\Method\methylpalmitate-20130323-150332.seq

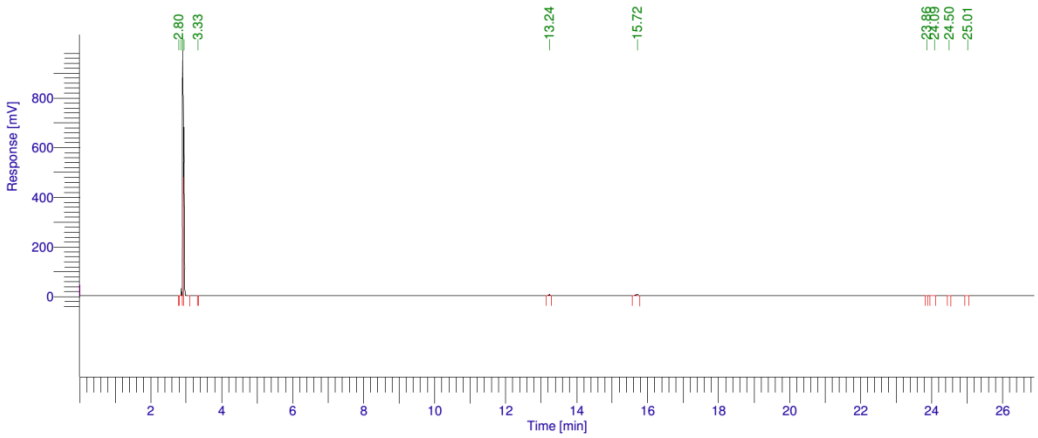

DEFAULT REPORT

Peak #	Time [min]	Area [µV·s]	Height [µV]	Area [%]	Norm. Area [%]	BL	Area/Height [s]
1	2.800	481.50	445.63	0.02	0.02	BV	1.0805
2	2.867	21789.55	28437.52	0.85	0.85	VV	0.7662
3	2.911	1568155.96	988884.29	61.00	61.00	VV	1.5858
4	2.940	948639.10	678152.71	36.90	36.90	VB	1.3989
5	3.333	22.12	25.80	0.00	0.00	BB	0.8573
6	13.236	10889.39	3774.44	0.42	0.42	BB	2.8850
7	15.715	20188.31	4778.55	0.79	0.79	BB	4.2248
8	23.863	38.20	16.80	0.00	0.00	BB	2.2736
9	24.091	147.60	22.55	0.01	0.01	BB	6.5467
10	24.501	222.80	88.55	0.01	0.01	BB	2.5160
11	25.015	93.19	21.09	0.00	0.00	BB	4.4191
		2570667.73	1.70e+06	100.00	100.00		

Software Version	: 6.3.1.0504	Date	: 3/26/2013 12:47:54 PM
Operator	: FES	Sample Name	:
Sample Number	:	Study	:
AutoSampler	: NONE	Rack/Vial	: 0/0
Instrument Name	: Clarus500	Channel	: A
Instrument Serial #	: 650N7041802	A/D mV Range	: 1000
Delay Time	: 0.00 min	End Time	: 26.89 min
Sampling Rate	: 12.5000 pts/s		
Sample Volume	: 1.000000 ul		
Sample Amount	: 1.0000	Area Reject	: 0.000000
Data Acquisition Time	: 3/11/2013 8:32:20 PM	Dilution Factor	: 1.00
		Cycle	: 1

Raw Data File : C:\Documents and Settings\FES\Desktop\Yong Sheng\Methyl Oleate.raw

Result File : C:\Documents and Settings\FES\Desktop\Yong Sheng\Methyl Oleate.rst [Editing in Progress]
Inst Method : C:\GC\Method\0_Biodiesel (20130308) from C:\Documents and Settings\FES\Desktop\Yong Sheng\Methyl Oleate.raw

Proc Method : C:\GC\Method\0_Biodiesel (20130308) from C:\Documents and Settings\FES\Desktop\Yong Sheng\Methyl Oleate.rst [Editing in Progress]

Calib Method : C:\GC\Method\0_Biodiesel (20130308) from C:\Documents and Settings\FES\Desktop\Yong Sheng\Methyl Oleate.rst [Editing in Progress]

Report Format File: C:\GC\Method\0_Biodiesel (20130308).rpt
Sequence File : C:\GC\Method\Methyl Oleate.seq

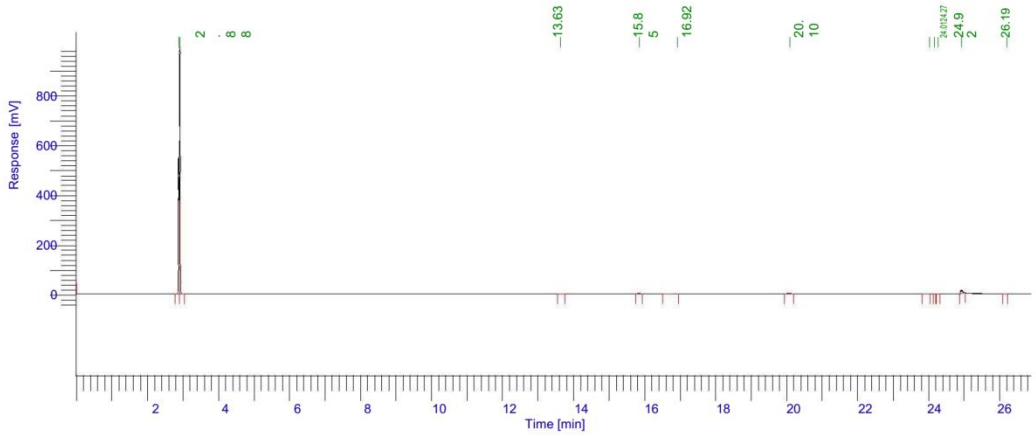

DEFAULT REPORT

Peak #	Time [min]	Area [µV·s]	Height [µV]	Area [%]	Norm. Area [%]	BL	Area/Height [s]
1	2.879	631346.06	551852.19	26.09	26.09	BV	1.1440
2	2.908	1712654.37	988878.23	70.76	70.76	VB	1.7319
3	13.629	550.60	96.65	0.02	0.02	BB	5.6965
4	15.854	6052.51	1645.73	0.25	0.25	BB	3.6777
5	16.923	900.56	24.32	0.04	0.04	BB	37.0250
6	20.099	12967.84	2270.14	0.54	0.54	BB	5.7124
7	24.013	174.82	21.95	0.01	0.01	BB	7.9632
8	24.153	75.61	37.30	0.00	0.00	BB	2.0272
9	24.270	318.33	115.56	0.01	0.01	BB	2.7546
		2420261.36	1.56e+06	100.00	100.00		

Software Version	: 6.3.1.0504	Date	: 3/26/2013 12:50:55 PM
Operator	: FES	Sample Name	:
Sample Number	:	Study	:
AutoSampler	: NONE	Rack/Vial	: 0/0
Instrument Name	: Clarus500	Channel	: A
Instrument Serial #	: 650N7041802	A/D mV Range	: 1000
Delay Time	: 0.00 min	End Time	: 26.89 min
Sampling Rate	: 12.5000 pts/s		
Sample Volume	: 1.000000 ul		
Sample Amount	: 1.0000	Area Reject	: 0.000000
Data Acquisition Time	: 3/23/2013 2:02:24 PM	Dilution Factor	: 1.00
		Cycle	: 1

Raw Data File : C:\Documents and Settings\FES\Desktop\Yong Sheng\methylsterate.raw
Result File : C:\Documents and Settings\FES\Desktop\Yong Sheng\methylsterate.rst [Editing in Progress]
Inst Method : C:\GC\Method\0_Biodiesel (20130308) from C:\Documents and Settings\FES\Desktop\Yong Sheng\methylsterate.raw
Proc Method : C:\GC\Method\0_Biodiesel (20130308) from C:\Documents and Settings\FES\Desktop\Yong Sheng\methylsterate.rst [Editing in Progress]
Calib Method : C:\GC\Method\0_Biodiesel (20130308) from C:\Documents and Settings\FES\Desktop\Yong Sheng\methylsterate.rst [Editing in Progress]
Report Format File: C:\GC\Method\0_Biodiesel (20130308).rpt
Sequence File : C:\GC\Method\methylsterate-20130323-140055.seq

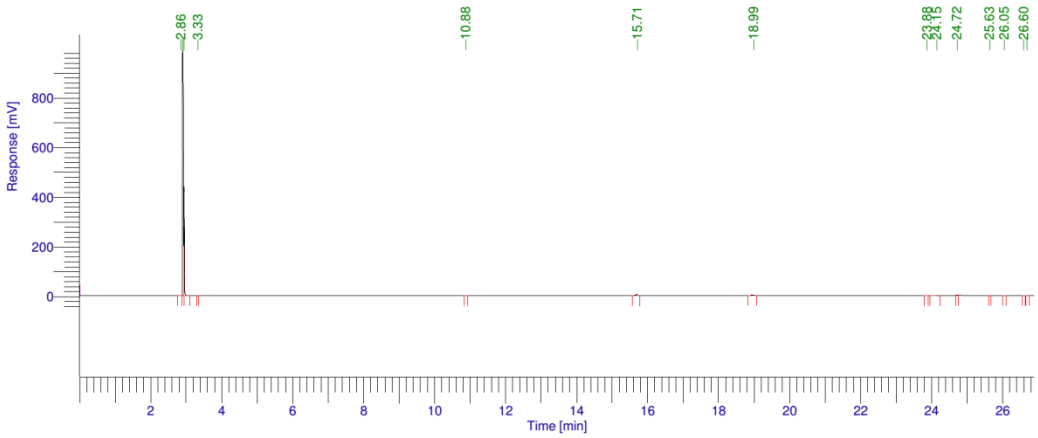

DEFAULT REPORT

Peak #	Time [min]	Area [µV·s]	Height [µV]	Area [%]	Norm. Area [%]	BL	Area/Height [s]
1	2.860	637.95	300.88	0.03	0.03	BV	2.1203
2	2.908	1776894.02	988884.70	77.31	77.31	VV	1.7969
3	2.946	487436.16	438319.23	21.21	21.21	VB	1.1121
4	3.331	24.34	26.26	0.00	0.00	BB	0.9267
5	10.883	84.58	32.07	0.00	0.00	BB	2.6378
6	15.714	19032.67	4606.13	0.83	0.83	BB	4.1320
7	18.985	12125.44	2481.60	0.53	0.53	BB	4.8861
8	23.878	96.79	25.73	0.00	0.00	BB	3.7612
9	24.153	1032.17	103.71	0.04	0.04	BB	9.9524
10	24.717	528.33	151.61	0.02	0.02	BB	3.4847
11	25.634	29.05	17.90	0.00	0.00	BB	1.6223
12	26.050	92.84	25.13	0.00	0.00	BB	3.6948
13	26.598	164.25	49.15	0.01	0.01	BV	3.3419
14	26.680	174.23	51.37	0.01	0.01	VB	3.3915
		2298352.80	1.44e+06	100.00	100.00		

Software Version	: 6.3.1.0504	Date	: 3/26/2013 12:48:58 PM
Operator	: FES	Sample Name	:
Sample Number	:	Study	:
AutoSampler	: NONE	Rack/Vial	: 0/0
Instrument Name	: Clarus500	Channel	: A
Instrument Serial #	: 650N7041802	A/D mV Range	: 1000
Delay Time	: 0.00 min	End Time	: 26.89 min
Sampling Rate	: 12.5000 pts/s		
Sample Volume	: 1.000000 ul		
Sample Amount	: 1.0000	Area Reject	: 0.000000
Data Acquisition Time	: 3/23/2013 2:33:44 PM	Dilution Factor	: 1.00
		Cycle	: 1

Raw Data File : C:\Documents and Settings\FES\Desktop\Yong Sheng\methyllinoleate.raw
Result File : C:\Documents and Settings\FES\Desktop\Yong Sheng\methyllinoleate.rst [Editing in Progress]
Inst Method : C:\GC\Method\0_Biodiesel (20130308) from C:\Documents and Settings\FES\Desktop\Yong Sheng\methyllinoleate.raw
Proc Method : C:\GC\Method\0_Biodiesel (20130308) from C:\Documents and Settings\FES\Desktop\Yong Sheng\methyllinoleate.rst [Editing in Progress]
Calib Method : C:\GC\Method\0_Biodiesel (20130308) from C:\Documents and Settings\FES\Desktop\Yong Sheng\methyllinoleate.rst [Editing in Progress]
Report Format File: C:\GC\Method\0_Biodiesel (20130308).rpt
Sequence File : C:\GC\Method\methyllinoleate-20130323-143215.seq

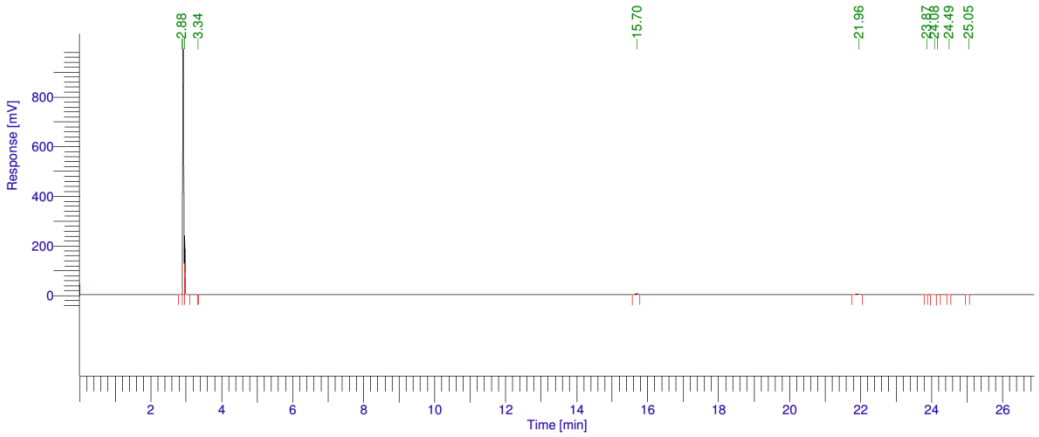

DEFAULT REPORT

Peak #	Time [min]	Area [µV·s]	Height [µV]	Area [%]	Norm. Area [%]	BL	Area/Height [s]
1	2.878	397.79	192.97	0.02	0.02	BV	2.0614
2	2.917	1908195.88	988886.12	88.00	88.00	VV	1.9296
3	2.962	228426.45	236590.45	10.53	10.53	VB	0.9655
4	3.337	24.03	25.13	0.00	0.00	BB	0.9563
5	15.704	17589.13	4103.91	0.81	0.81	BB	4.2859
6	21.955	12705.69	1983.08	0.59	0.59	BB	6.4070
7	23.867	65.02	21.13	0.00	0.00	BB	3.0776
8	24.080	518.17	75.26	0.02	0.02	BV	6.8855
9	24.162	346.66	85.28	0.02	0.02	VB	4.0650
10	24.485	106.53	28.85	0.00	0.00	BB	3.6921
11	25.050	92.38	12.16	0.00	0.00	BB	7.5991
		2168467.74	1.23e+06	100.00	100.00		

APPENDIX D

Condition: 80 ºC reaction temperature, 2 wt% sulfonated Al_20_3 (5M acid concentration and 18 hours immersion time) to PFAD mass ratio, 20:1 methanol to PFAD molar ratio, 6 hours reaction time

Predicted FAME yield = 56.25 %
Experimental FAME yield = 57.49 %

Percentage error, % = $\frac{57.49-56.25}{56.25} \; x \; 100 \; \%$ = 2.2 %

APPENDIX E

Preparation of Solutions Used in ICP-OES

i. Preparation of 8 M HNO_3

$$\text{Molarity for 65 \% of } HNO_3 = \frac{\text{Density of } HNO_3}{\text{Molecular Weight of } HNO_3} \times \frac{65}{100} \times 1000$$

$$= \frac{1.4090 \text{ g cm}^{-1}}{63.0130 \text{ g mol}^{-1}} \times \frac{65}{100} \times 1000$$

$$= 14.5343 \text{ mol L}^{-1}$$

$$= 14.5343 \text{ M}$$

$M_1V_1 = M_2V_2$

where,

M_1 = concentration of 65 % of HNO_3 (14.5343 M)

V_1 = volume of 65 % of HNO_3

M_2 = concentration of 8 M HNO_3

V_2 = volume of 8 M HNO_3

$M_1V_1 = M_2V_2$

(14.5343 M) V_1 = (8 M)(250 mL)

$$V_1 = \frac{(8 \text{ M})(250 \text{ mL})}{14.5343 \text{ M}}$$

$$= 137.65 \text{ mL}$$

Thus, 137.65 mL of 65 % of HNO_3 was diluted to 250 mL with deionised water.

ii. Preparation of Stock Solution of Sulphur, S

Molecular weight of $Al_2(SO_4)_3 \cdot 16H_2O$

= [(26.9815 x 2)+ (32.0660+(15.9994 x 4)) x 3 + 16 x (1.0079 x 2 + 15.9994)] $gmol^{-1}$

= 630.3984 $g\ mol^{-1}$

Atomic weight of S = 32.0660 $g\ mol^{-1}$

50 ppm of stock solution for S = 50 $mg\ L^{-1}$

= 0.05 $g\ L^{-1}$

$$\text{Number of mole of S} = \frac{0.05 \text{ g L}^{-1}}{32.0660 \text{ g mol}^{-1}}$$

$$= 1.5590 \times 10^{-3} \text{ mol L}^{-1}$$

Mass of $Al_2(SO_4)_3 \cdot 16H_2O_4$ = 1.5590×10^{-3} mol L^{-1} × 630.3984 $g\ mol^{-1}$

= 0.9830 $g\ L^{-1}$

Thus, 0.9830 g of $Al_2(SO_4)_3 \cdot 16H_2O_4$ was transferred into 1000 mL volumetric flask and top up with deionised water.

Preparation of standard solution of Sulphur, S

$M_1V_1 = M_2V_2$

where,

M_1 = concentration of stock solution (50 ppm)

V_1 = volume of stock solution

M_2 = concentration of standard solution

V_2 = volume of standard solution (250 mL)

Example of calculation for standard solution of 20 ppm

$M_1V_1 = M_2V_2$

(50 ppm) V_1 = (20 ppm)(250 mL)

$$V_1 = \frac{(20 \text{ ppm})(250 \text{ mL})}{50 \text{ ppm}}$$

$$= 100 \text{ mL}$$

Thus, 100 mL of stock solution for sulphur was dissolved in 8 M HNO_3 then diluted to 250 mL with deionised water to produce 20 ppm standard solution of sulphur.

APPENDIX F

BET Isotherm

Thermo
ELECTRON CORPORATION
Instrument type : Sorptomatic 1990
Sample name : Al2O3_Analysis.199
Filename : D:\Backup\Data SO1990\Fong\BET\bet_LATEST\al2o3\Al2O3_Analysis.199

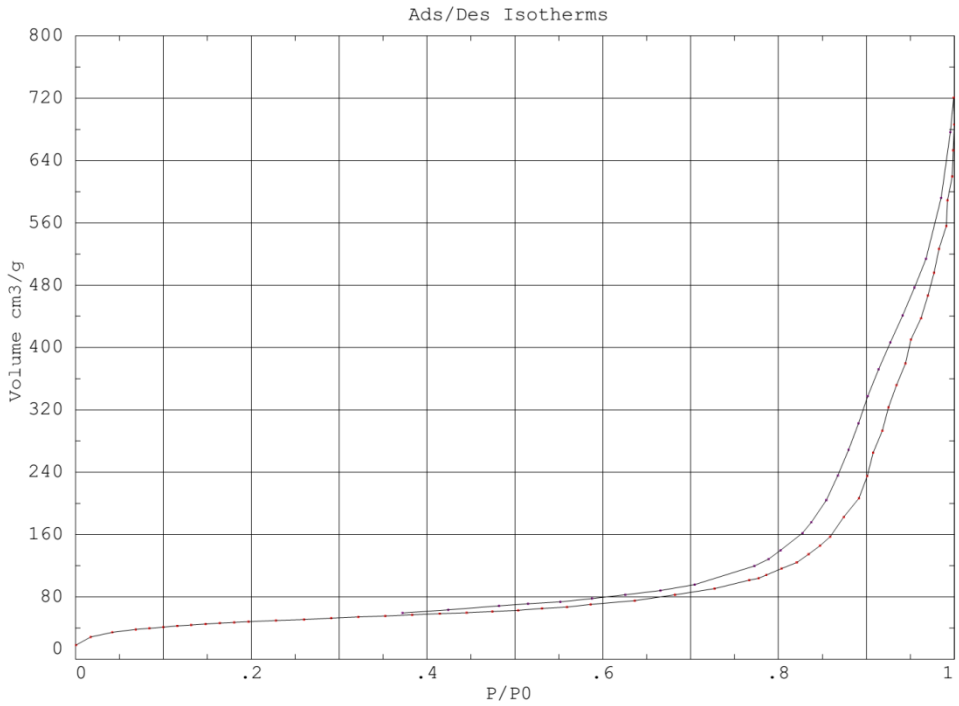

RESULTS

Calculation Method < B.E.T. >	
<B.E.T.> Initial-final P/P0 :	.04 - .3
Specific surface calculations	
Monolayer volume (cm3/g) :	38.4791565
Specific surface area (m²/g) :	167.507431
C value of BET equation :	310.8982
Correlation factor :	.9989203
Pore specific volume (cm3/g) :	.58699828
Pore specific volume at P/P0 :	.95
Total Adsorbed volume (cm3/g) :	720.61008
(Dol./Heal)	
Cumulative area max. (m²/g) :	182.172989
Pore volume max. (cm3/g) :	.698932827

Thermo
Instrument type : Sorptomatic 1990
Sample name : Al2O3_2M_6hAnalysis.199
Filename : D:\Backup\Data SO1990\Fong\BET\2m_6h\Al2O3_2M_6hAnalysis.199

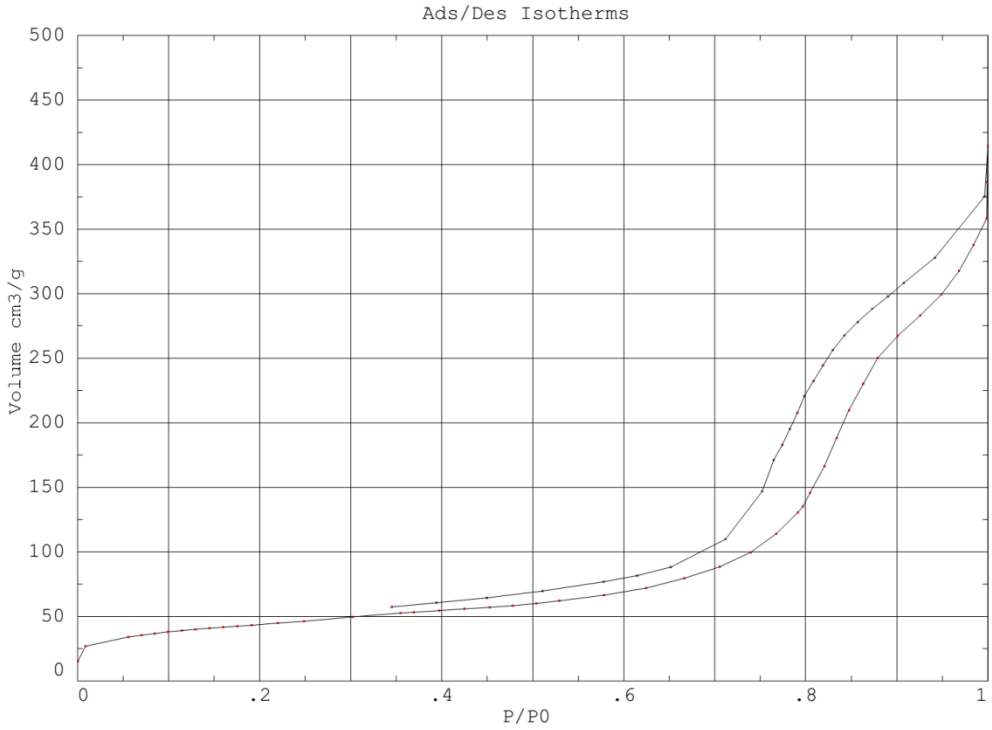

RESULTS

Calculation Method < B.E.T. >	
<B.E.T.> Initial-final P/P0 :	.04 - .3
Specific surface calculations	
Monolayer volume (cm3/g) :	35.5942345
Specific surface area (m²/g) :	154.948792
C value of BET equation :	209.3775
Correlation factor :	.999779
Pore specific volume (cm3/g) :	.46260551
Pore specific volume at P/P0 :	.95
Total Adsorbed volume (cm3/g) :	414.48088
(Dol./Heal)	
Cumulative area max. (m²/g) :	206.442322
Pore volume max. (cm3/g) :	.536776304

Thermo
ELECTRON CORPORATION

Instrument type : Sorptomatic 1990
Sample name : Al2O3_2M_12hAnalysis.199
Filename : D:\Backup\Data SO1990\Fong\BET\bet_LATEST\2m_12h\Al2O3_2M_12hAnalysis.199

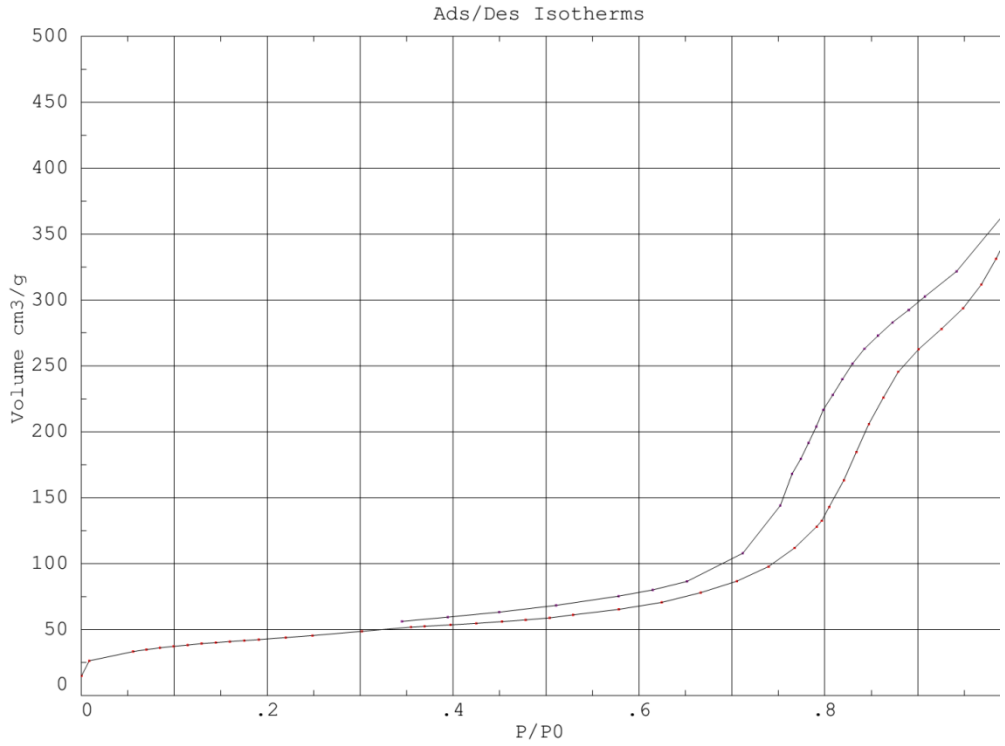

RESULTS

Calculation Method < B.E.T. >	
<B.E.T.> Initial-final P/P0 :	.04 - .3
Specific surface calculations	
Monolayer volume (cm3/g) :	34.9371109
Specific surface area (m²/g) :	152.088196
C value of BET equation :	209.3773
Correlation factor :	.999779
Pore specific volume (cm3/g) :	.45406511
Pore specific volume at P/P0 :	.95
Total Adsorbed volume (cm3/g) :	406.82895
(Dol./Heal)	
Cumulative area max. (m²/g) :	202.631073
Pore volume max. (cm3/g) :	.526866734

Thermo
ELECTRON CORPORATION
Instrument type : Sorptomatic 1990
Sample name : Al2O3_2M_18hAnalysis.199
Filename : D:\Backup\Data SO1990\Fong\BET\2m_18h\Al2O3_2M_18hAnalysis.199

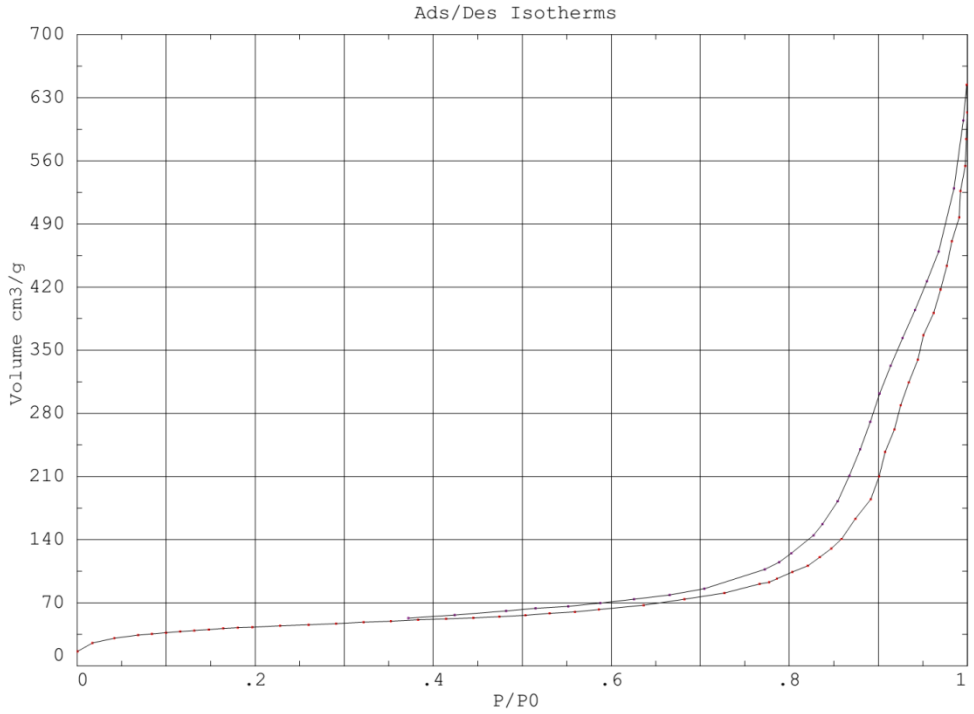

RESULTS

Calculation Method < B.E.T. >	
<B.E.T.> Initial-final P/P0 :	.04 - .3
Specific surface calculations	
Monolayer volume (cm3/g) :	34.4106102
Specific surface area (m²/g) :	149.796234
C value of BET equation :	310.8989
Correlation factor :	.9989203
Pore specific volume (cm3/g) :	.52493274
Pore specific volume at P/P0 :	.95
Total Adsorbed volume (cm3/g) :	644.41723
(Dol./Heal)	
Cumulative area max. (m²/g) :	162.911133
Pore volume max. (cm3/g) :	.625032008

Thermo
ELECTRON CORPORATION
Instrument type : Sorptomatic 1990
Sample name : Al2O3_3M_6hAnalysis.199
Filename : D:\Backup\Data SO1990\Fong\BET\bet_LATEST\3m_6h\Al2O3_3M_6hAnalysis.199

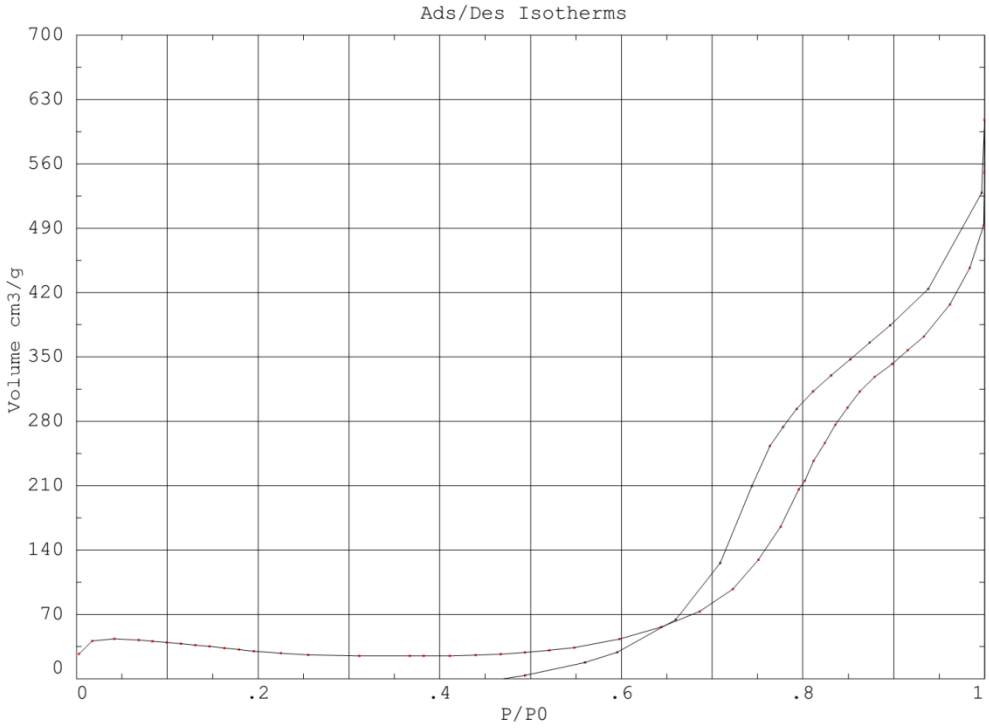

RESULTS

Calculation Method < B.E.T. >	
<B.E.T.> Initial-final P/P0 :	.04 - .3
Specific surface calculations	
Monolayer volume (cm3/g) :	18.7157326
Specific surface area (m²/g) :	81.473312
C value of BET equation :	-20.7481
Correlation factor :	.9794891
Pore specific volume (cm3/g) :	.57520217
Pore specific volume at P/P0 :	.95
Total Adsorbed volume (cm3/g) :	607.89817
(Dol./Heal)	
Cumulative area max. (m²/g) :	399.877991
Pore volume max. (cm3/g) :	.91187048

Thermo
ELECTRON CORPORATION
Instrument type : Sorptomatic 1990
Sample name : Al2O3_3M_12hAnalysis.199
Filename : D:\Backup\Data SO1990\Fong\BET\3m_12h\Al2O3_3M_12hAnalysis.199

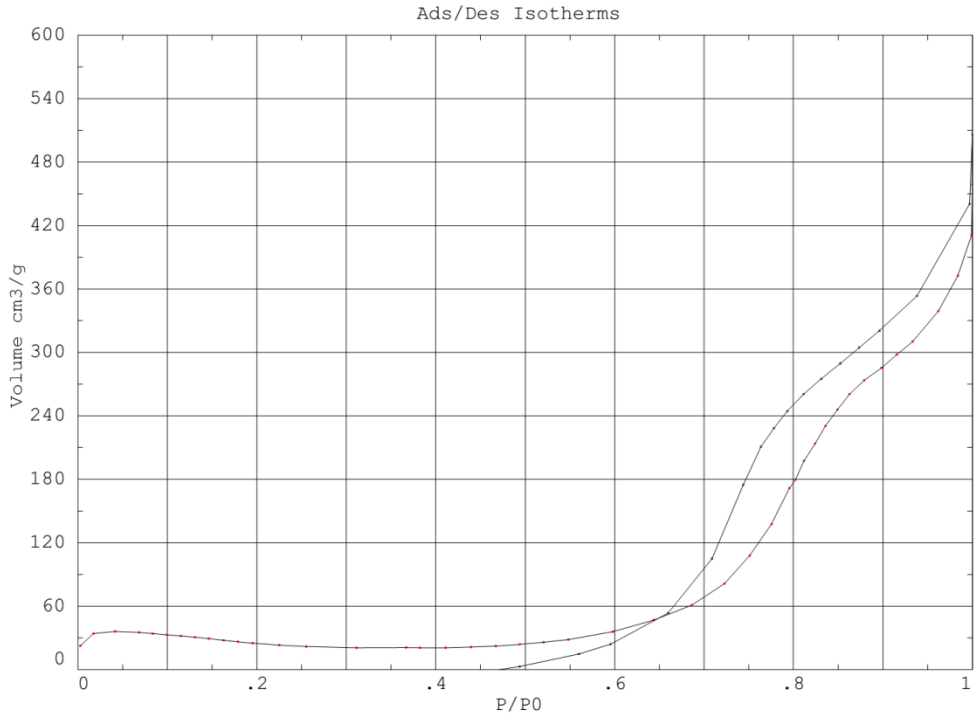

RESULTS

Calculation Method < B.E.T. >	
<B.E.T.> Initial-final P/P0 :	.04 - .3
Specific surface calculations	
Monolayer volume (cm3/g) :	15.5964432
Specific surface area (m²/g) :	67.894424
C value of BET equation :	-20.7481
Correlation factor :	.9794891
Pore specific volume (cm3/g) :	.47933519
Pore specific volume at P/P0 :	.95
Total Adsorbed volume (cm3/g) :	506.58183
(Dol./Heal)	
Cumulative area max. (m²/g) :	333.231659
Pore volume max. (cm3/g) :	.759891987

Thermo
ELECTRON CORPORATION

Instrument type : Sorptomatic 1990
Sample name : AlO(3M-18h)analysis
Filename : D:\Backup\Data SO1990\Fong\BET\3m_18h\AlO(3M-18h)analysis.199

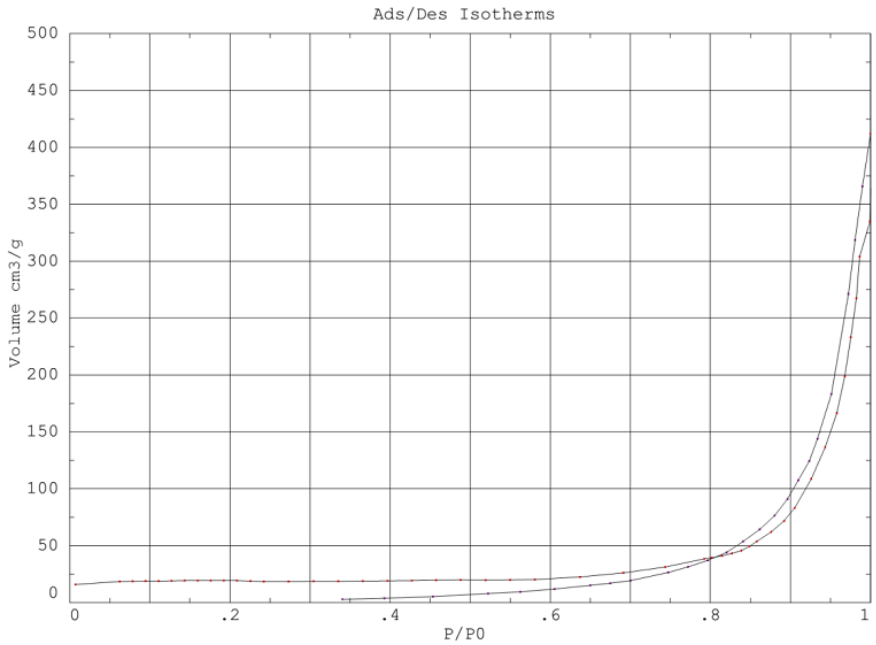

RESULTS

Calculation Method < B.E.T. >	
<B.E.T.> Initial-final P/P0 :	.04 - .3
Specific surface calculations	
Monolayer volume (cm3/g) :	13.2582169
Specific surface area (m^2/g) :	57.715656
C value of BET equation :	-37.7029
Correlation factor :	.994343
Pore specific volume (cm3/g) :	.65482533
Pore specific volume at P/P0 :	.95
Total Adsorbed volume (cm3/g) :	412.05936
(Dol./Heal)	
Cumulative area max. (m^2/g) :	69.601189
Pore volume max. (cm3/g) :	.257331133

Thermo
ELECTRON CORPORATION
Instrument type : Sorptomatic 1990
Sample name : Al2O3_4M_6hAnalysis.199
Filename : D:\Backup\Data SO1990\Fong\BET\bet_LATEST\4m_6h\Al2O3_4M_6hAnalysis.199

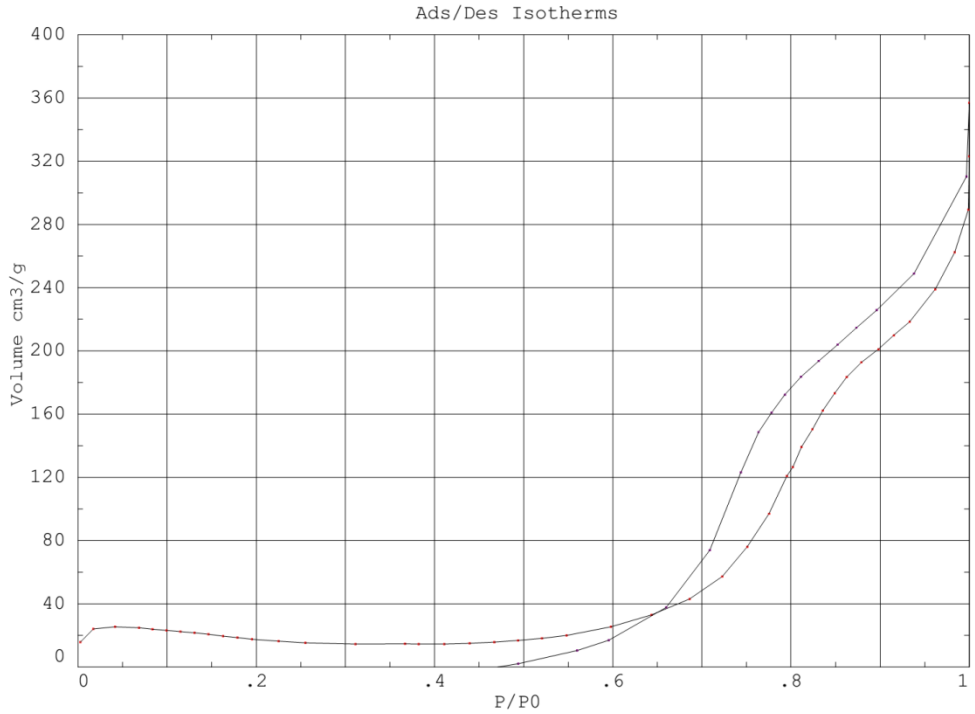

RESULTS

Calculation Method < B.E.T. >	
<B.E.T.> Initial-final P/P0 :	.04 - .3
Specific surface calculations	
Monolayer volume (cm3/g) :	10.9898605
Specific surface area (m²/g) :	47.841049
C value of BET equation :	-20.7481
Correlation factor :	.9794891
Pore specific volume (cm3/g) :	.33775818
Pore specific volume at P/P0 :	.95
Total Adsorbed volume (cm3/g) :	356.95722
(Dol./Heal)	
Cumulative area max. (m²/g) :	234.807968
Pore volume max. (cm3/g) :	.535449445

Thermo
ELECTRON CORPORATION
Instrument type : Sorptomatic 1990
Sample name : Al2O3_4M_12hAnalysis.199
Filename : D:\Backup\Data SO1990\Fong\BET\bet_LATEST\4m_12h\Al2O3_4M_12hAnalysis.199

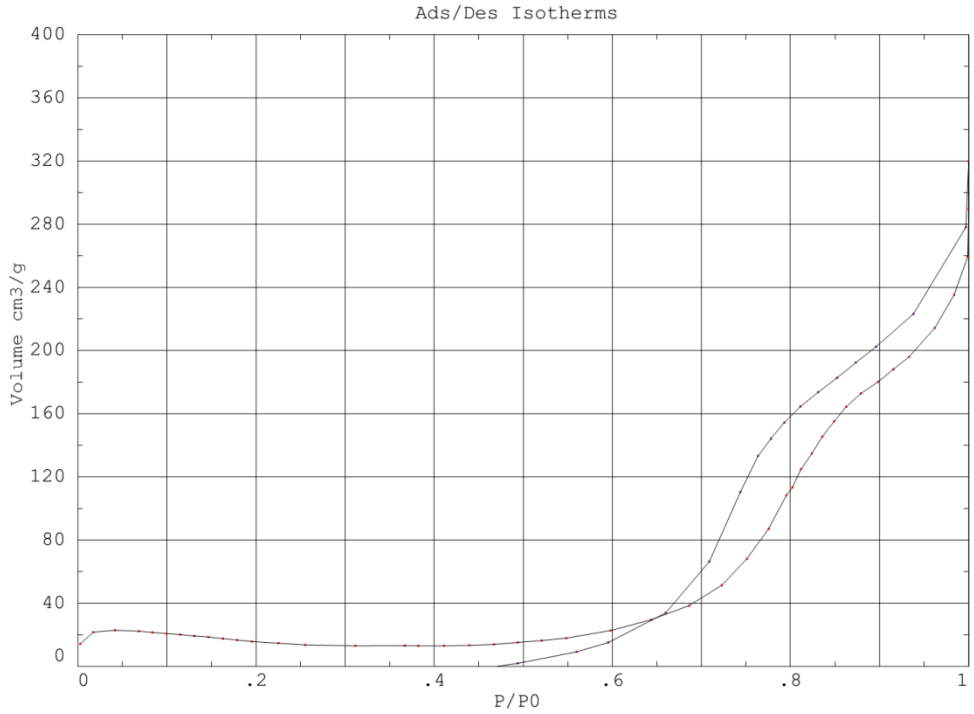

RESULTS

Calculation Method < B.E.T. >	
<B.E.T.> Initial-final P/P0 :	.04 - .3
Specific surface calculations	
Monolayer volume (cm3/g) :	9.8503857
Specific surface area (m²/g) :	42.880692
C value of BET equation :	-20.7481
Correlation factor :	.9794891
Pore specific volume (cm3/g) :	.30273801
Pore specific volume at P/P0 :	.95
Total Adsorbed volume (cm3/g) :	319.94641
(Dol./Heal)	
Cumulative area max. (m²/g) :	210.462097
Pore volume max. (cm3/g) :	.479931742

Thermo
ELECTRON CORPORATION

Instrument type : Sorptomatic 1990
Sample name : AlO(4M18h)Analysis
Filename : D:\Backup\Data SO1990\Fong\BET\bet_LATEST\4m_18h\AlO(4M18h)Analysis.199

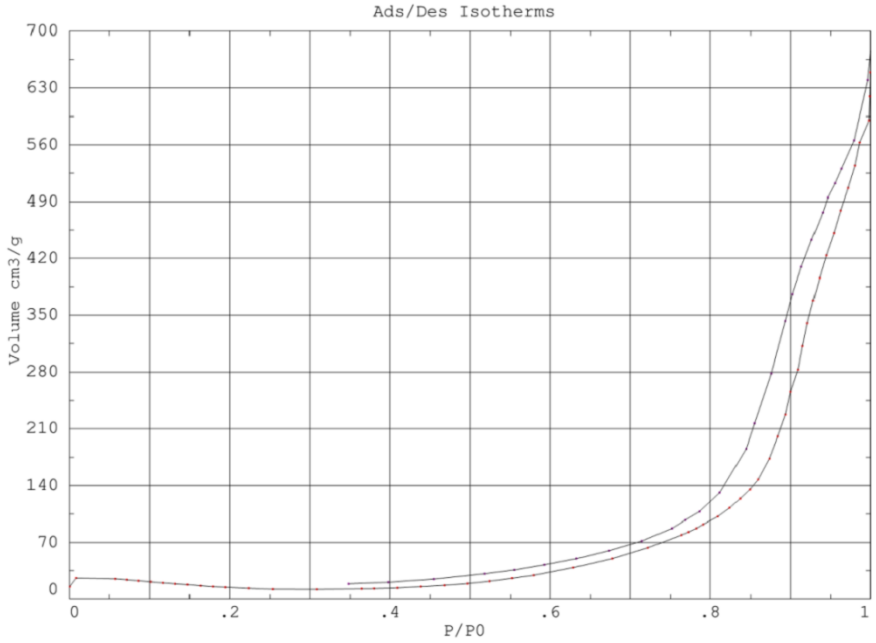

RESULTS

Calculation Method < B.E.T. >	
<B.E.T.> Initial-final P/P0 :	.04 - .3
Specific surface calculations	
Monolayer volume (cm3/g) :	8.3585997
Specific surface area (m²/g) :	36.38665
C value of BET equation :	-16.5568
Correlation factor :	.9777771
Pore specific volume (cm3/g) :	.21104057
Pore specific volume at P/P0 :	.95
Total Adsorbed volume (cm3/g) :	679.11366
(Dol./Heal)	
Cumulative area max. (m²/g) :	232.642792
Pore volume max. (cm3/g) :	.882085919

Thermo
ELECTRON CORPORATION
Instrument type : Sorptomatic 1990
Sample name : Al2O3_5M_6hAnalysis.199
Filename : D:\Backup\Data SO1990\Fong\BET\5m_6h\Al2O3_5M_6hAnalysis.199

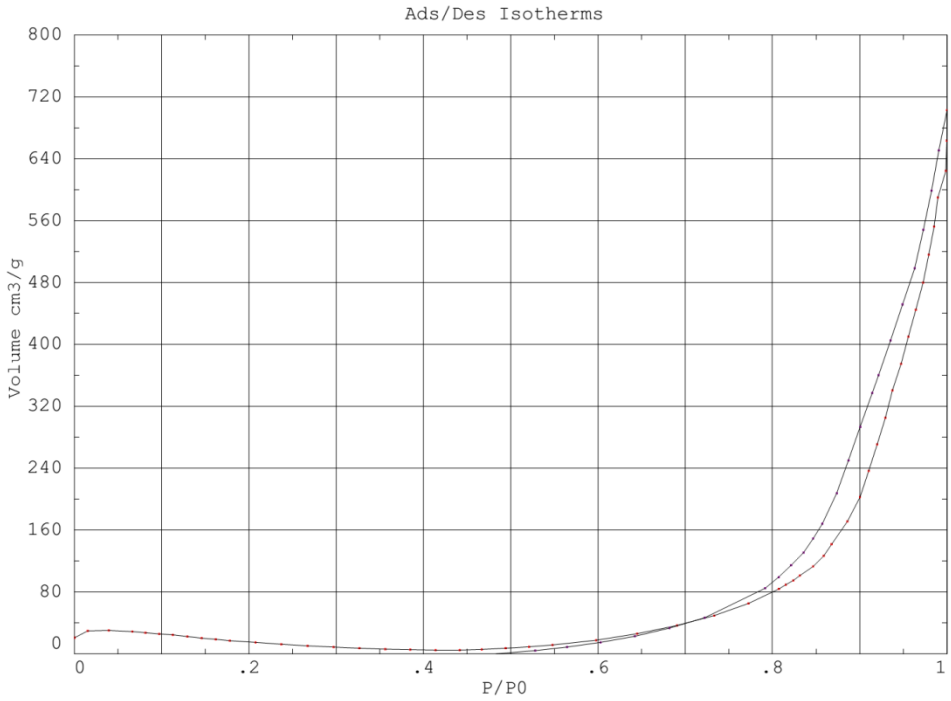

RESULTS

Calculation Method < B.E.T. >	
<B.E.T.> Initial-final P/P0 :	.04 - .3
Specific surface calculations	
Monolayer volume (cm3/g) :	5.9429779
Specific surface area (m²/g) :	25.870966
C value of BET equation :	-10.9187
Correlation factor :	.9510931
Pore specific volume (cm3/g) :	.57905567
Pore specific volume at P/P0 :	.95
Total Adsorbed volume (cm3/g) :	702.82118
(Dol./Heal)	
Cumulative area max. (m²/g) :	212.505676
Pore volume max. (cm3/g) :	.838473737

Thermo
ELECTRON CORPORATION
Instrument type : Sorptomatic 1990
Sample name : Al2O3_5M_12hAnalysis.199
Filename : D:\Backup\Data SO1990\Fong\BET\5m_12h\Al2O3_5M_12hAnalysis.199

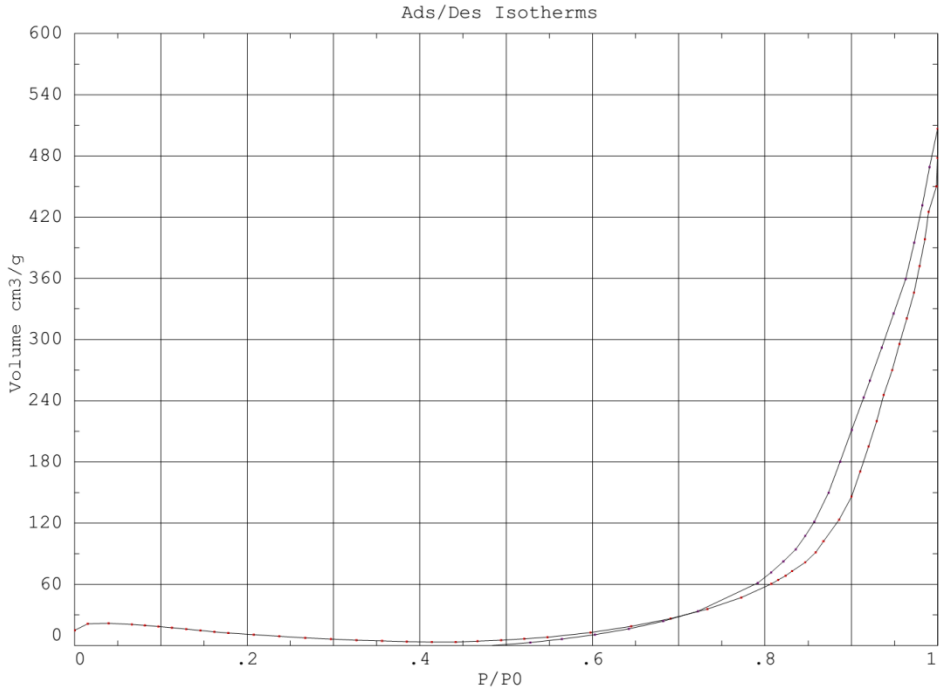

RESULTS

Calculation Method < B.E.T. >	
<B.E.T.> Initial-final P/P0 :	.04 - .3
Specific surface calculations	
Monolayer volume (cm3/g) :	4.2843304
Specific surface area (m^2/g) :	18.650543
C value of BET equation :	-10.9187
Correlation factor :	.951093
Pore specific volume (cm3/g) :	.41744488
Pore specific volume at P/P0 :	.95
Total Adsorbed volume (cm3/g) :	506.66822
(Dol./Heal)	
Cumulative area max. (m^2/g) :	153.196686
Pore volume max. (cm3/g) :	.604460835

Thermo
ELECTRON CORPORATION
Instrument type : Sorptomatic 1990
Sample name : AlO(5M_18h)Analysis
Filename : D:\Backup\Data SO1990\Fong\BET\5m_18h\AlO(5M_18h)Analysis.199

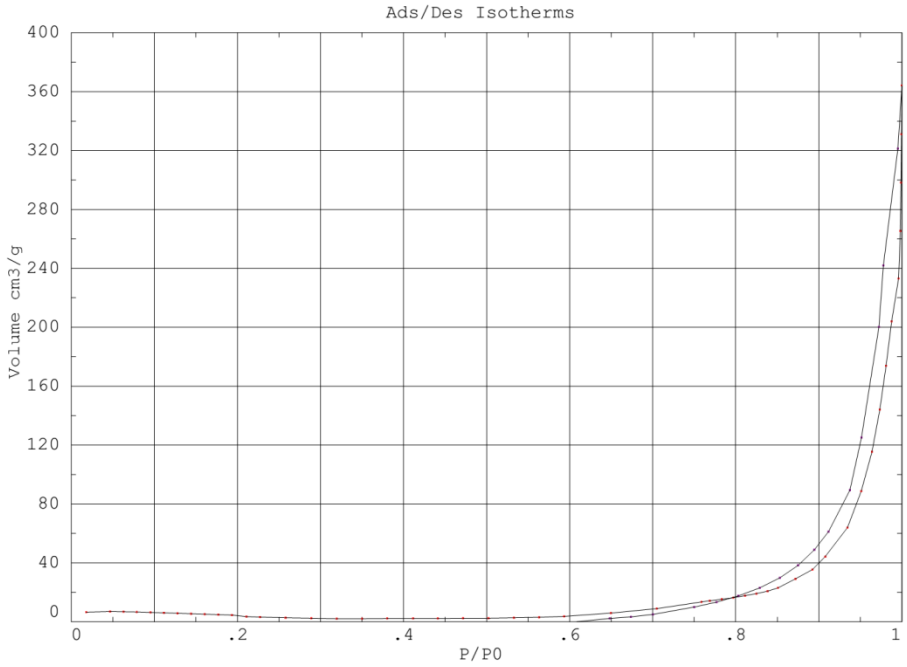

RESULTS

Calculation Method < B.E.T. >	
<B.E.T.> Initial-final P/P0 :	.04 - .3
Specific surface calculations	
Monolayer volume (cm3/g) :	1.7560308
Specific surface area (m^2/g) :	7.644351
C value of BET equation :	-12.9801
Correlation factor :	.9378971
Pore specific volume (cm3/g) :	.09869891
Pore specific volume at P/P0 :	.95
Total Adsorbed volume (cm3/g) :	364.30033
(Dol./Heal)	
Cumulative area max. (m^2/g) :	40.839214
Pore volume max. (cm3/g) :	.16644907

Thermo
ELECTRON CORPORATION
Instrument type : Sorptomatic 1990
Sample name : AlO(5M_18h_Calcined)analysis
Filename : D:\Backup\Data SO1990\Fong\BET\5m_18h_c\AlO(5M-Calcined)analysis.199

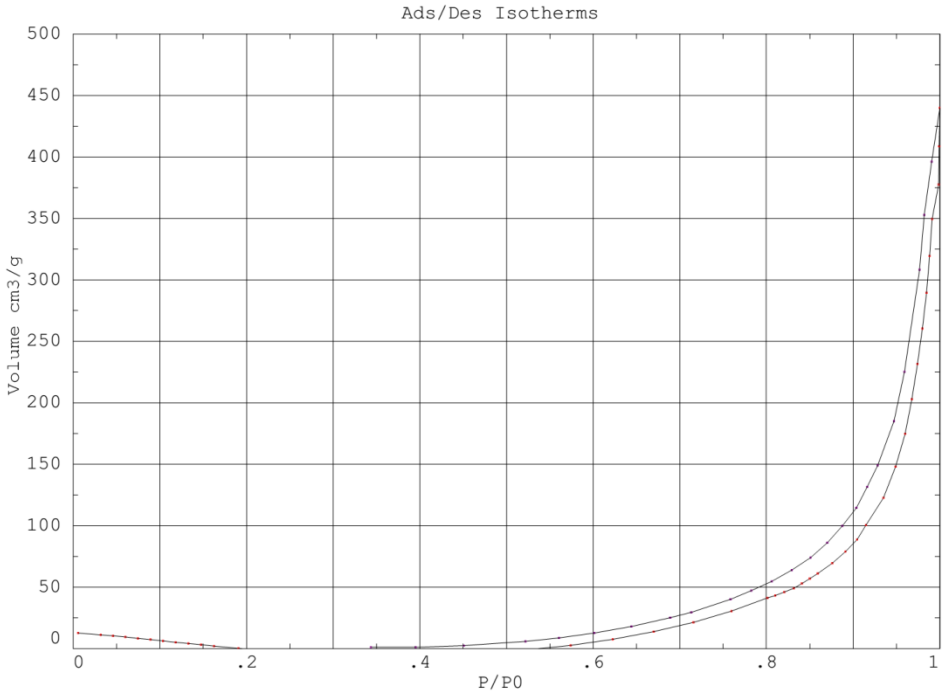

RESULTS

Calculation Method < B.E.T. >	
<B.E.T.> Initial-final P/P0 :	.04 - .3
Specific surface calculations	
Monolayer volume (cm3/g) :	1.2809646
Specific surface area (m²/g) :	5.576294
C value of BET equation :	469.743
Correlation factor :	.1748207
Pore specific volume (cm3/g) :	.22883496
Pore specific volume at P/P0 :	.95
Total Adsorbed volume (cm3/g) :	439.74659
(Dol./Heal)	
Cumulative area max. (m²/g) :	96.104698
Pore volume max. (cm3/g) :	.339993

APPENDIX G

Al_2O_3

Element	*Wt%*	*At%*
OK	35.46	48.09
AlK	64.54	51.91
Matrix	Correction	MThin

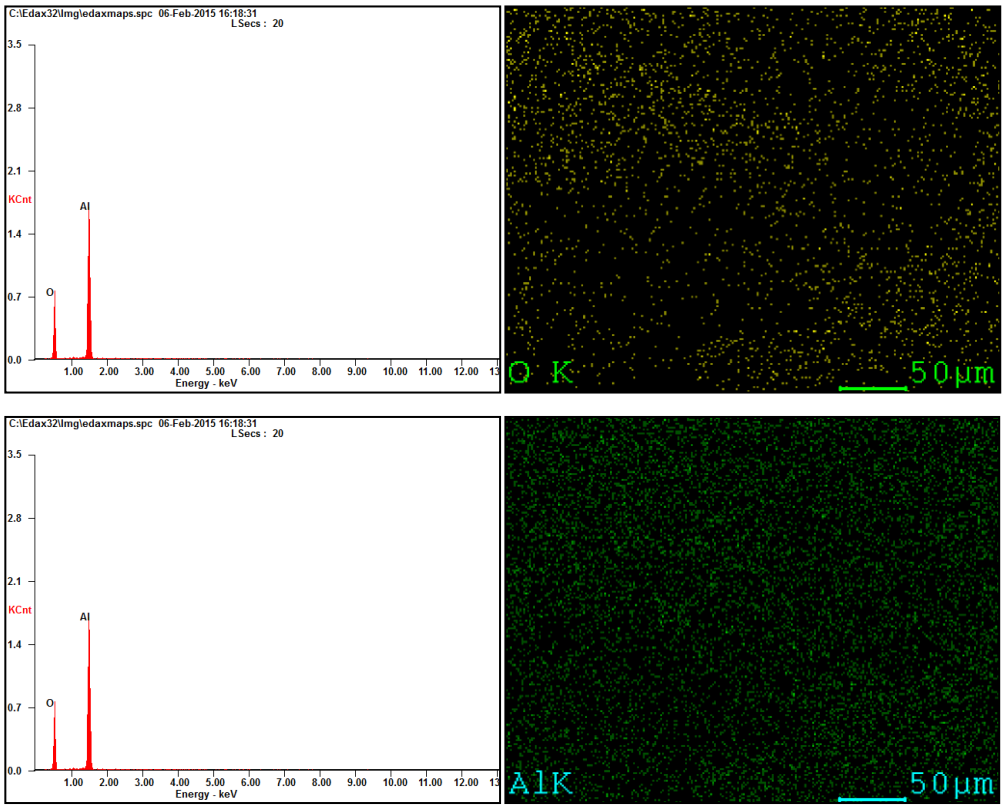

Al_2O_3-SO_3H (with calcinations treatment)

Element	*Wt%*	*At%*
OK	38.02	51.04
AlK	58.99	46.96
SK	02.98	02.00
Matrix	Correction	MThin

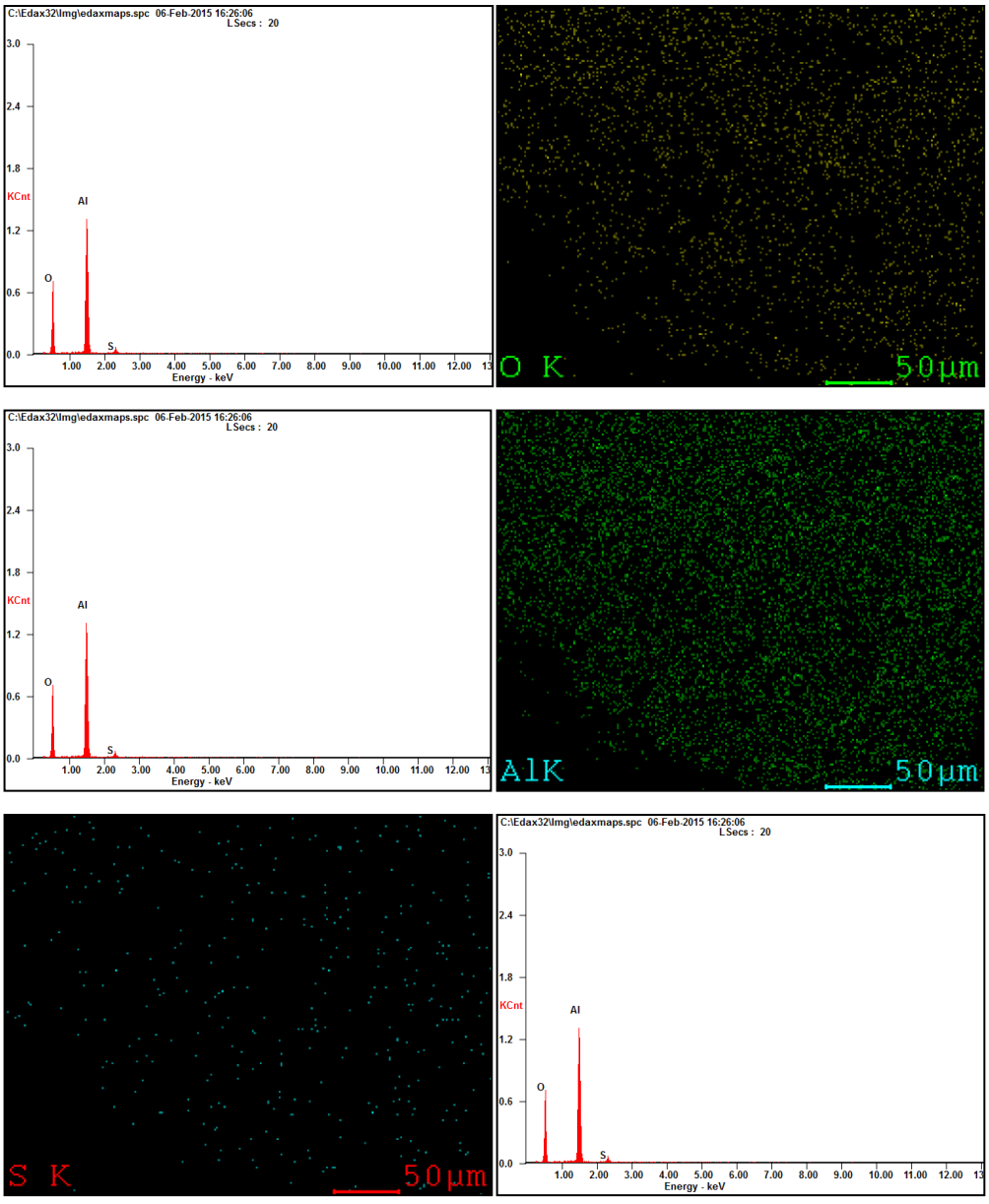

Al_2O_3-SO_3H (without calcinations treatment)

Element	*Wt%*	*At%*
OK	41.03	54.30
AlK	54.37	42.66
SK	04.60	03.04
Matrix	Correction	MThin

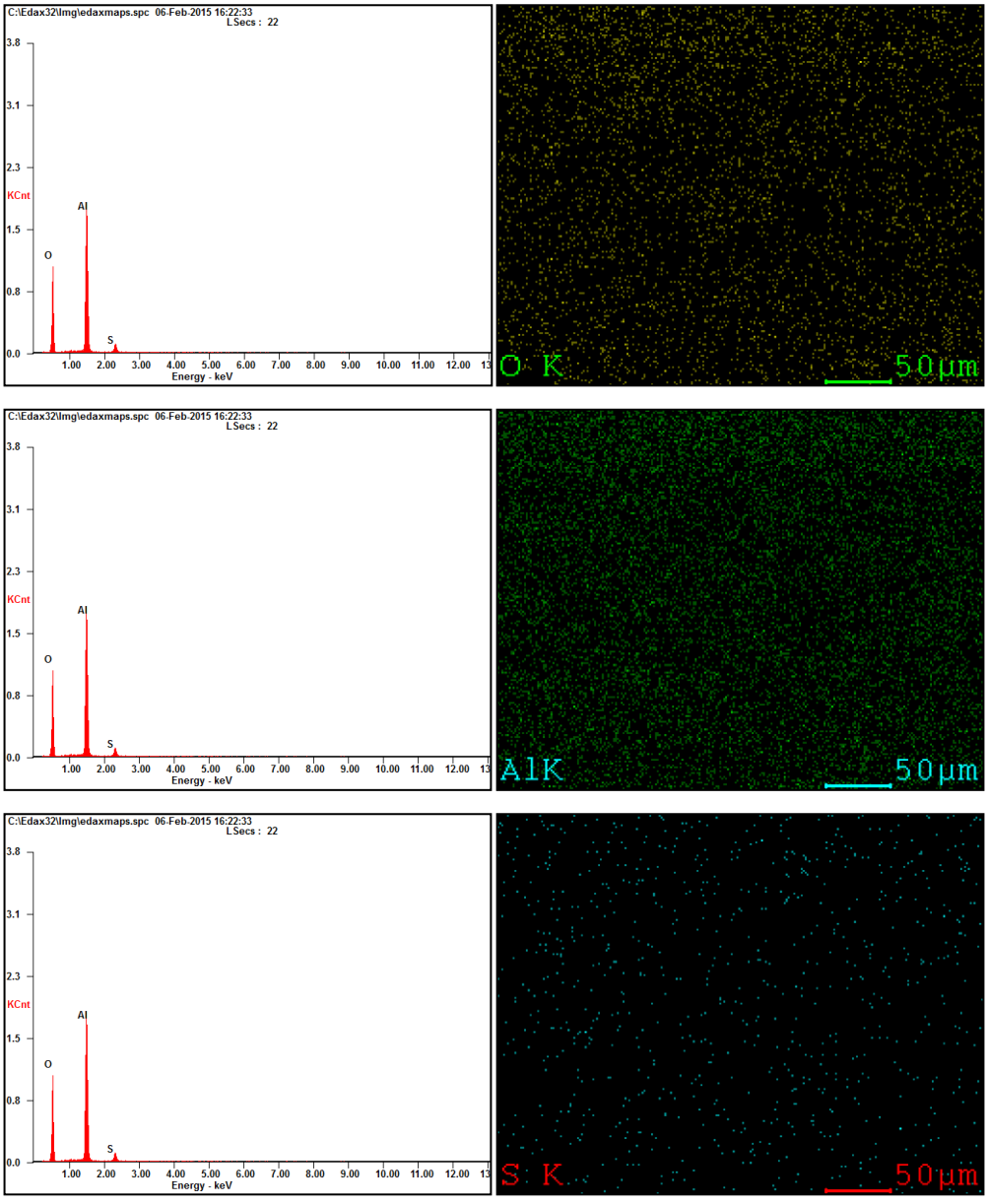

SiO_2

Element	*Wt%*	*At%*
OK	38.47	52.32
SiK	61.53	47.68
Matrix	Correction	MThin

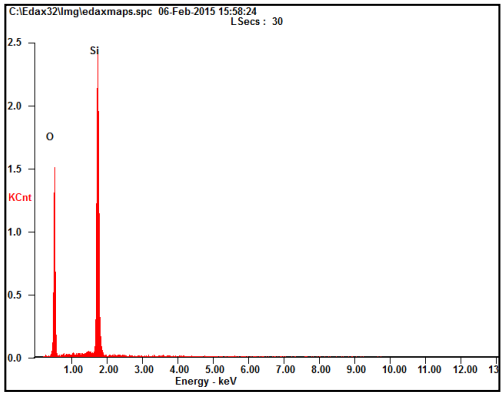

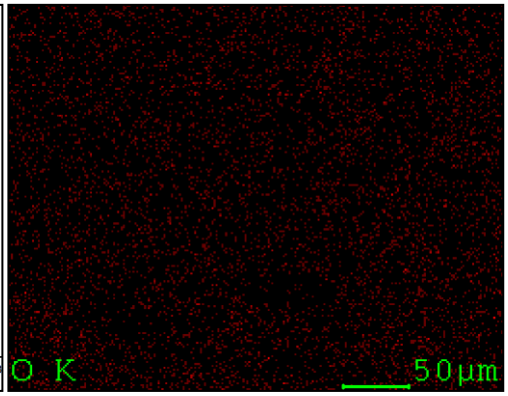

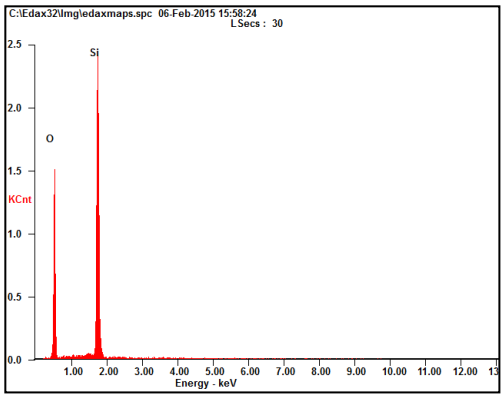

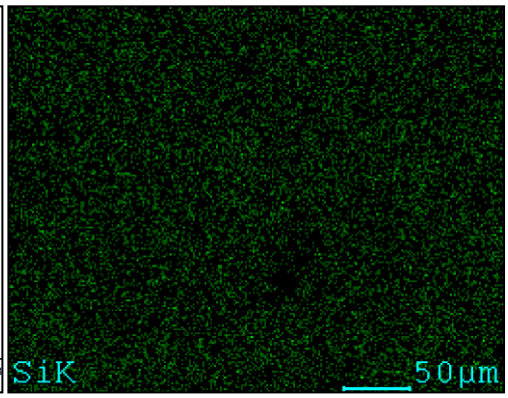

SiO_2-SO_3H (with calcinations treatment)

Element	*Wt%*	*At%*
OK	35.46	49.11
SiK	64.40	50.80
SK	00.13	00.09
Matrix	Correction	MThin

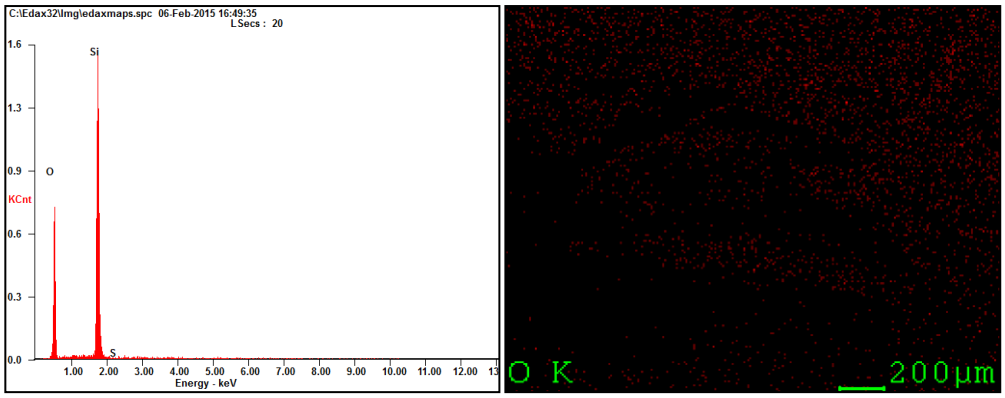

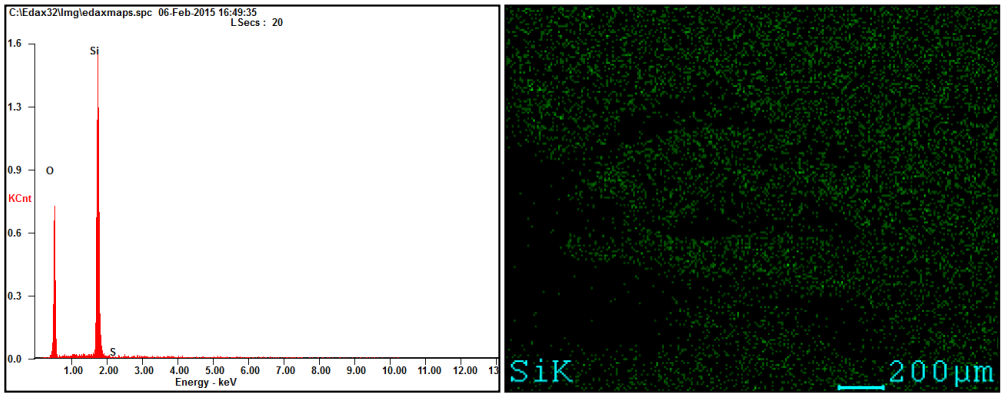

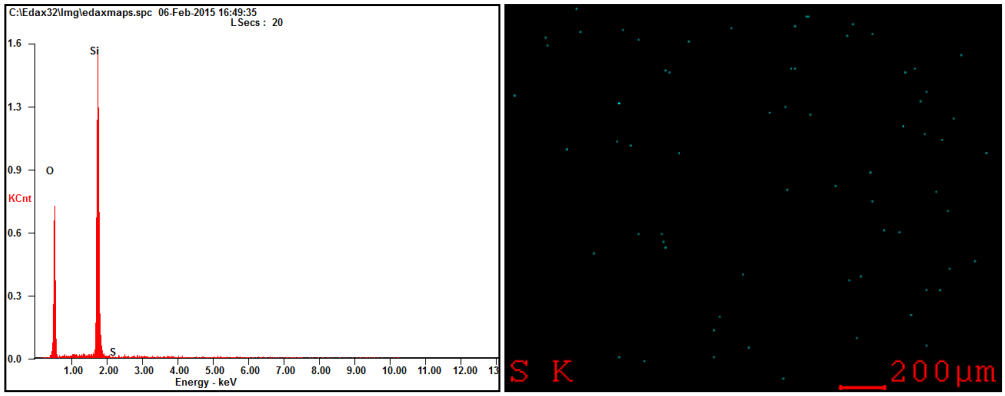

SiO_2-SO_3H (without calcinations treatment)

Element	*Wt%*	*At%*
OK	32.87	46.23
SiK	66.94	53.63
SK	00.19	00.14
Matrix	Correction	MThin

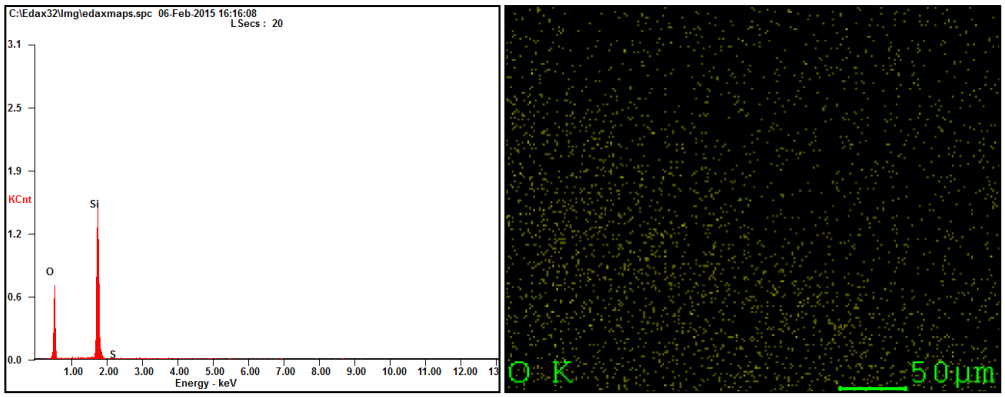

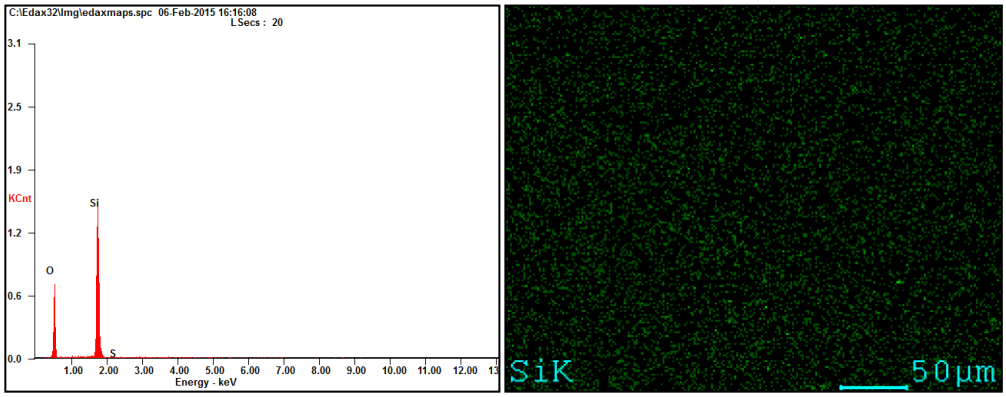

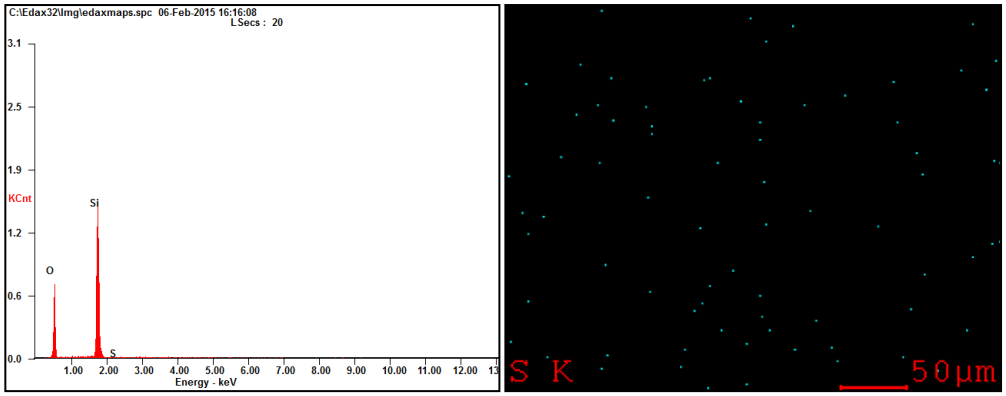

TiO_2

Element	*Wt%*	*At%*
OK	05.40	14.60
TiK	94.60	85.40
Matrix	Correction	MThin

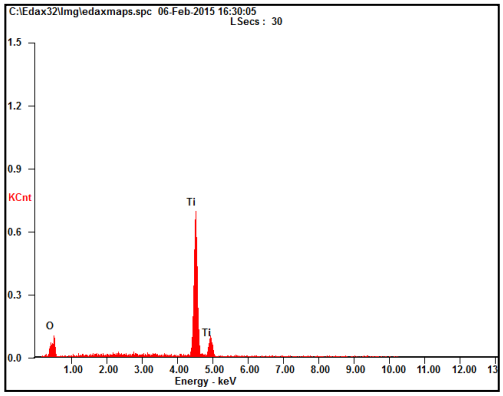

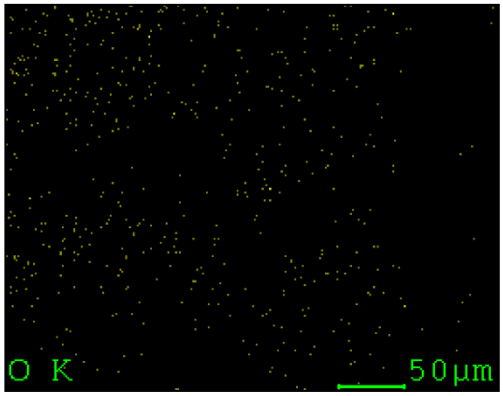

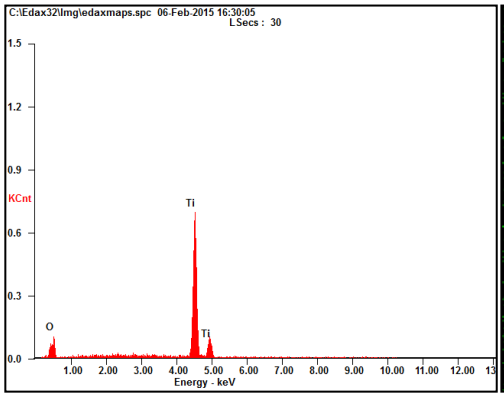

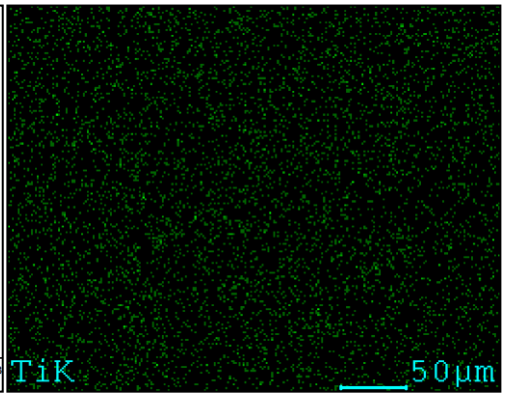

TiO_2-SO_3H (with calcinations treatment)

Element	*Wt%*	*At%*
OK	12.48	29.89
SK	00.23	00.28
TiK	87.29	69.84
Matrix	Correction	MThin

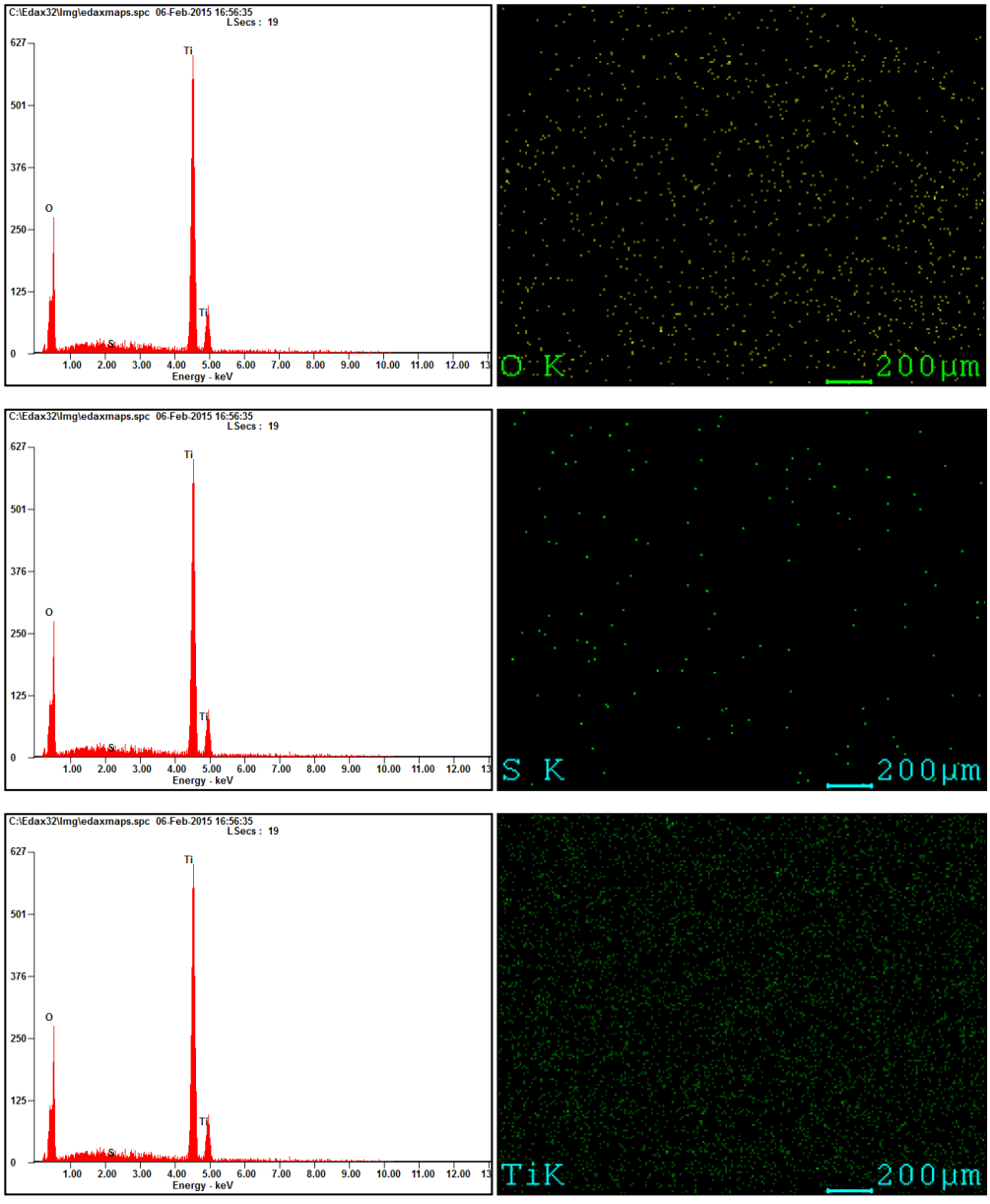

TiO_2-SO_3H (without calcinations treatment)

Element	*Wt%*	*At%*
OK	08.05	20.74
SK	00.28	00.36
TiK	91.67	78.91
Matrix	Correction	MThin